THE EFFECTS OF EXPLOSIVES ON THE PHYSICAL PROPERTIES OF SNOW

by

Robyn Elaine Wooldridge

A thesis submitted in partial fulfillment
of the requirements for the degree

of

Master of Science

in

Earth Sciences

MONTANA STATE UNIVERSITY
Bozeman, Montana

January, 2013

APPROVAL

of a thesis submitted by

Robyn Elaine Wooldridge

This thesis has been read by each member of the thesis committee and has been found to be satisfactory regarding content, English usage, format, citation, bibliographic style, and consistency and is ready for submission to The Graduate School.

Dr. Jordy Hendrikx

Approved for the Department of Earth Sciences

Dr. David Mogk

Approved for The Graduate School

Dr. Ronald W. Larsen

STATEMENT OF PERMISSION TO USE

In presenting this thesis in partial fulfillment of the requirements for a master's degree at Montana State University, I agree that the Library shall make it available to borrowers under rules of the Library.

If I have indicated my intention to copyright this thesis by including a copyright notice page, copying is allowable only for scholarly purposes, consistent with "fair use" as prescribed in the U.S. Copyright Law. Requests for permission for extended quotation from or reproduction of this thesis in whole or in parts may be granted only by the copyright holder.

Robyn Elaine Wooldridge

January, 2013

ACKNOWLEDGEMENTS

This research was made possible by the support and assistance of various people and organizations. I would like to thank my committee chair, Jordy Hendrikx, for his open door and willingness to help at any time. I would also like to thank my other committee members, Karl Birkeland and Dan Miller, for their help and patience over the course of this research project.

Moonlight Basin, Montana, and the Moonlight Basin Ski Patrol provided my primary study site, logistical support, and explosives. I would especially like to thank Brad Carpenter, Randy Spence and the snow safety team for their continued help over the course of two years.

I would also like to thank Snowmass Ski Area, Colorado, and the Snowmass Ski Patrol for fostering my interest in avalanche mitigation and explosives control work; and also for providing my initial study site, explosives, and personnel to act as field assistants. Thanks especially to Craig Chalmers, Matt Huber and the Snowmass snow safety department.

I thank both the American Avalanche Association and the American Alpine Club for research grants that provided financial support for this study.

Finally, I would like to thank my family for being my best cheerleaders. I cannot thank them enough for always encouraging me and believing in my goals.

TABLE OF CONTENTS

LIST OF TABLES

Table Page

LIST OF FIGURES

Figure Page

LIST OF FIGURES – CONTINUED

Figure Page

LIST OF FIGURES – CONTINUED

Figure Page

ABSTRACT

Explosives are a critically important component of avalanche control programs. They are used to both initiate avalanches and to test snowpack instability by ski areas, highway departments and other avalanche programs around the world. Current understanding of the effects of explosives on snow is mainly limited to shock wave behavior demonstrated through stress wave velocities, pressures and attenuation. This study seeks to enhance current knowledge of how explosives physically alter snow by providing data from field-based observations and analyses that quantify the effect of explosives on snow density, snow hardness and snow stability test results. Density, hardness and stability test results were evaluated both before and after the application of 0.9 kg cast pentolite boosters as surface and air blasts. Changes in these properties were evaluated at specified distances up to 5.5 meters (m) from the blast center for surface blasts and up to 4 m from the blast center for air blasts. A density gauge, hand hardness, a ram penetrometer, Compression Tests (CTs), and Extended Column Tests (ECTs) were used. In addition to the field based observations, the measurement error of the density gauge was established in laboratory tests. Results from surface blasts did not provide conclusive data. Air blasts yielded statistically significant density increases out to a distance of 1.5 m from the blast center and down to a depth of 50 centimeters (cm). Statistically significant density increases were also observed at the surface (down to 20 cm) out to a distance of 4 m. Hardness data showed little to no measurable change. Results from CTs showed a statistically significant decrease in the number of taps needed for column failure 4 m from the blast center in the post-explosive tests. A smaller data set of ECT results showed no overall change in ECT score. The findings of this study provide a better understanding of the physical changes in snow following explosives, which may lead to more effective and efficient avalanche risk mitigation.

1. INTRODUCTION

Explosives are a critically important component of avalanche risk mitigation programs. They are used by ski areas, highway departments and other avalanche programs to both initiate avalanches and to test snowpack instability. Despite their importance, knowledge about the effects of explosives on the physical properties of snow is limited. This research provides experimental, field-based observations and analyses of the changes in snow density, snow hardness and snow stability test results after the application of explosives, thereby contributing to the understanding of how explosives affect the physical properties of snow.

While knowledge of the physical effects of explosives on snow is limited, many prior studies have examined shock wave propagation through the snowpack, focusing on stress wave velocities, pressures and attenuation (e.g. Livingston, 1968; Lyakhov et al., 1989; Mellor, 1973; Wisotski and Snyer, 1966; Bones et al., 2012). Livingston (1968) examined explosives induced failure processes in snow and concluded that snow is unique from other materials such as rock, glacier ice and some soils in its failure process. Two notable differences, both due to the large amount of pore space in snow, are abatement of the disturbance before peak pressures are reached and a considerable recovery of potential energy during unloading. This recovery of potential energy occurs as peak under-snow pressures decline and implosion occurs in the crater zone (Livingston, 1968). Mellor (1973) also illustrated differences between snow's response to explosives and that of materials more commonly coupled with explosives such as rock. Snow demonstrates peak pressures that are about 100 times less than those measured in

granite and also shows much more rapid attenuation of stress waves (Mellor, 1973). He discussed the importance of impedance matching in shockwave propagation. For effective explosives-materials coupling, the product of detonation velocity and explosive density should be nearly equal to the product of acoustic velocity and density of the medium (Mellor, 1973). Mellor (1973) emphasized the impedance mismatch between snow and explosives and the resulting shockwave attenuation that is not seen in materials with better coupling like rock or frozen soil. Gubler (1977) examined stress wave attenuation as a result of charge size, placement, type of explosive, snow type and ground type. He normalized his results to a standard charge of 1kg with a detonation velocity of 6900 m/s and a density of 1.4 kg/m^3 which is comparable to a 0.9 kg charge of pentolite which has a detonation velocity of approximately 7900 m/s and a density of 1.6 kg/m^3 (Orica Ltd., 2010). He determined that the most effective charge placement was one to two meters above the snow surface. Ueland (1992) investigated the effectiveness of different charge types and sizes in various snowpacks and confirmed the effectiveness of air blasts suspended above the snow surface. Contrary to Gubler's findings, Ueland argued that snow hardness influences shock wave attenuation more than density, with softer snow exhibiting stronger attenuation than harder snow.

This rapid attenuation of shock waves demonstrates how snow behaves differently from previously mentioned materials (Mellor, 1968; Wisotski and Snyer, 1966; Livingston, 1968). In experiments involving above-snow explosive blasts, Mach-region peak pressures were found to be lower over snow than over bare ground or concrete. This was attributed to shockwave attenuation upon contact with the snow surface, once

again demonstrating much higher shock wave attenuation rates in snow (Wisotski and Snyer, 1966; Bones et al., 2012). This rapid attenuation is a unique response that sets snow apart from those other materials and may be a result of the unique structure and composition of snow. Snow is structured in layers that form as it accumulates and metamorphoses and is made up of two physically different components, air and ice or water, that remain separate within the medium (Livingston, 1968) rather than mixing like in more homogenous materials.

When explosives are in direct contact with snow, the normal explosive reaction is impeded. The presence of carbon in the crater region after detonations of explosives on or near the snow surface suggests the likelihood of an incomplete reaction (Wisotski and Snyer, 1966). Wisotski and Snyer (1966) documented anomalies and scatter in their peak pressure and velocity data calculated from snowpack measurements and proposed that this is a feature of snow and explosives coupling. Snow is a composite material made up of air, ice and/or water. Pore space between the solid components makes up 45-97% of total snow volume (McClung and Schaerer, 2006), a much larger percentage than in most other materials. For example, the porosity of rock is 1-40% and that of concrete is 1-10% (Wisconsin Geological and Natural History Survey, 2011; Klieger and Lamond, 2006). This large pore space in snow, a non-elastic medium, allows for permanent compaction as the momentum behind the shockwave is transferred to the snow and the shockwave is attenuated (Johnson et. al, 1994). Johnson et al. (1993) show that higher pressures are necessary to compact snow with lower initial densities; and that snow will eventually be compacted to a critical density where elevated pressures are needed to

cause further densification. They also fit a power law to their shockwave attenuation data (Johnson et. al, 1994). Because shockwave attenuation occurs simultaneously with snow compaction and densification, it is possible that density change as a function of initial density could also be characterized by a power law.

Brown (1981) predicted that snow density would increase in the immediate area surrounding a blast, but the author did not provide data to support this prediction. Frigo et al. (2010) detonated dynamite and emulsion charges above, on and below the snow surface and made snowpack measurements including snow density, but density was only measured at the blast crater and their results were inconclusive.

Miller et al. (2011) presented a model predicting some of the responses of snow to an explosive blast. An explosion is characterized by an increase in pressure and temperature across the shock front (Mellor, 1973; Miller et al., 2011). Creating this sudden increase in pressure that ideally leads to weak layer failure is the goal of avalanche control operations using explosives. Miller et al. (2011) use ANSYS/AUTODYN, a program commonly used for assessing the movement of rock during an explosion, to create an explicit model of snow behavior during such an event. The model is ideal for characterizing the rapid increase in pressure across the shock front because of its ability to predict changes in nonlinear solids and gases at the same time (Miller et al., 2011). Miller et al. (2011) evaluated pressure and stress waves from both surface and air blasts of 0.9 kg and 1.8 kg pentolite charges and examined the decrease in both as a result of geometric expansion and snow attenuation of the shock wave. They also used their model to evaluate density changes, predicting increasing density in the

region below the explosive (Miller et al., 2011). Miller et al. (2011) theorized that the region affected by a stress wave might provide a gauge of the effectiveness of explosives in avalanche control work.

All of these studies provide insight into the behavior of shock waves in snow, but there is still a lack of information and observational data on the physical changes in snow that occur as a result of using explosives. Quantifying changes in physical snow properties such as density and hardness at different distances from a blast could help to define the area of influence of explosives commonly used for avalanche mitigation applications. These results could either strengthen or contradict the work done by Miller et al. (2011) and others prior (e.g. Johnson et al., 1993). Furthermore, examining changes in stability test results after the use of explosives may also provide information about how far from the blast center snow stability, as measured by Compression Tests (CTs) and Extended Column Tests (ECTs), is being affected and whether the snowpack is gaining or losing strength.

1.2 Aims / Research Questions

Throughout this thesis, pre- and post-explosives use changes in snow density, snow hardness and snow stability test results will be quantified, as will the distances over which those changes can be measured. The following research questions will be addressed:

1) After the application of explosives as surface blasts and air blasts, is there a change in snow density and to what distances and depths can that change be measured in the field?

2) After the application of explosives as surface blasts and air blasts, is there a change in snow hardness and to what distances and depths can that change be measured in the field?

3) After the application of explosives as surface blasts and air blasts, is there a change in stability test results as shown by Compression Tests and/or Extended Column Tests, and at what distances can those changes be quantified?

To answer these questions, snow density and snow hardness were measured before and after applying explosives as both surface and air blasts at four distances from the blast center and down to a depth of 1 meter (m). Compression Tests (Jamieson and Johnston, 1996) were conducted before and after both surface and air blast detonation at two distances from center for each detonation. Extended Column Tests (Simenhois and Birkeland, 2006) were performed before and after air blasts only. Repeated measurements of the changes in snow density, snow hardness and snow stability test results following detonation of explosives have not previously been made. This research provides observational data and analyses which will help bridge the gap between theoretical knowledge and practical field-based knowledge on how snow responds to explosives and may lead to improvements in avalanche control operations.

2. METHODS

2.1 Study Sites

Data for this study was collected from three field sites in three different mountain ranges with snow climates that have been classified as both continental and intermountain depending on conditions in a given year (Mock and Birkeland, 2000). The three study areas were located in central Colorado and southwestern Montana. Based on average monthly air temperatures during the winters of 2010/2011 and 2011/2012, when this study was conducted, the Colorado site was representative of a continental snow climate and the Montana study sites demonstrated temperatures characteristic of intermountain snow climates. Selected test sites received no avalanche mitigation and little to no skier compaction in an effort to preserve natural snow conditions. Sites with low slope angles were chosen to minimize snow loss through avalanching and to reduce personnel avalanche risk during data collection. All surface blasts were performed in the Colorado study site and all air blasts were conducted in the Montana study sites.

2.1.1 Snowmass Study Area

A total of eight explosives tests were conducted as surface blasts at Snowmass Ski Area in the Elk Mountain Range located in west-central Colorado between December 27, 2010 and January 6, 2011 (Figure 1). The northeast corner of the Snowmass study area is located at approximately 39.1705° north and 106.9345° west and has an elevation of 3,330 m. The test site lies in an open meadow within ski area boundaries in a clearing surrounded by evergreen forest composed mostly of lodgepole pine and subalpine spruce

trees (Figure 2). Test slopes formed a small basin with slope angles ranging from 6° to 13° and sites facing East-northeast, East-southeast or North-northwest. Because the test site provides poor access to desirable ski terrain and has low slope angles, it receives little to no skier compaction and no avalanche mitigation.

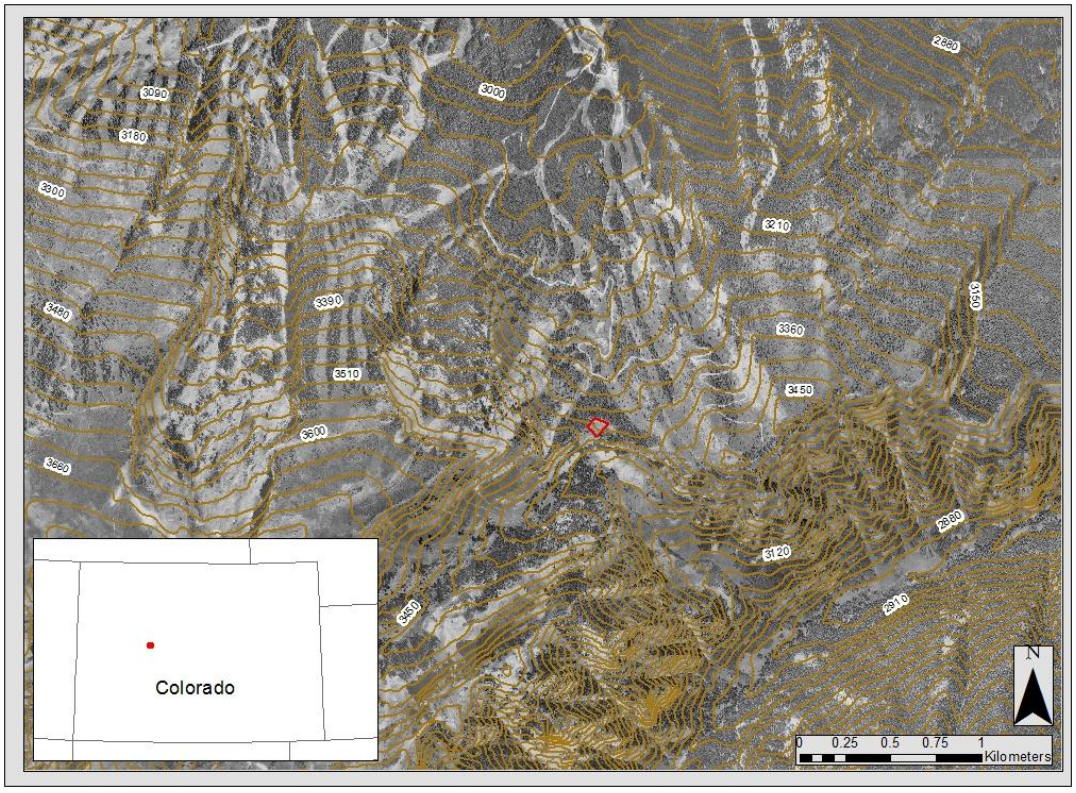

Figure 1: Map showing the location of the Snowmass study area outlined in red and its relative position within Colorado as indicated by the red dot in the inset. Elevations are shown in meters. The contour interval is 30 m.

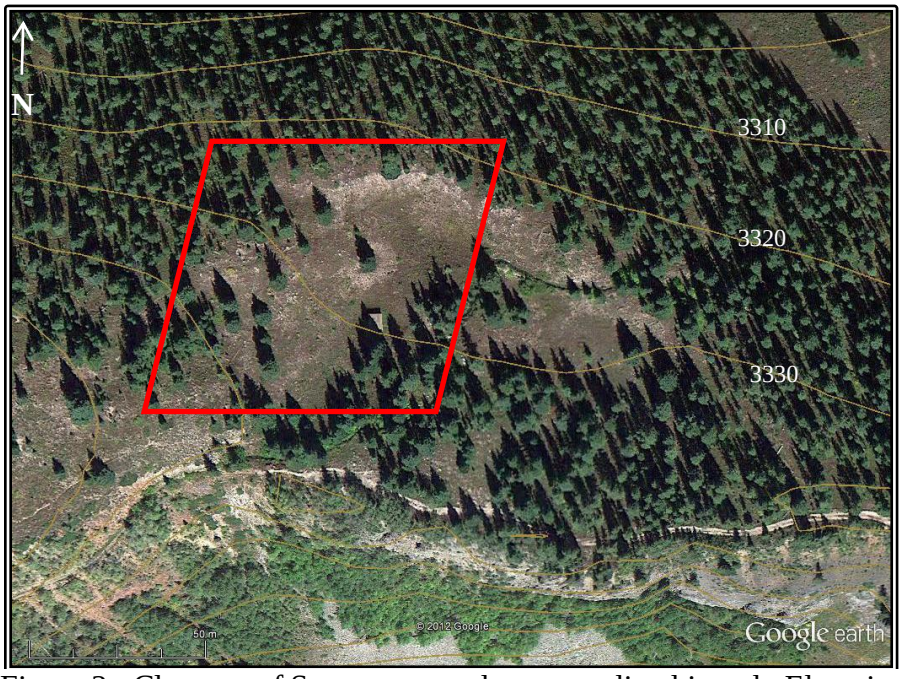

Figure 2: Close-up of Snowmass study area outlined in red. Elevations are shown in meters and the contour interval is 10 m.

2.1.2 Montana Study Areas

Twenty-five tests of air blast explosions were conducted at Moonlight Basin during the winters of 2010/2011 and 2011/2012 and two were conducted at Bridger Bowl in January of 2011. The majority of the data collected during this study was gathered at Moonlight Basin Ski Resort in the Madison Mountain Range in southwestern Montana. The Northeast corner of the Moonlight Basin Study site is located at approximately 45.3028° north, 111.4545° west and an elevation of 2,155 m (Figure 3). This site lies within the ski area boundaries in a closed area that was cut as a ski trail, but never opened to skier access. The slope is completely free of trees and other obstacles and is flanked by forest cover. Slope angles at this site range from 7° to 20°. Due to its closed status

and gentle slope angles this site was free from skier traffic and avalanche mitigation (Figure 4).

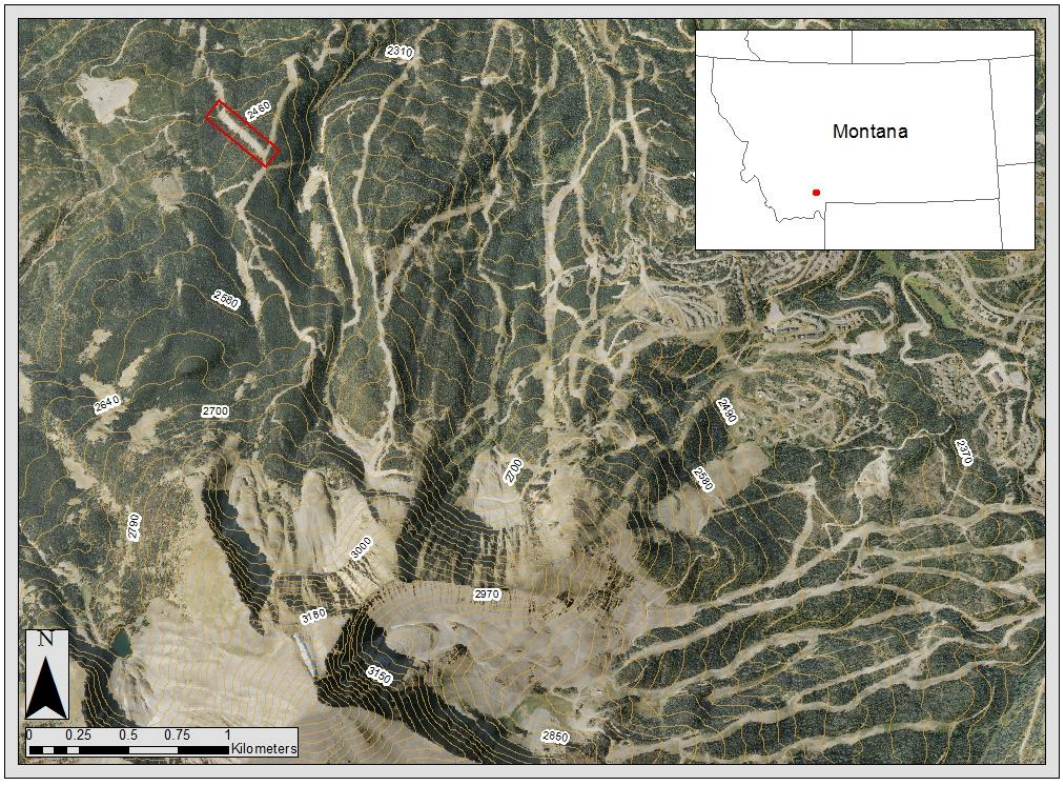

Figure 3: Map showing the location of the Moonlight Basin study area outlined in red and its location within Montana as indicated by the red dot in the inset. Elevations are shown in meters and the contour interval is 30 m.

Figure 4: Close up of Moonlight Basin study area outlined in red. Elevations are shown in meters and the contour interval is 10 m.

The second study area in southwestern Montana is located at Bridger Bowl Ski Area in the Bridger Mountain Range at approximately 45.8060° north, 110.9108° west with an elevation of 2,066 m (NE corner) (Figure 5). This site was in an open meadow surrounded by open evergreen canopy and was located in a permanently closed area. Slope angles at the Bridger Bowl site ranged from 7° to 20° (Figure 6).

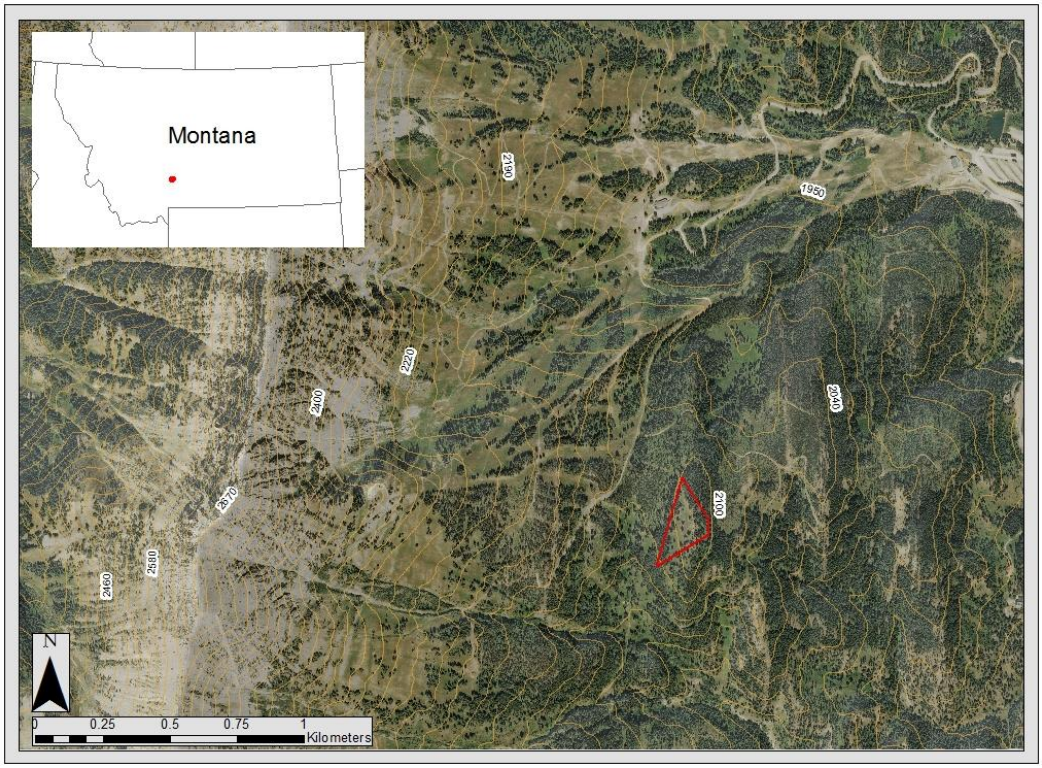

Figure 5: Map showing the location of the Bridger Bowl study area outlined in red and its location within Montana as indicated by the red dot in the inset. Elevations are shown in meters. The contour interval is 30 m.

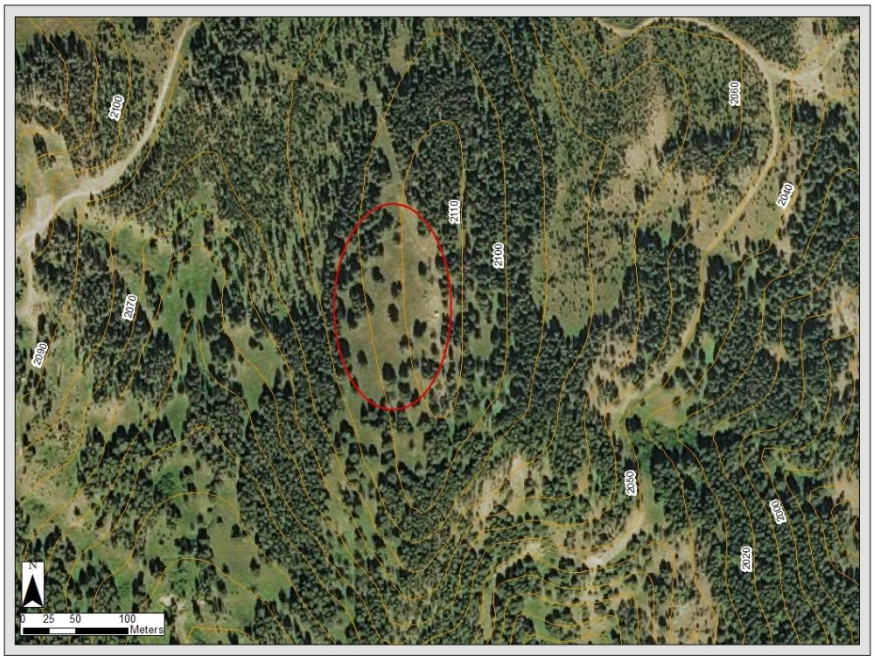

Figure 6: Close up of Bridger Bowl study area circled in red. Elevations are shown in meters and the contour interval is 10 m.

2.2 Field Methods

Snow density and snow hardness were measured before and after applying explosives as both surface blasts and air blasts at four distances from the blast center. Compression Tests (Jamieson and Johnston, 1996) were also conducted before and after using explosives at two distances from the blast center. For tests of air blasts, Extended Column Tests (Simenhois and Birkeland, 2006) were conducted at two distances from center for each detonation. Methods of data collection were similar for both the 8 surface blasts and the 27 air blasts. Four pre-blast snowpits were dug and sampled, an explosive was detonated and four post-blast snowpits were excavated and sampled, however the distance was altered for the surface blasts. The procedure follows. A blast center was selected based on consistency of slope angle, snow depth and proximity to previous tests. Uniform slope angle and uniform snow depth were desired, as was a gap of at least 4 m between other blast centers and the intended snowpit locations in order to preserve natural snow conditions. At each test site, four snowpit locations were measured at specified distances from the blast center and marked without disturbing snow between the blast center and the pit locations. These sites were determined to be the exact locations of the post-blast snowpits. To ensure that the post-blast measurements would be made exactly at these marked locations in undisturbed snow, pre-blast snowpits were located approximately 0.5 m downhill of the marked locations. Surface blast pit distances were chosen in an attempt to avoid post-blast sampling of mechanically mixed snow within the blast craters. A surface blast results in a crater where snow is moved and mixed within the crater and some snow is relocated to the outside of the crater along with

black soot. One initial surface blast was conducted to test the sampling methods and establish crater size. The crater resulting from this initial surface blast measured 1.75 m in radius, therefore post-explosives surface blast pits were located 2, 2.5, 3 and 5.5 m from the blast center (Figure 7) in order to be outside the crater zone. Snowpits in all post-explosives air blast tests were placed at distances of 0.5, 1, 1.5 and 4 m from the blast center (Figure 7). Although one representative snowpit for each detonation would have been sufficient for baseline measurements, a pre-blast pit was dug for each distance. This was done to minimize the possible effects of spatial variability. The air blast distances are much closer than those used in the surface blast tests and were established through one initial air blast test. Air blasts create a circular zone where snow is compacted rather than displaced like it is in surface blasts. An air blast has a circular depression that was measured in the initial air blast test out to a radius of 1.5 m from the blast center. At a distance of 1 m from the blast center, there was a decrease in snow surface height due to compaction that measured up to 10 cm. Because of differences in cratering and compaction between surface and air blasts, post-air blast measurements were made adjacent to the blast center in snow that was not displaced by the blast.

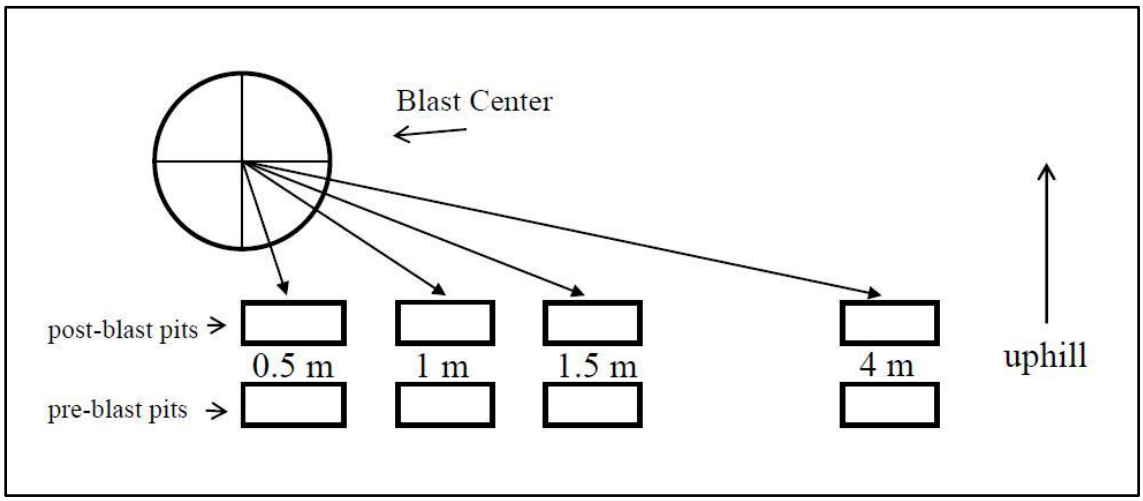

Figure 7: Diagram of sampling design, showing the pre- and post-blast pit locations for air blasts and the blast center. Pre-blast pits were located 0.5 m downhill of post-blast distances in order to leave undisturbed snow at the distances indicated for post-blast sampling. Post-blast pits for surface blasts were located at distances of 2, 2.5, 3 and 5.5 m from the blast center.

The snowpits were dug to a depth of 1 m where the snow cover exceeded 1 m and to the ground where snow height was less than 1 m. These depths are based on the model by Miller et al. (2011), which predicts that the compaction zone from a 1.8 kg surface blast will reach a depth of 0.8 m and on calculations by Johnson et al. (1994) determining that the zone of compaction is 1 m for a 1 kg charge buried in snow. Both the depth predicted by Miller et al. (2011) and the area of compaction observed by Johnson et al. (1994) are associated with surface blasts. Because a surface blast will affect snow to a greater depth within a smaller area than a suspended blast (Miller et al., 2011) it was expected that a depth of 1 m would be adequate to capture density and hardness changes resulting from air blasts. These depths were also believed to be appropriate for surface blast pits because the 0.9 kg charge size used here was smaller than the sizes of the charges used in both studies. Snowpits where CTs or ECTs were conducted were

approximately 100 cm wide and those where neither a CT nor ECT were performed were approximately 50 cm wide. Occasionally this caused pits, especially post-blast pits, to run together, but care was taken to sample at the distances indicated in the sampling design. Snow density and hardness were assessed in 10 cm increments with the first measurements taken at a depth of 5 cm from the snow surface. Measurements of densities and hardness before and after surface blasts were made every 10 cm from the snow surface down to a depth of 50 cm after which measurements were made only at depths of 70-80 cm and 90-100 cm because it was believed that there would be very little detectable change at these depths. It should be noted that the complete set of 8 surface blast tests were conducted before any of the 27 air blasts were performed. As a result, some elements of the study design were changed for air blasts in order to better measure the parameters of interest.

Density and hardness for air blast tests were assessed every 10 cm to a depth of 1 m to provide a more complete and continuous data set. Density was measured using a Strong Stitch density gauge by Winter Engineering equipped with a 100 cm^3 cylindrical cutter and a mass balance gauge reading from 0% to 60% water content (Figure 8) in both surface and air blasts. All density samples were obtained with the long axis of the cutter oriented horizontally across the slope. Hardness was determined using the hand hardness test (Greene et al., 2010). The hardness index described by Greene et al. (2010) was used for surface blast hardness measurements and data analysis (Table 1). After conducting the surface blasts, an index with more sensitivity was desired, so the above hardness

index was modified to include an upper, middle and lower hardness level within each hardness category (Table 2).

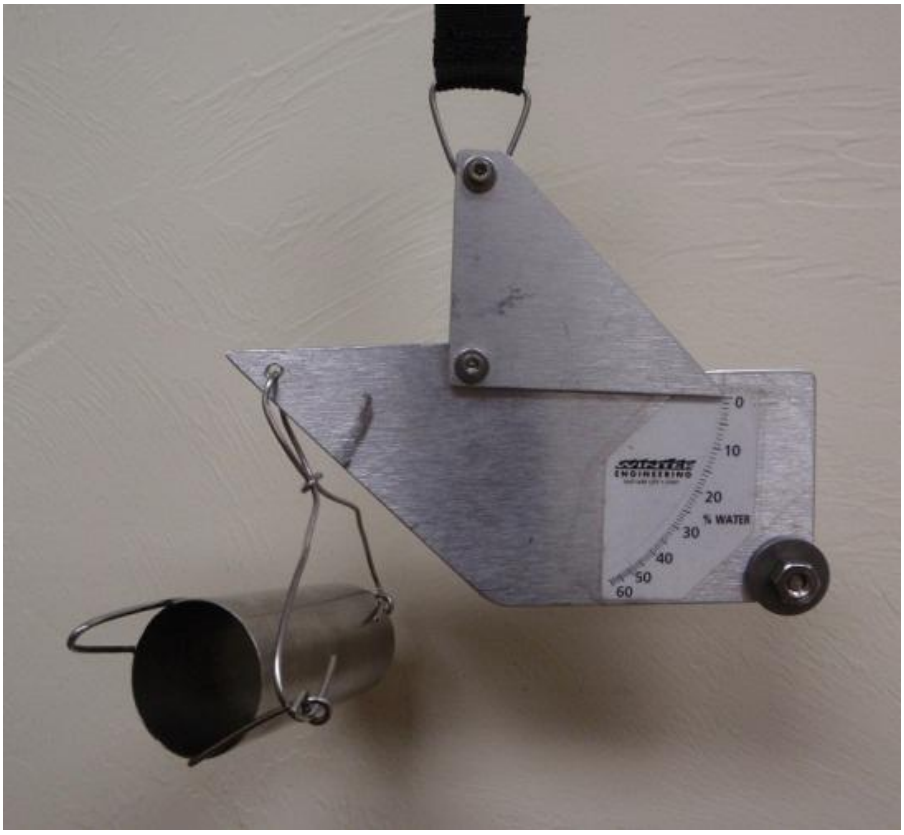

Figure 8: Strong Stitch Density Gauge by Winter Engineering showing the 100 cm^3 cylindrical cutter and the mass balance gauge with a measurement scale of 0-60% water.

Table 1: Hardness Classifications used in determining hand hardness in surface blast tests and assigned numerical codes used to calculate hardness change.

Hardness Code	Hardness	Analysis Code
F	fist	1
4F	4-finger	2
1F	1-finger	3
P	pencil	4
K	knife	5

Table 2: Hardness Classifications used in determining hand hardness in air blasts and assigned numerical codes used to calculate hardness change.

Hardness Code	**Hardness**	**Analysis Code**
F-	softer than fist	1
F	fist	2
F+	harder than fist	3
4F-	softer than 4-finger	4
4F	4-finger	5
4F+	harder than 4-finger	6
1F-	softer than 1-finger	7
1F	1-finger	8
1F+	harder than 1-finger	9
P-	softer than pencil	10
P	pencil	11
P+	harder than pencil	12
K-	softer than knife	13
K	knife	14
K+	harder than knife	15

Compression Tests were performed for 6 of the 8 surface blast detonations. The Compression Test distinguishes weak layers in the snowpack and the relative ease that failure takes place at a particular weak layer interface (Jamieson and Johnston, 1996). The technique for conducting a compression test involves isolating a 30 x 30 cm column to a depth of 100 – 120 cm and tapping on it 30 times. An avalanche shovel blade is placed on top of the column and the taps are applied to the shovel to prevent destruction of the column. The initial 10 taps are light taps from wrist using the fingertips, the next 10 are moderate taps from the elbow using the fingertips and the final 10 taps are hard taps from the shoulder using the palm or fist (Jamieson and Johnston, 1996). The results of a Compression Test include the number of taps at which the column failed, the depth of the layer where failure occurred and the shear quality, or the smoothness, of the failure surface. Changes in CT score and shear quality (Greene et al., 2010) were recorded. For

each of those 6 tests, CTs were conducted at distances of 2 and 3 m from the blast center. Extended Column Tests were not performed during surface blast tests.

Compression Tests were also performed for 25 of the 27 air blast detonations and changes in CT score and shear quality (Greene et al., 2010) were documented. For each of those 25 tests, CTs were conducted at two of the four snowpit locations that were dug at various distances from the blast center. After conducting 9 explosive tests, the locations of CTs were changed from 0.5 m and 1.5 m from the blast center to 1 m and 4 m in order to better explore the spatial changes in snow properties with greater distance from the blast center. Of particular interest were changes in stability test results at a distance close to the blast center (1 m) as compared to those farther away (4 m). Extended Column Tests were conducted at distances of 1 m and 4 m from the blast center in 10 of the 27 air blasts. The procedure for performing Extended Column Tests is the same as for Compression Tests, except the column length is increased to 90 cm, the shovel blade is placed over the end of the column rather than the middle, and the occurrence or absence of propagation is recorded (Simenhois and Birkeland, 2006). ECTs were chosen as an additional stability test because of their ability to provide information about fracture propagation that cannot be obtained through the use of CTs.

In tests of surface blasts, snow hardness was also assessed using a ram penetrometer, or Swiss Rammsonde (Gray and Male, 1981), before and after explosives applications. The ram penetrometer was used as a second measure of snow hardness to provide a more complete profile of pre- and post-blast hardness since it makes continuous measurements throughout the snowpack rather than making intermittent measurements.

Ram hardness was measured before and after explosive detonation at all four distances from the blast center in 7 of the 8 surface blast tests. The ram penetrometer is used to create a vertical snow hardness profile by measuring the force necessary for the ram to penetrate different layers of the snowpack. The ram is a pole or tube with a pointed end that penetrates the snow. Cylindrical hammers are dropped from designated heights and the depth of penetration along with the drop height and numbers of drops are used to calculate the ram hardness at various depths (Gray and Male, 1981). The ram penetrometer had a tube weight of 0.69 kg and was used with a hammer weighing 0.25 kg. In tests of air blasts, ram hardness was not measured. For air blasts, obtaining densities every 10 cm to a depth of 1 m rather than sampling intermittently was considered to be more important than measuring ram hardness since one method of evaluating snow hardness was already being used. Time did not allow for both measurements to be made.

Pre-blast measurements for surface blasts were made in the afternoon the day before conducting the explosives detonations. Explosives were applied in the mornings under the conditions that there was no overnight snowfall or heavy wind. Light to moderate winds were not problematic because the study site used for surface blasts was well protected and not easily affected by wind (Figure 2). At the location of the bamboo marking the intended blast center, a 0.9 kg cast pentolite booster, armed with safety fuse and a number 8 blasting cap, was ignited using a pull-wire igniter and placed on the snow surface with the closed end of the blasting cap oriented in the downward direction. Blasting caps were uniformly oriented in order to eliminate any effects of directional

variation. After explosive detonation, new pit locations were measured from the blast center at the locations previously discussed, snowpits were dug and all pre-blast measurements were repeated as before.

After initial setup and pre-blast measurements were completed in tests of air blasts, a 0.9 kg cast pentolite booster was taped to the bamboo located at the blast center. The center of the booster was positioned exactly 1 m above the snow surface in keeping with current industry standards and with the closed end of the blasting cap oriented in the downward direction. As in the surface blasts, blasting caps were uniformly oriented. After explosive detonation, post-blast pits were excavated and all pre-blast measurements were repeated.

3. DATA ANALYSIS AND LABORATORY TESTS

3.1 Laboratory Comparisons of Density Gauges and Analysis of Laboratory Data

To establish the accuracy and precision of the density gauge used for field measurements, densities were measured and compared using three different methods in a laboratory setting. The Strong Stitch Snow Density Gauge, produced by Winter Engineering (WE) was used for field measurements in this study because of its size, portability, and lack of electronic or battery powered components. It consists of a 100 cm^3 cylindrical cutter and a mass balance scale reading from 0% to 60% water content (Figure 8). The accuracy of the cutter used with a digital scale was documented by Conger and McClung (2009) to be from $\pm$ 1 to 4 %, but they did not establish this for the cutter and mass balance scale together. Therefore, the overall device accuracy and precision were determined for improved interpretation of this study's results.

Accuracy of the WE gauge was tested by comparing the sampled median lab snow density with the bulk density of the lab snow. Precision was determined to be the deviation from the median, or the median absolute deviation (MAD). Accuracy and precision of density measurements taken with the gauge were tested in the Subzero Science and Engineering Research Facility (SSERF) at Montana State University during the summer and fall of 2012. Two separate experiments were conducted in low and medium density snow representative of the snow sampled in the field. Comparison of measurement instruments in low density snow was conducted using new snow made in the cold hydrodynamics chamber in the subzero facility by Dr. Ladean McKittrick, the

facility coordinator, the night before measurements were made. Measurements of medium density snow were made in laboratory-made snow that had been stored for approximately 2-4 weeks. Density measurements were performed in the same manner in both types of snow.

Prior to taking any densities, the snow was prepared for testing to ensure uniformity. Initially, it was sifted into a box. The inner box dimensions were measured and snow height was recorded. Snow did not completely fill the box due to snow availability, but snow depths in the box were adequate for sampling. The box was weighed to establish the bulk snow density and turned on its side to simulate a snowpit wall. Thirty snow densities were taken in the low density snow using three different methods resulting in a total of ninety densities. In the medium density snow, twenty-nine densities per method were sampled resulting in a total of 87 measurements. Density cutters that would fit within layers of snow 10 cm deep were chosen so that theoretically they could be used within the field sampling design. The first two density measurement methods used the same sample obtained with the 100 cm^3 cylindrical cutter from the Winter Engineering gauge. The sample was initially weighed with the included mass balance and then with a digital scale. The third method employed the use of a 200 cm^3 triangular cutter and the same digital scale as used previously with the 100 cm^3 cutter (Figure 9). The digital scale used was an Acculab vic-4kg with a 1 gram (g) resolution. For each snow sample obtained using the cylindrical cutter, an adjacent density was taken using the triangular cutter. All densities were sampled with the long axis of the cutters oriented horizontally.

The Kruskal-wallis test, a nonparametric analysis of variance test for equal medians (Kruskal and Wallis, 1952), was used to check for a median difference between the three sampling methods. This nonparametric test was used because data distributions were non-normal. The interquartile range and the median absolute deviation were determined for each density measurement method.

Figure 9: The 200 cm^3 triangular cutter with lid. The triangular base is pushed into a snow layer and the lid is slid over the top to cut the snow.

3.2 Analysis of Field Data

All air blast and surface blast data were visually analyzed, but statistical tests were only performed on air blast data due to the small sizes of the surface blast data sets (Table 3). Initial analysis of density, hardness and CT data from both surface and air blasts was undertaken by comparing median changes displayed in box and whisker plots. ECT data from air blasts was also examined using the same method. Because compaction occurred in the blast region, pre- and post-blast snow heights changed in the

pits close to the blast center. This necessitated matching pre- and post-blast measurements for data analysis. In both surface and air blasts, snow was compacted in the locations of the pre- and post-blast pits rather than being displaced or removed. In surface blasts, pits were far enough away from the blast center that some snow and soot were dislocated from the crater to the planned locations of the post-blast pits, but snow was not removed from the sites of the pre- or post-blast pits. After air blasts, a depression around the blast center could be seen to distances of 1.5 m from the blast center, but snow had not been removed or displaced from the area near the blast center or the pit locations. This reinforces the concept of decreasing snow height after a blast due to compaction rather than snow displacement or removal. Because of this compaction and because air blast and surface blast data showed similar characteristics, surface down matching of measurements, as opposed to ground up matching, was considered to be most appropriate.

Percent change in density data and hardness change data were analyzed in 10 cm increments using the 10 cm increments used in data collection. Each 10 cm increment was considered a separate layer. Before- and after-blast density and hardness measurements were compared by using the snow surface as a measurement reference and matching pre- and post-blast observations down to 1 m. The per layer data of percent change in density from the 8 surface blast explosions were matched from the surface down and not from the ground up, because pairing them from the ground up resulted in a loss of measurements below a depth of 50 cm. Since measurements were not made every 10 cm below a depth of 50 cm, the before- and after-blast measurements at depths of 70-

80 cm and 90-100 cm were offset when paired from the ground up in cases where snow height decreased after a blast. If snow height remained the same or if measurements were matched from the snow surface down, this offset did not occur. Air blast measurements were paired from both the snow surface down and the ground up. Data were examined to determine whether the same trends were present. This additional analysis was undertaken to ensure that the results were not a product of methodology, and that similar trends could be replicated regardless of the starting point for comparison of the pre- and post-blast density and hardness of individual layers as discussed above. Changes in CT and ECT score were examined by comparing the number of pre-and post-blast taps at column failure. Changes in CT shear quality from air blasts were also compared using box and whisker plots. Box and whisker plots show the median line, the interquartile range (IQR) representing the middle 50% of the data as boxes, and include data out to 1.5 IQRs within the whiskers. CT shear quality from surface blast tests was not evaluated due to the limited amount of data.

Pre- and post-blast ram hardness profiles were created and compared to further examine changes in hardness as a result of surface blasts. These profiles were also used to verify proper matching of measurements from the snow surface down.

Preliminary analysis of air blast data was undertaken to determine whether parametric statistical methods were appropriate. Surface blast data were not tested for statistical significance due to the small sizes of the data sets (n=8). Data for each air blast parameter was analyzed using an appropriate method of statistical analysis (Table 3).

Table 3: Statistical analysis performed on each parameter for air blasts. Boxes that include an 'x' indicate analysis with the listed method.

Parameter	**Test Type**		
	Boxplots	Wilcoxon sign-rank	Bootstrapped 95% confidence interval for the mean
Percent change in density	x	x	x
Hardness	x		x
CT score	x	x	
ECT Score	x	x	
CT shear quality	x		

Air blast density data deviated from normality as demonstrated by histograms and normal probability plots; and Lillefors tests of normality indicated non-normal distributions. Therefore, the Wilcoxon sign-rank test, a nonparametric comparison test (Wilcoxon, 1945), was used to test for a statistically significant change in both snow density and CT score at the 5% significance level ($p=0.05$). CT score data included outliers and displayed non-normal distributions in histograms and normal probability plots. Therefore, these data were also appropriate for analysis with the Wilcoxon sign-rank test. Hardness data were highly skewed with the lower ends of the distributions lying on the medians in many cases, thereby violating the assumption of symmetry required by the Wilcoxon test.

Bootstrapping (Efron and Tibshirani, 1993) was used for analysis of air blast hardness data to produce a theoretical population distribution from which parametric statistics were obtained. Density data was bootstrapped to provide a more complete analysis. The techniques used here involve randomly sampling the existing data sets, with replacement, to create 5000 new data sets from which 95% confidence intervals were constructed for mean changes in hardness and density. The BCA, or bias corrected

and accelerated method of bootstrapping, was utilized for its ability to better approximate the endpoints of the confidence intervals and to correct for non-normal distributions (Higgins, 2004). The 5% significance level and bootstrapped sample sizes of 5000 used here are within limits established by Higgins (2004), who recommends using a confidence interval of 90% or 95% and between 1000 – 5000 bootstrap samples. These sample sizes are also well above the minimum sample size of 1000 established by Efron and Tibshirani (1993).

In addition, the relationship between initial snow density and percent change in density was examined for air blast measurements matched from the snow surface down. A single term power function was fit to the data for each depth and each distance from the blast center. Other functions were also tested to assess for best fit. For each fitted function, R^2, standard squared error (SSE) and root mean squared error (RMSE) were computed to assess model fit.

4. RESULTS

4.1 Surface Blasts

Data from surface blasts conducted at Snowmass Ski Area show increases in density at the snow surface (depth of 0-10 cm) out to 3 m from the blast center. Below a depth of 10 cm only two locations exhibit density increases larger than 10%. These occur at a depth of 10-20 cm and a distance of 2 m from the blast center and at a depth of 20-30 cm and a distance of 2.5 m from the blast center (Figure 10). Aside from the changes at the snow surface, density change follows no apparent pattern. Because data sets consisted of 8 or fewer measurements for each distance in each layer, statistical tests were not conducted.

Pre- and post-blast hardness data show no median change in the upper snowpack at all distances from the blast center and very little to no median change at depths below 40 cm. While still small, the greatest hardness changes were observed at a depth of 90-100 cm and a distance of 5.5 m from the blast center (Figure 11). Hardness change was not tested for statistical significance because median values were extremely close to zero and because the data set only consisted of 8 measurements at each location.

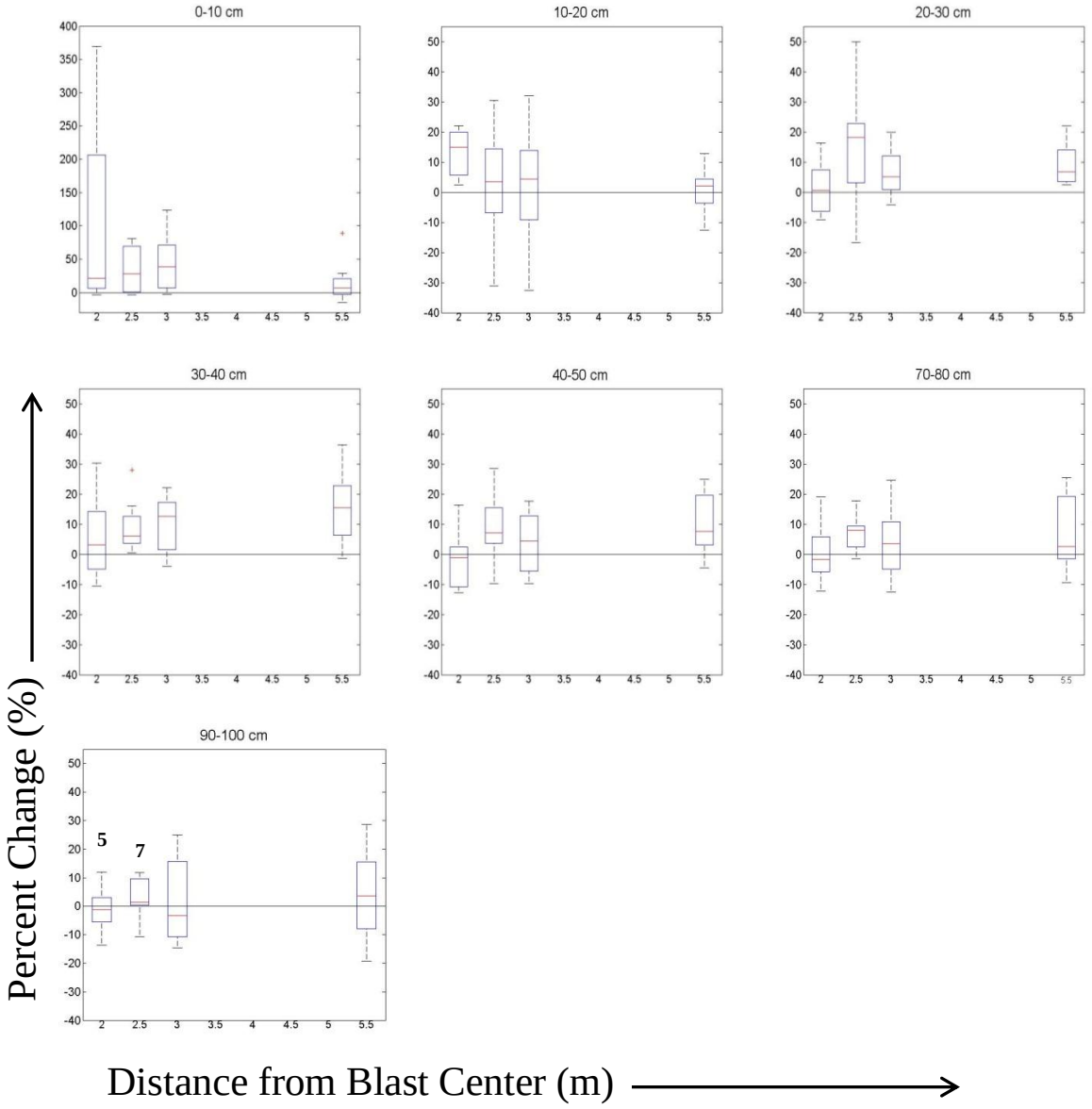

Figure 10: Box and whisker plots showing percent change in density for each distance and depth for surface blast data matched from the **snow surface down**. Each plot is labeled at the top to indicate the depth. Values on the y-axis represent percent change (from +50 to -40%) and values on the x-axis represent distance from the blast center in meters (from 2 to 5.5 m). On each box, the line is the median, the edges of the box are the interquartile range (IQR) representing the middle 50% of the data and the whiskers extend to 1.5 IQRs. Outliers are represented by plus signs. The 0-10 cm plot is scaled differently than the other plots because percent increases were much greater at this depth. Sample sizes are n = 8 except at a depth 90-100 cm where sample size is indicated above the plots.

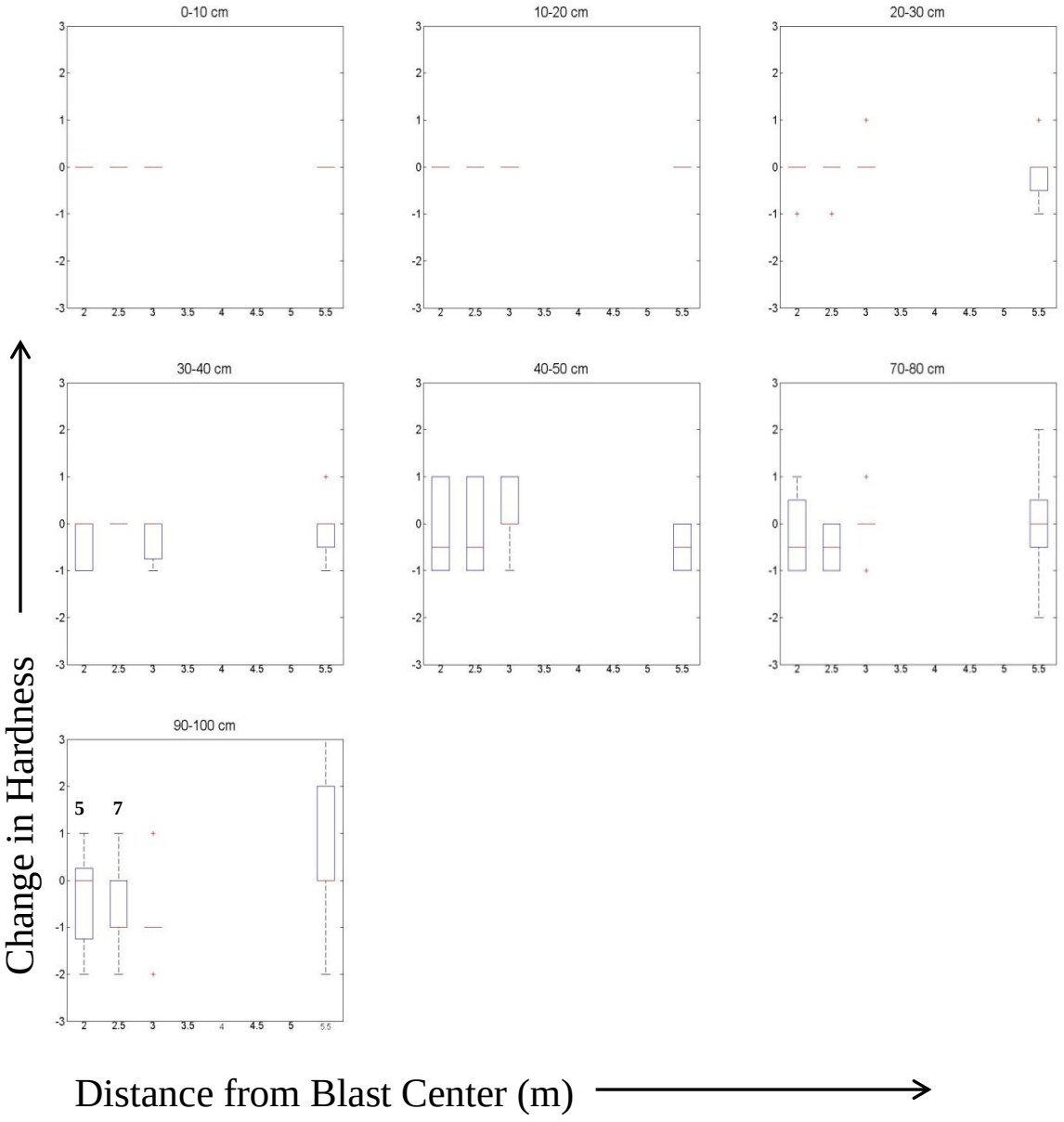

Figure 11: Box and whisker plots showing change in hardness for each distance and depth for surface blast data matched from the **snow surface down**. Each plot is labeled at the top to indicate the depth. Values on the y-axis represent change in hardness (from +3 to -3) (Table 1) and values on the x-axis represent distance from the blast center in meters (from 2 to 5.5 m). On each box, the line is the median, the edges of the box are the interquartile range (IQR) representing the middle 50% of the data and the whiskers extend to 1.5 IQRs. Outliers are represented by plus signs. Sample size is 8 except at 3 m from the blast center where n =7 due to sampling error and at a depth of 90-100 cm where sample size is indicated above the plots.

Ram hardness profiles did not display strong evidence for or against changes in hardness (Figures 12-15; Table 4; Appendix Figures A1-A21). Of the 21 profiles used to evaluate hardness change, 9 profiles showed increasing hardness, 7 showed decreasing hardness, 2 indicated both increases and decreases, and 3 showed no change. The profiles were also used to evaluate the validity of surface down measurement matching and indicated that layer matching benefitted from using the snow surface as a measurement reference rather than the ground (Figures 12-15; Table 4; Appendix Figures A1-A21). Before- and after-blast snow height data was available for 21 of the surface blast ram profiles. Of these profiles, 9 showed a 0-3 cm decrease in snow height, 7 showed a decrease of 4-8 cm and 5 showed a change of 9 cm or more. Of the 9 profiles with no change, 6 showed poor pre- and post-blast layer matching that was not improved by correcting for decreases in snow height and 3 showed reasonable layer alignment with no correction. Of the 7 profiles where height decreased 4-8 cm, 4 displayed satisfactory alignment of layers with no height adjustment (Figure 12), 2 were better aligned with adjustment and 1 had poor matching which could not be improved with height adjustments (Figure 13). Of the 5 profiles where snow height decreased by 9 or more cm, 2 profiles showed adequate alignment of layers with no height adjustment (Figure 14) and 3 benefitted from a small height adjustment that did not compensate for the total decrease in snow height (Figure 15).

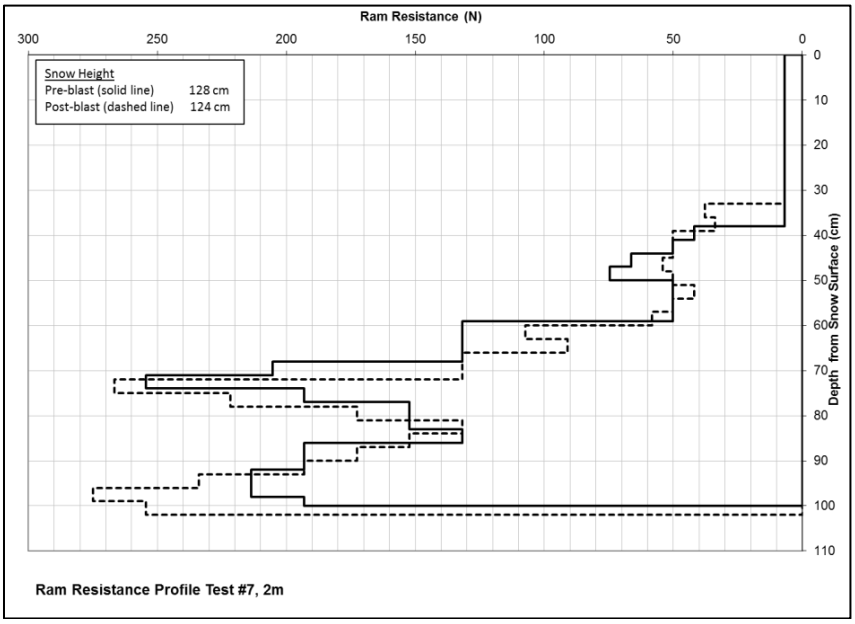

Figure 12: Pre-blast (bold line) and post-blast (dashed line) ram resistance profiles showing ram resistance in newtons along the x-axis versus depth in cm along the y-axis. This profile shows good alignment of layers with no adjustment for the 4 cm decrease in post-blast snow height. Decreases in ram resistance are visible at shallower depths while an increase in resistance is evident at a depth of approximately 90-100 cm.

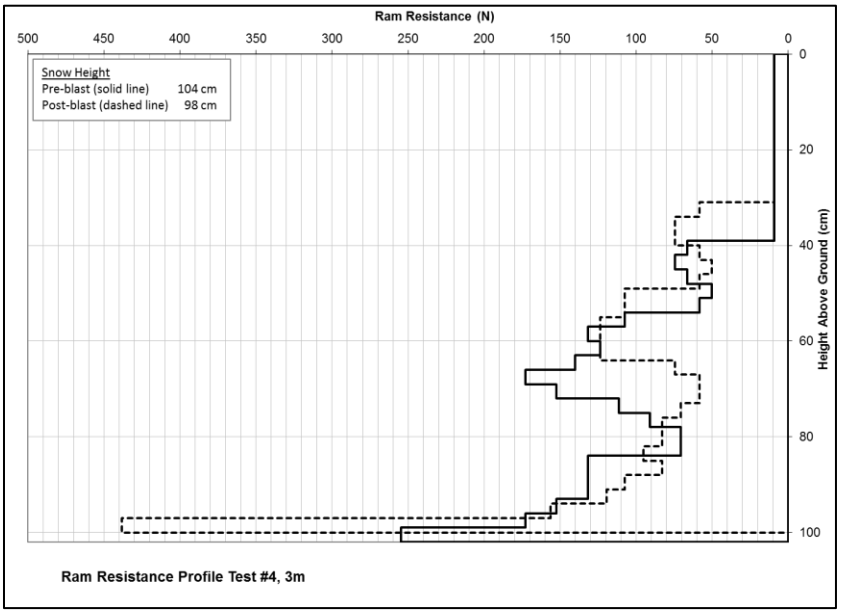

Figure 13: Pre-blast (bold line) and post-blast (dashed line) ram resistance profiles showing ram resistance in newtons along the x-axis versus depth in cm along the y-axis. This profile shows pre- and post-blast layers with poor alignment when not adjusted for the 6 cm decrease in post-blast snow height. With layers better aligned, there appears to be a decrease in hardness in the middle of the profile and a possible increase near a depth of 1 m.

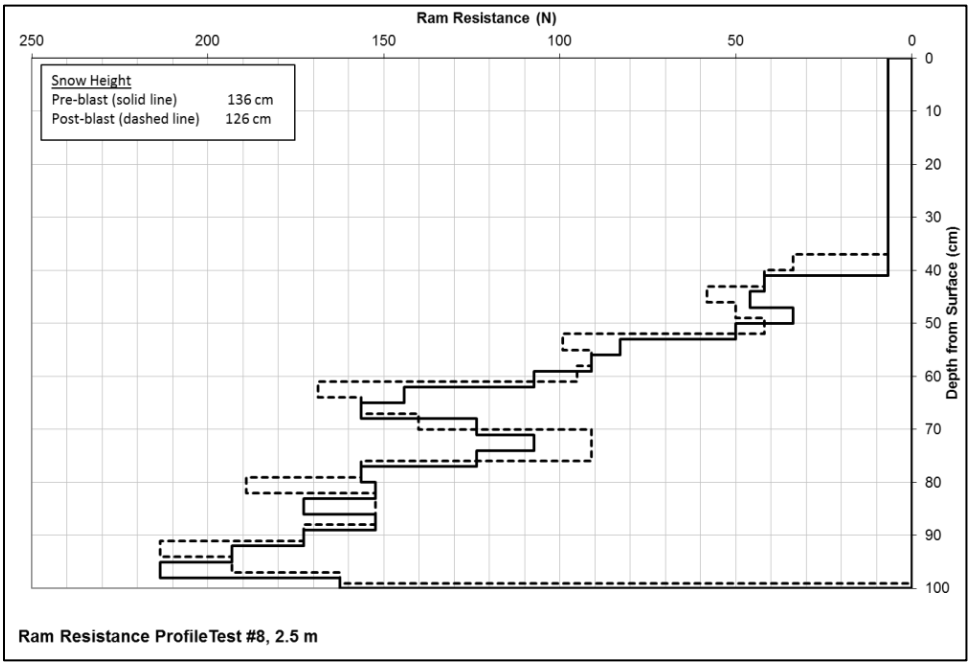

Figure 14: Pre-blast (bold line) and post-blast (dashed line) ram resistance profiles showing ram resistance in newtons along the x-axis versus depth in cm along the y-axis. This profile shows good alignment of layers with no adjustment for the 10 cm decrease in post-blast snow height. This profile indicates small increases in hardness at various depths.

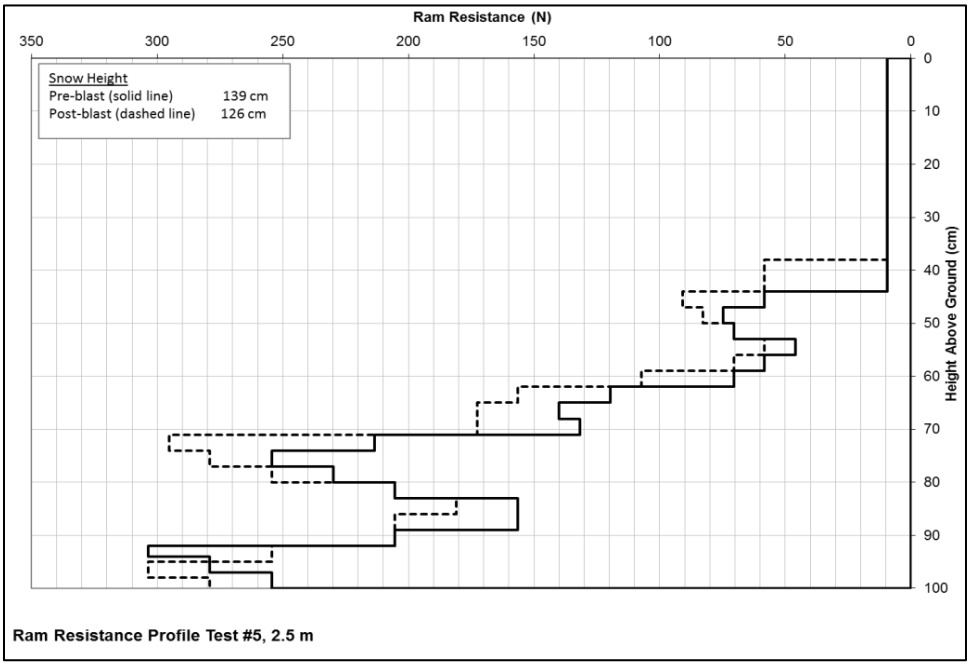

Figure 15: Pre-blast (bold line) and post-blast (dashed line) ram resistance profiles showing ram resistance in newtons along the x-axis versus depth in cm along the y-axis. Layer alignment would be improved with a partial height adjustment. This profile shows increases in hardness at various depths.

Table 4: Pre- and post-blast layer alignment from 21 Ram Resistance profiles. Only 4 profiles displayed improved layer alignment when post-blast profiles were adjusted to account for some or all of the decrease in snow height.

	Decrease in snow surface height		
Number of ram resistance profiles with:	**0-3 cm**	**4-8 cm**	**≥ 9 cm**
good alignment; no adjustment needed	2	4	3
poor alignment; no improvement with adjustment	7	1	0
improved alignment with partial height adjustment	0	0	2
improved alignment with full height adjustment	0	2	0

Compression Test results show a slight decrease in median CT score after a blast at locations 2 m from the blast center. Data from CTs show no median change in CT score with the interquartile range also being zero (Figure 16).

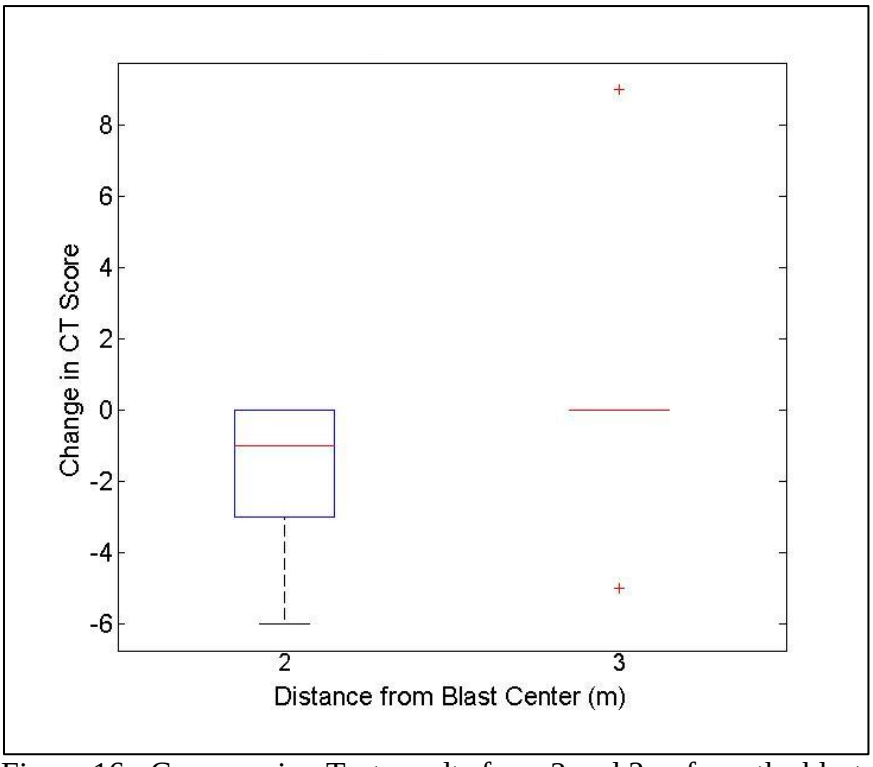

Figure 16: Compression Test results from 2 and 3 m from the blast center for 6 surface blasts. On each box, the red line is the median, the edges of the box are the interquartile range (IQR) representing the middle 50% of the data and the whiskers extend to 1.5 IQRs. Outliers are represented by plus signs. The line representing the 3 m data indicates that the IQR at this location equals zero.

4.2 Air Blasts

Density change measurements matched both from the snow surface down (Figure 17) and the ground up (Figure 18), indicate density increases at locations that are both near the blast center and the snow surface. Results from statistical tests of data matched from the surface down indicate that density increases significantly in the region extending out to a distance of 1.5 m from the blast center and down to a depth of 60 cm below the snow surface (Table 5). Statistically significant increases in density also occurred out to a distance of 4 m at the snow surface (down to 20 cm) (Table 5). Significant density increases are also evident deeper in the snowpack out to 1.5 m from the blast center (Table 5). In addition, statistical tests of percent change in density data matched from the ground up show statistically significant increases in density, but to a smaller extent than surface down data (Table 6).

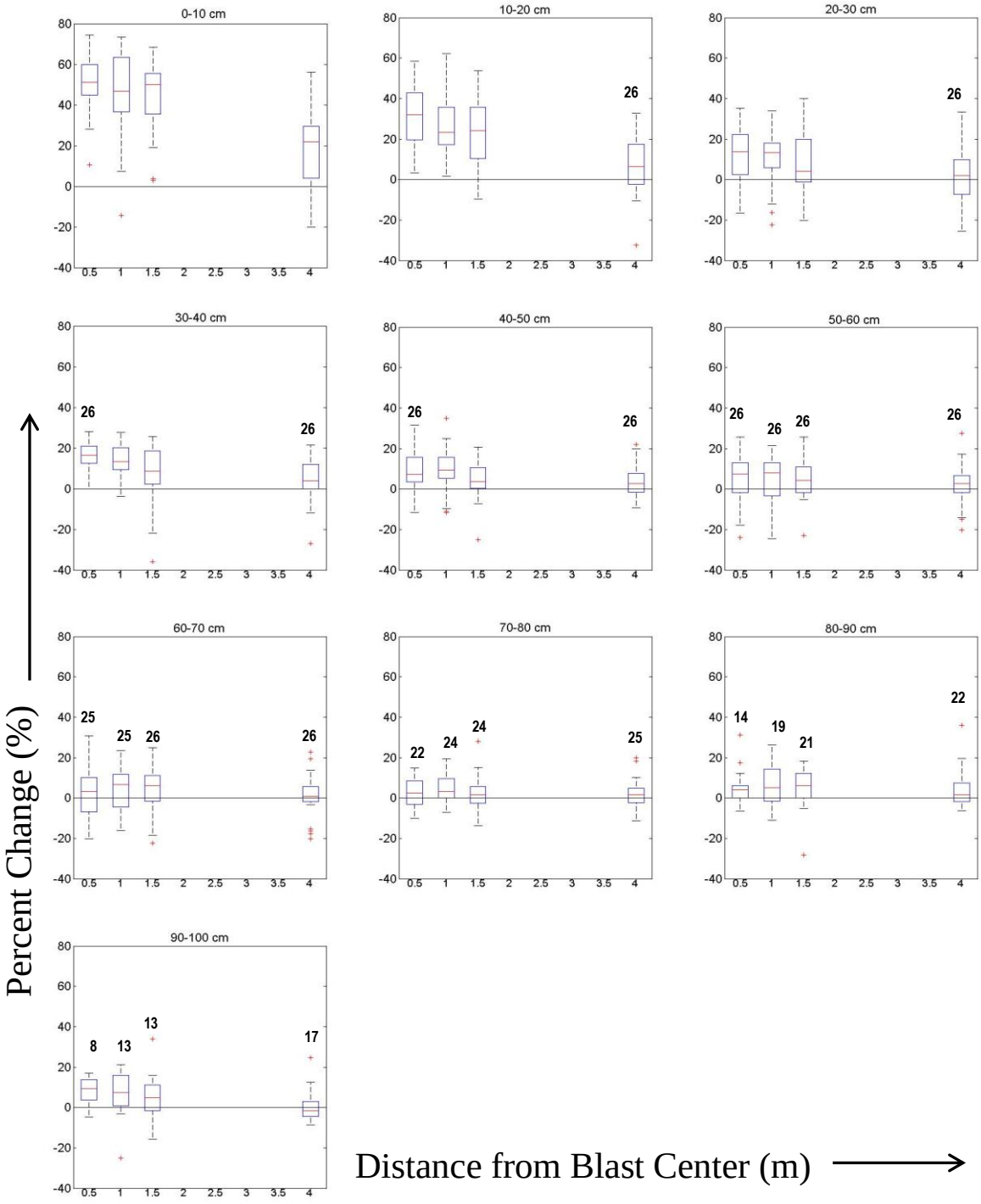

Figure 17: Box and whisker plots showing percent change in density for each distance and depth for air blast data measurements matched from the **snow surface down**. Each plot is labeled at the top to indicate the depth. Values on the y-axis represent percent change (from +80 to -40%) and values on the x-axis represent distance from the blast center in meters (from 0.5 to 4 m). On each box, the line is the median, the edges of the box are the interquartile range (IQR) representing the middle 50% of the data and the whiskers extend to 1.5 IQRs. Outliers are represented by plus signs. Sample size is 27 except where indicated by a number above the plot. Small sample sizes are a result of snow compaction or shallow snow cover.

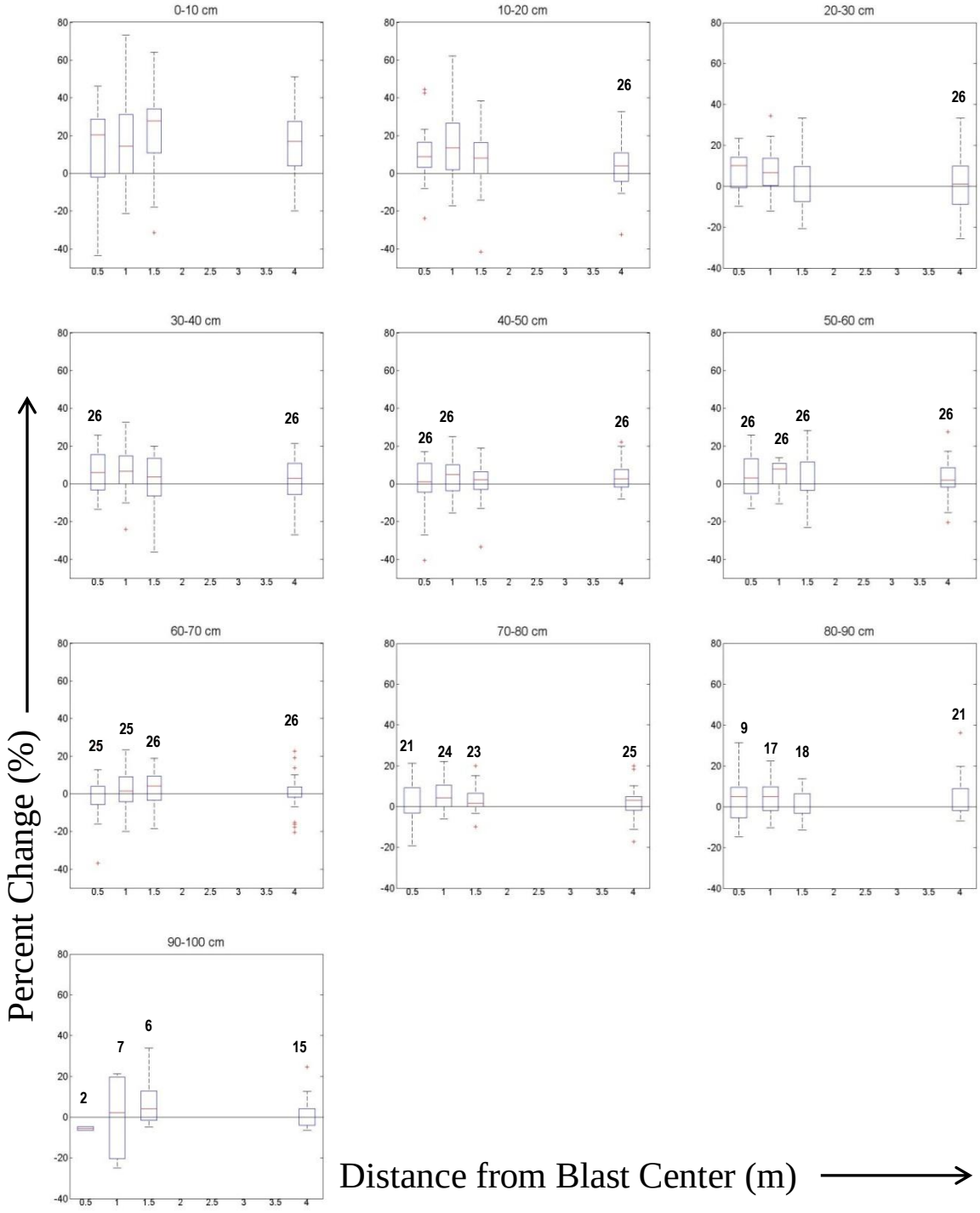

Figure 18: Box and whisker plots showing percent change in density for each distance and depth for air blast data measurements matched from the **ground up**. Each plot is labeled at the top to indicate the depth. Values on the y-axis represent percent change (from +80 to -50%) and values on the x-axis represent distance from the blast center in meters (from 0.5 to 4 m). On each box, the line is the median, the edges of the box are the interquartile range (IQR) representing the middle 50% of the data and the whiskers extend to 1.5 IQRs. Outliers are represented by plus signs. Sample size is 27 except where indicated by a number above the plot.

Table 5: P values generated from the Wilcoxon sign-rank test, testing percent change in density data from air blasts for a median of zero. P values less than 0.05 are shaded and indicate a statistically significant change in density. Layers are matched from the **snow surface down**. Data sets contain 27 measurements except where indicated. Small sample sizes are a result of snow compaction or shallow snow cover.

Distance→ Depth↓	**0.5m**	**1m**	**1.5m**	**4m**
0-10cm	5.6×10^{-6}	5.5×10^{-6}	5.6×10^{-6}	1.1×10^{-4}
10-20cm	5.6×10^{-6}	5.6×10^{-6}	3.0×10^{-5}	1.5×10^{-2} (n=26)
20-30cm	1.6×10^{-4} (n=26)	2.3×10^{-3}	1.8×10^{-2}	0.6 (n=26)
30-40cm	1.2×10^{-5} (n=26)	9.8×10^{-6}	1.4×10^{-2}	5.3×10^{-2} (n=26)
40-50cm	2.5×10^{-4} (n=26)	2.2×10^{-3}	3.4×10^{-3}	2.6×10^{-2} (n=26)
50-60cm	5.0×10^{-2} (n=26)	1.8×10^{-2} (n=26)	1.2×10^{-2} (n=26)	9.3×10^{-2} (n=26)
60-70cm	0.5 (n=25)	6.7×10^{-2} (n=25)	7.1×10^{-2} (n=26)	0.3 (n=26)
70-80cm	0.2 (n=22)	1.5×10^{-2} (n=24)	0.4 (n=24)	0.4 (n=25)
80-90cm	2.4×10^{-2} (n=14)	3.0×10^{-2} (n=19)	1.1×10^{-2} (n=21)	7.7×10^{-2} (n=22)
90-100cm	2.3×10^{-2} (n=8)	8.0×10^{-2} (n=13)	0.1 (n=13)	1.0 (n=17)

Table 6: P values generated from the Wilcoxon sign-rank test, testing percent change in density data from air blasts for a median of zero. P values less than 0.05 are shaded and indicate a statistically significant change in density. Measurements are matched from the **ground up**. Data sets contain 27 measurements except where indicated. Small sample sizes are a result of snow compaction or shallow snow cover.

Distance→ Depth↓	**0.5m**	**1m**	**1.5m**	**4m**
0-10cm	8.8×10^{-3}	2.1×10^{-3}	1.9×10^{-4}	1.5×10^{-4} (n=26)
10-20cm	6.0×10^{-4}	1.9×10^{-3}	2.1×10^{-2}	0.1 (n=26)
20-30cm	3.4×10^{-4}	1.9×10^{-3}	0.9	0.9 (n=26)
30-40cm	1.2×10^{-2} (n=26)	3.6×10^{-3}	0.2	0.2 (n=26)
40-50cm	0.3 (n=26)	0.1 (n=26)	0.2	2.9×10^{-2} (n=26)
50-60cm	0.1 (n=26)	8.6×10^{-4} (n=26)	0.2 (n=26)	0.1 (n=26)
60-70cm	0.7 (n=25)	0.5 (n=25)	0.1 (n=26)	0.6 (n=26)
70-80cm	0.3 (n=21)	3.6×10^{-3} (n=24)	6.8×10^{-2} (n=23)	0.3 (n=25)
80-90cm	0.4 (n=9)	3.5×10^{-2} (n=17)	0.5 (n=18)	0.2 (n=21)
90-100cm	*(n=2)	*(n=7)	*(n=6)	0.7 (n=15)

Bootstrapping the density data matched from the snow surface down resulted in 95% confidence intervals for the mean percent increase in density at each sampled location. Mean percent increases in density occurred in a continuous area down to a depth of 50 cm and out to a distance of 1.5 m from the blast center. On the surface (down to 20 cm), mean density increases were observed out to a distance of 4 m from the blast center (Table 7). Deeper in the snowpack there were also mean increases in snow density. These percent increases occurred from a depth of 80-100 cm at a distance of 0.5 m from the blast center, from a depth of 70-90 cm 1 m from the blast center, from 90-100 cm in depth at a distance of 1.5 m from center and from a depth of 80-90 cm 4 m from center.

Bootstrapped 95% confidence intervals for density data matched from the ground up also show statistically significant percent increases in mean density, indicated by confidence intervals that exclude 0, in a continuous region extending out from the blast center to a distance of 1 m and down to a depth of 40 cm (Table 8). At distances of 1.5 m and 4 m from the blast center density increases only occurred at the surface (down to a depth of 20 cm). At depths of 70-100 cm and distances of 1 and 1.5 m from the blast center there were also increases in density, although they did not occur in a continuous region.

Table 7: Bootstrapped 95% confidence intervals for mean percent change in density calculated from 5000 resampled data sets for air blast data measurements matched from the **snow surface down**. Boxes are shaded to illustrate the distances and depths where the 95% confidence interval for mean percent increase in density does not include zero, indicating that there was a statistically significant increase in density at these locations. Sample size is 27 except where indicated next to the sample mean.

Depth↓ Distance→	**0.5m**		**1m**		**1.5m**		**4m**	
	sample mean	**95% CI**	**sample mean**	**95% CI**	**sample mean**	**95% CI**	**sample mean**	**95% CI**
0-10 cm	52	46 - 56	45	36 - 52	45	38 - 50	20	13 - 27
10-20 cm	32	26 - 37	27	23 - 33	24	17 - 30	7.1 (n=26)	1.4 - 12
20-30 cm	14	8.7 - 18	10	4.7 - 15	7.1	2.0 - 13	1.8 (n=26)	-2.9 - 6.9
30-40 cm	16 (n=26)	13 - 18	14	10 - 17	6.9	0.4 - 12	3.9 (n=26)	-0.7 - 7.7
40-50 cm	9.4 (n=26)	5.6 - 13	8.9	4.6 - 13	4.7	0.8 - 7.6	3.9 (n=26)	1.1 - 7.2
50-60 cm	4.4 (n=26)	-2.0 - 9.2	4.7 (n=26)	-0.1 - 8.3	4.6 (n=26)	0.5 - 8.0	2.7 (n=26)	-1.2 - 6.3
60-70 cm	2.0 (n=25)	-2.3 - 6.8	4.1 (n=25)	-0.3 - 8.2	4.3 (n=26)	-0.5 - 8.5	0.9 (n=26)	-3.2 - -4.6
70-80 cm	2.1 (n=22)	-0.6 - 5.2	4.1 (n=24)	1.3 - 6.9	2.0 (n=24)	-1.0 - 5.9	-0.1 (n=25)	-8.0 - 3.5
80-90 cm	6.0 (n=14)	2.3 - 12	6.6 (n=19)	2.4 - 11	4.5 (n=21)	-1.1 - 7.8	4.8 (n=22)	-1.6 - 11
90-100 cm	8.2 (n=8)	2.9 - 12	6.2 (n=13)	-2.3 - 11	5.3 (n=13)	-0.2 - 13	1.0 (n=17)	-2.0 - 6.1

Table 8: Bootstrapped 95% confidence intervals for mean percent change in density calculated from 5000 resampled data sets for air blast data measurements matched from the **ground up**. Boxes are shaded to illustrate the distances and depths where the 95% confidence interval for mean percent increase in density does not include zero, indicating that there was a statistically significant increase in density at these locations. Sample size is 27 except where indicated next to the sample mean.

Distance→ Depth↓	**0.5m**		**1m**		**1.5m**		**4m**	
	sample mean	**95% CI**	**sample mean**	**95% CI**	**sample mean**	**95% CI**	**sample mean**	**95% CI**
0-10 cm	13	3.4 - 21	18	9.3 - 28	23	13 - 31	16 (n=26)	10 - 21
10-20 cm	10	5.2 - 16	13	6.9 - 21	7.1	0.6 - 13	1.8 (n=26)	-7.4 - 7.5
20-30 cm	7.9	4.5 - 11	7.3	3.5 - 12	0.7	-3.9 - 5.7	0.3 (n=26)	-4.8 - 5.6
30-40 cm	5.7 (n=26)	1.8 - 9.7	7.6	3.0 - 12	2.5	-3.0 - 6.9	2.5 (n=26)	-1.9 - 6.8
40-50 cm	0.6 (n=26)	-5.6 - 4.7	3.3 (n=26)	-0.4 - 7.3	1.9	-2.8 - 5.4	3.9 (n=26)	1.2 - 7.2
50-60 cm	4.1 (n=26)	0.1 - 8.6	5.8 (n=26)	2.9 - 8.0	3.4 (n=26)	-0.7 - 7.7	2.6 (n=26)	-1.2 - 6.3
60-70 cm	-1.1 (n=25)	-6.0 - 2.9	2.1 (n=25)	-1.8 - 6.3	2.7 (n=26)	-1.2 - 6.2	0.5 (n=26)	-3.5 - 4.2
70-80 cm	1.9 (n=21)	-1.7 - 5.8	5.6 (n=24)	2.8 - 8.8	2.8 (n=23)	0.6 - 5.9	-0.3 (n=25)	-8.0 - 3.5
80-90 cm	5.0 (n=9)	-2.6 - 14	5.4 (n=17)	1.6 - 9.7	1.0 (n=18)	-2.3 - 4.1	4.5 (n=21)	0.9 - 10
90-100 cm	* (n=2)	N/A	* (n=7)	N/A	* (n=6)	N/A	1.9 (n=15)	-1.3 - 7.0

Greater percent increases in density are seen both closer to the surface and when initial densities are lower (Figures 19-21). At the snow surface (to a depth of 20 cm) out to a distance of 1.5 m from the blast center, a power function was somewhat successful in modeling the relationship between initial density and change in density (as a %). In this region, between 50% and 70% of the variation in the data could be explained using a single term power function (Table 9; Equation 1).

Equation 1: $$f(x) = a \times x^b$$

Below a depth of 20 cm, power function fits were poor except at a depth of 90-100 cm at farther distances from the blast center. Linear, quadratic, exponential and rational fits were also tested with this data. Fits were poor for all functions except a linear function (Equation 2).

Equation 2: $$f(x) = mx + b$$

A linear fit was capable of explaining between 54% and 79% of the variation in the data out to a distance of 1.5 m from the blast center and down to a depth of 20 cm (Table 9). A linear fit returned R^2 values above 0.5 for all distances at a depth of 50-60 cm and from 60-80 cm at a distance of 0.5 m from the blast center (Table 9).

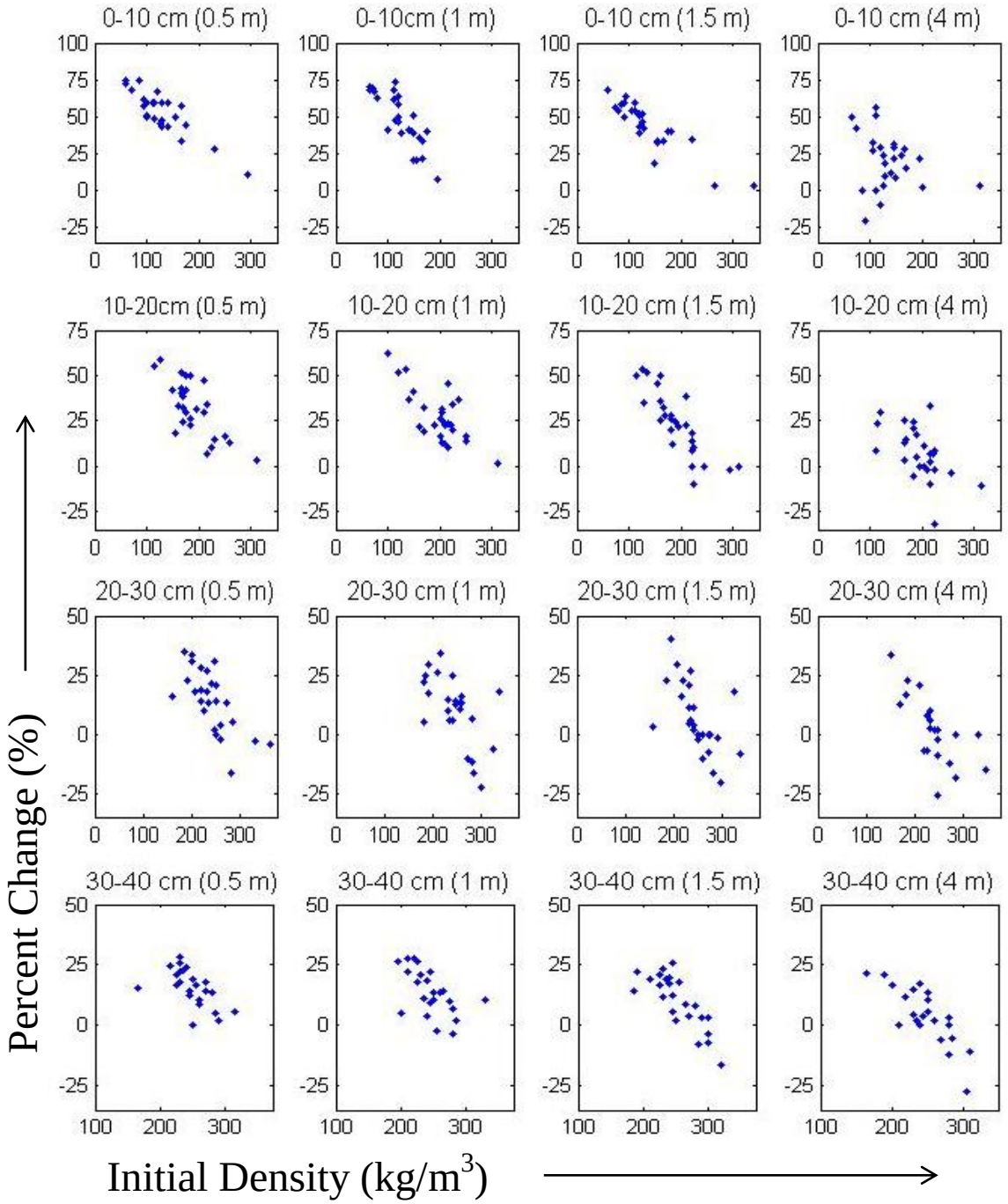

Figure 19: Percent change in density data versus initial density data from air blasts at each distance from center for depths from 0 – 40 cm. Each plot is labeled at the top to indicate the depth and the distance from the blast center. Values on the x-axis represent initial density in kg/m^3 and y-axis values represent percent change in density. Both x and y axes are scaled the same for each depth.

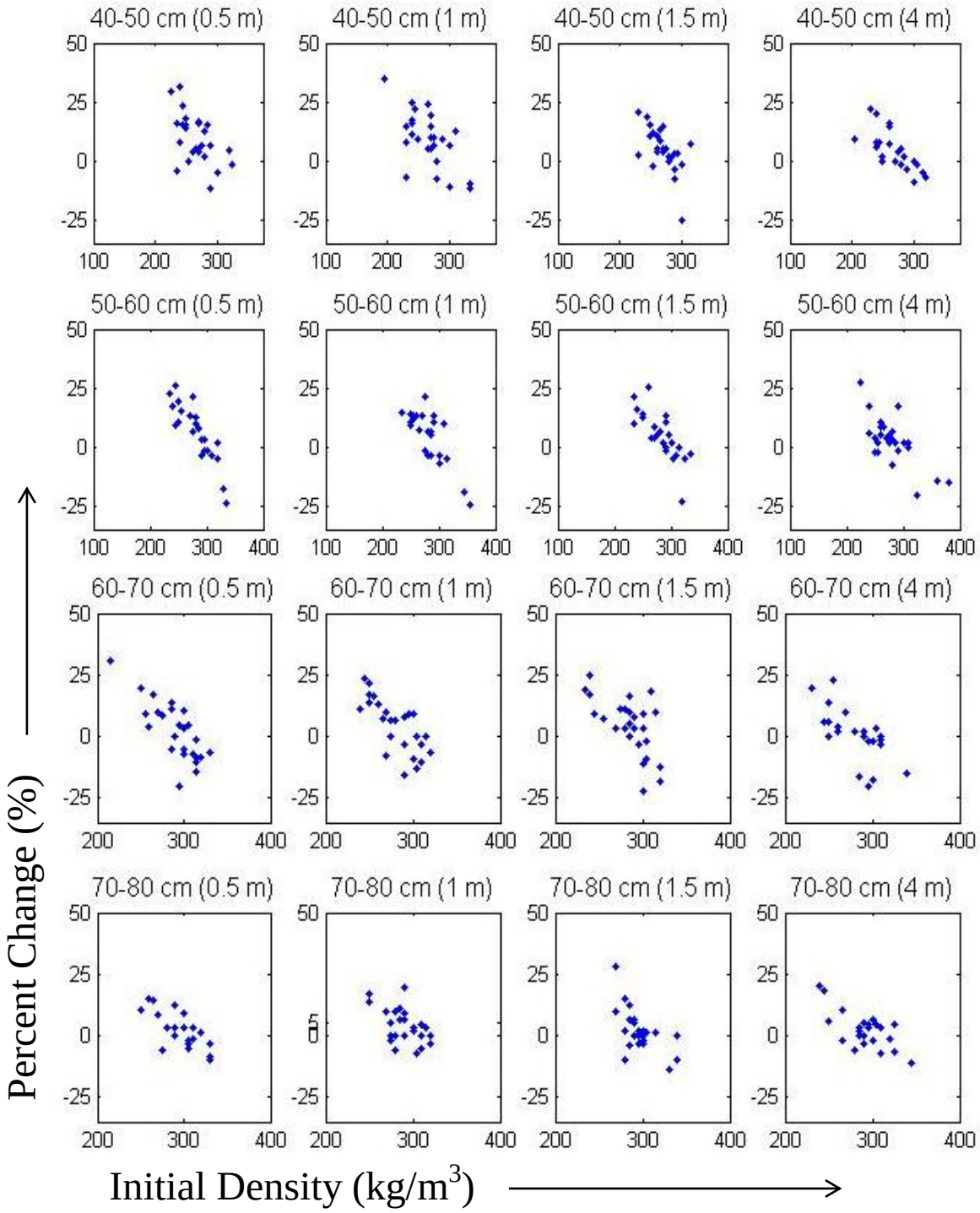

Figure 20: Percent change in density data versus initial density data at each distance from center for depths from 40 – 80 cm. Each plot is labeled at the top to indicate the depth and the distance from the blast center. Values on the x-axis represent initial density in kg/m^3 and y-axis values represent percent change in density. Both x and y axes are scaled the same for each depth.

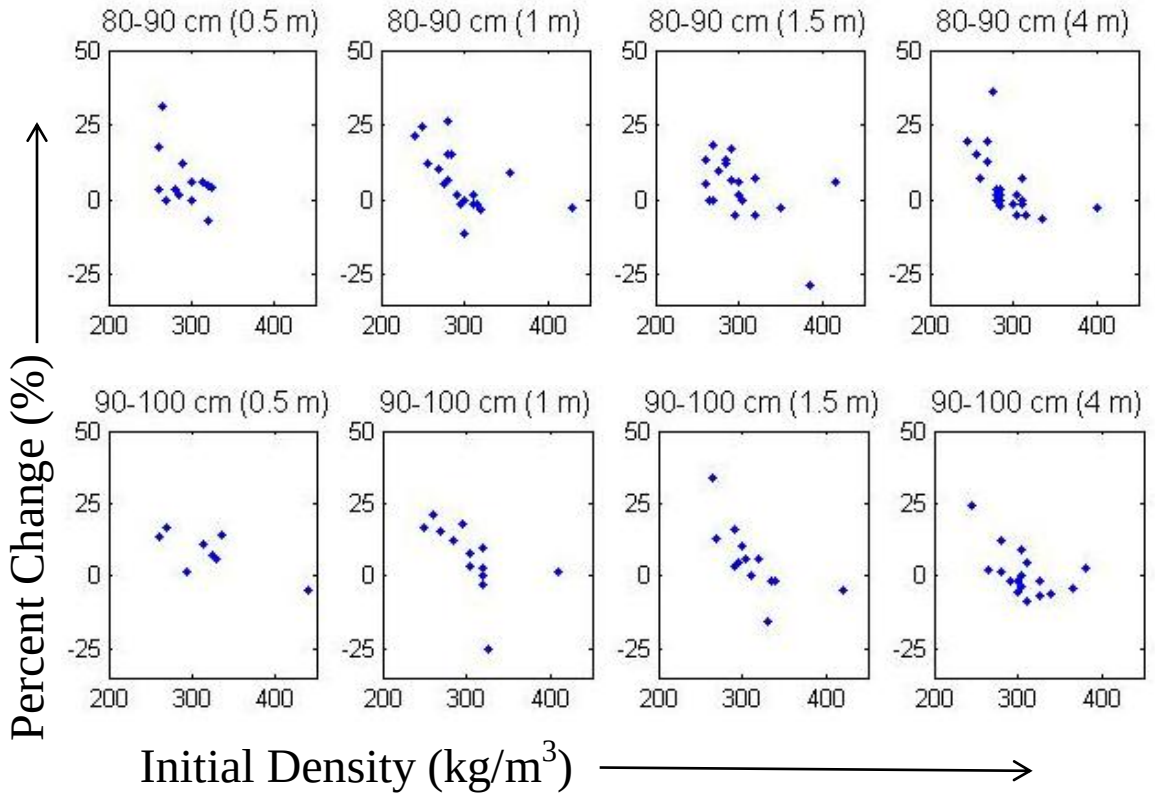

Figure 21: Percent change in density versus initial density data at each distance from center for depths from 80 – 100 cm. Each plot is labeled at the top to indicate the depth and the distance from the blast center. Values on the x-axis represent initial density in kg/m^3 and y-axis values represent percent change in density. Both x and y axes are scaled the same for each depth.

Table 9: Goodness of fit data. R^2, standard squared error (SSE), and root mean squared error (RMSE) for power fits and linear fits at each location. Shaded boxes indicate fits with an R^2 of better than 0.5.

Power Fit						**Linear Fit**				
	0.5 m	**1 m**	**1.5 m**	**4 m**			**0.5 m**	**1 m**	**1.5 m**	**4 m**
0-10cm						**0-10cm**				
R^2	0.68	0.62	0.70	0.073		**R^2**	0.76	0.75	0.79	0.064
SSE	1785	4491	2127	8034		SSE	1298	2683	1381	7613
RMSE	8.44	13.4	9.22	18.3		RMSE	7.35	10.6	7.59	18.2
10-20cm						**10-20cm**				
R^2	0.50	0.60	0.66	0.19		**R^2**	0.54	0.54	0.70	0.29
SSE	3087	2145	2841	4278		SSE	2828	2434	2483	3708
RMSE	11.1	9.26	10.7	13.4		RMSE	10.6	9.87	9.97	12.4
20-30cm						**20-30cm**				
R^2	0.33	0.28	0.20	0.40		**R^2**	0.47	0.36	0.36	0.46
SSE	3049	3638	4524	2643		SSE	2424	3240	3630	2384
RMSE	11.0	12.1	13.5	10.5		RMSE	9.85	11.4	12.1	9.97
30-40cm						**30-40cm**				
R^2	0.20	0.32	0.33	0.33		**R^2**	0.33	0.31	0.73	0.40
SSE	1041	1329	3855	1975		SSE	877.8	1339	1545	1773
RMSE	6.59	7.29	12.4	9.07		RMSE	6.05	7.32	7.86	8.60
40-50cm						**40-50cm**				
R^2	0.31	0.35	0.25	0.29		**R^2**	0.31	0.41	0.35	0.51
SSE	1850	2286	1589	1095		SSE	1870	2055	1377	755.7
RMSE	8.78	9.56	7.97	6.75		RMSE	8.83	9.07	7.42	5.61
50-60cm						**50-60cm**				
R^2	0.38	0.31	0.41	0.38		**R^2**	0.85	0.65	0.59	0.52
SSE	3394	2037	1407	1565		SSE	851.9	1048	981.2	1202
RMSE	11.9	9.21	7.66	8.08		RMSE	6.61	6.61	6.39	7.08
60-70cm						**60-70cm**				
R^2	0.40	0.46	0.32	0.27		**R^2**	0.62	0.55	0.39	0.42
SSE	2003	1563	2343	1907		SSE	1267	1297	2089	1516
RMSE	9.33	8.25	9.88	8.91		RMSE	7.42	7.51	9.33	7.95
70-80cm						**70-80cm**				
R^2	0.37	0.30	0.41	0.18		**R^2**	0.54	0.28	0.35	0.27
SSE	667.1	794.3	1014	3431		SSE	487.3	806.8	1110	3048
RMSE	5.78	6.01	6.79	12.2		RMSE	4.94	6.06	7.10	11.5
80-90 cm						**80-90cm**				
R^2	0.27	0.46	0.19	0.37		**R^2**	0.24	0.29	0.28	0.31
SSE	806.5	1028	1685	1389		SSE	844.2	1350	1479	1523
RMSE	8.20	7.78	9.42	8.33		RMSE	8.39	8.91	8.82	8.73
90-100cm	(n=8)	(n=13)	(n=13)	(n=17)		**90-100cm**	(n=8)	(n=13)	(n=13)	(n=17)
R^2	0.43	0.37	0.66	0.57		**R^2**	0.56	0.30	0.44	0.29
SSE	208.1	1111	579.8	471.0		SSE	160.8	1226	942.1	773.3
RMSE	5.89	10.1	7.26	5.60		RMSE	5.18	10.6	9.25	7.18

Hardness plots show little to no change (Figure 22; Figure 23) when measurements are matched both from the snow surface down and from the ground up.

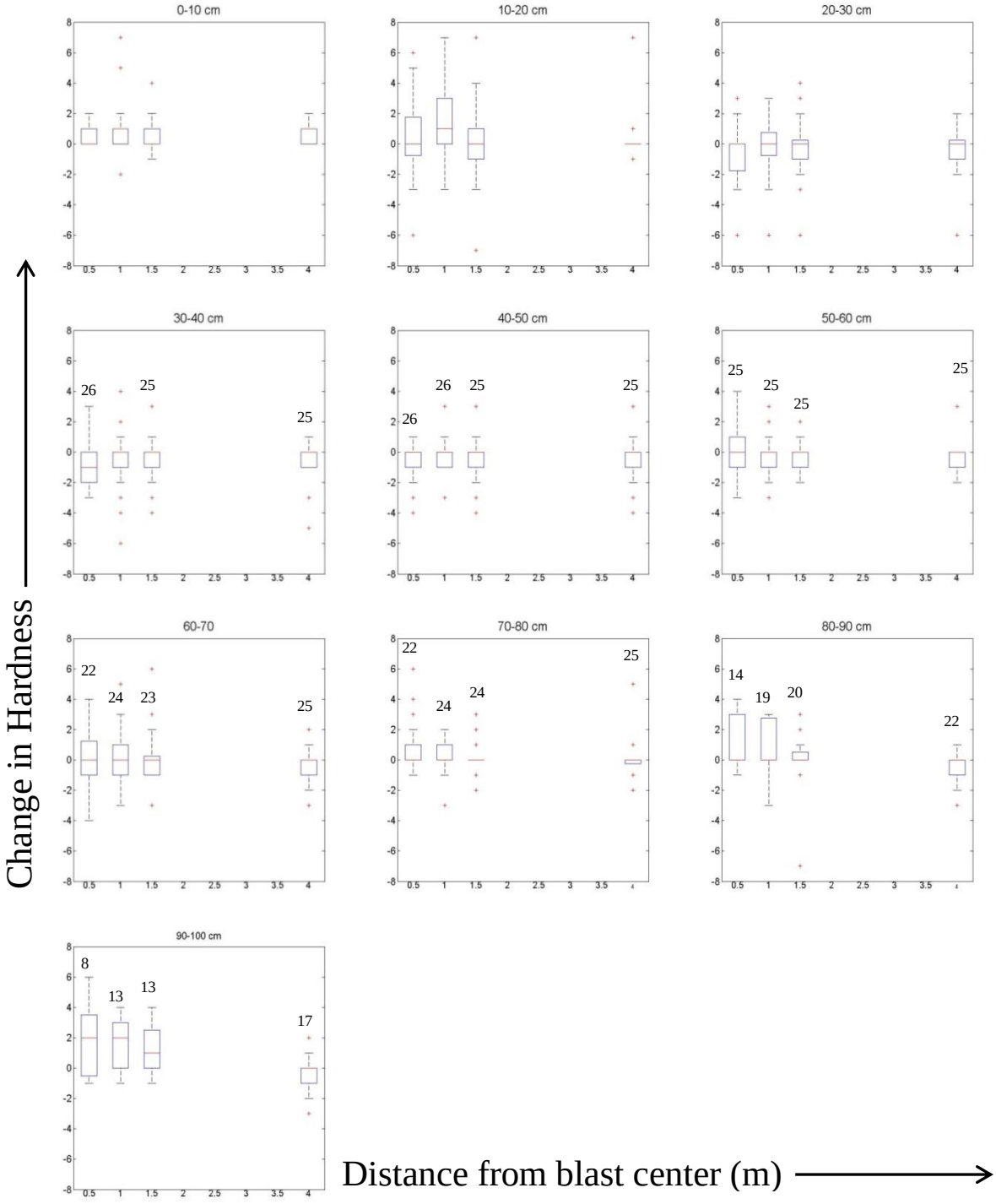

Figure 22: Box and whisker plots showing change in hardness for air blast data matched from the **snow surface down**. Each plot is labeled at the top to indicate the depth. Values on the y-axis represent change in hardness (from +8 to -8) and values on the x-axis represent distance from the blast center in meters (from 0.5 to 4 m). On each box, the line is the median, the edges of the box are the interquartile range (IQR) representing the middle 50% of the data and the whiskers extend to 1.5 IQRs. Outliers are represented by plus signs. Sample size is 27 except where indicated by a number above the plot.

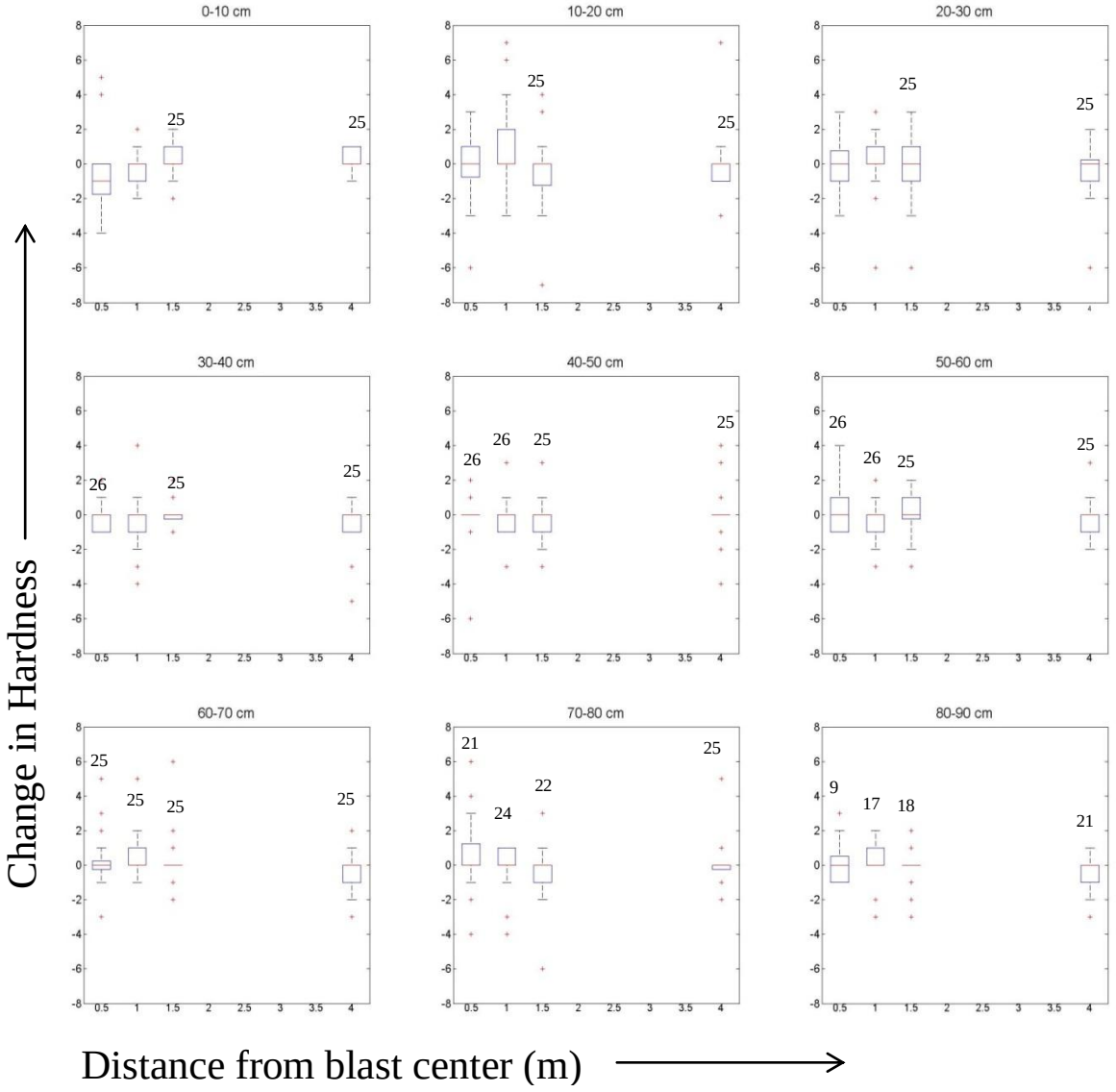

Figure 23: Box and whisker plots showing change in hardness for each distance and depth for air blast data matched from the **ground up**. Each plot is labeled at the top to indicate the depth. Values on the y-axis represent change in hardness (from +8 to -8) and values on the x-axis represent distance from the blast center in meters (from 0.5 to 4 m). On each box, the line is the median, the edges of the box are the interquartile range (IQR) representing the middle 50% of the data and the whiskers extend to 1.5 IQRs. Outliers are represented by plus signs. Data was not available at a depth of 90-100 cm. Sample size is 27 except where indicated by a number above the plot.

The 95% confidence intervals generated from bootstrapping the surface down data indicate slight mean increases (less than 1 step using the modified hand hardness scale discussed earlier) (Table 2) at the snow surface out to a distance of 4 m from the blast center (Table 10). The bootstrapped confidence intervals also show a mean increase in hardness deeper in the snowpack. Increases are evident at a distance of 0.5 m from the blast center and depths from 70-100 cm. At a depth of 90-100 cm increases occur out to a distance of 1.5 m from the blast center (Table 10). Two areas of hardness decrease are exposed in the confidence interval data. These occur at depths of 30-40 cm at both 0.5 and 4 m from the blast center (Table 8). These decreases are very small, with the largest decreases being approximately one step in the modified hardness scale previously described.

Bootstrapping data matched from the ground up resulted in 95% confidence intervals showing small mean increases in hardness and mean decreases in hardness that occurred at various distances and depths from the blast center, but lacked any clear pattern (Table 11). Mean changes in hardness were less than a 1 step change in the modified hardness scale previously discussed. The 95% confidence intervals that do not include zero indicate a statistically significant change in hardness.

Table 10: Bootstrapped 95% confidence intervals calculated from 5000 resampled data sets for the change in hardness for air blast data matched from the **snow surface down**. Blocks of dark shading indicate locations where a mean increase in hardness is included in the 95% confidence interval generated from bootstrapping. Blocks of lighter shading depict locations where the 95% confidence interval indicates a mean decrease. Sample size is 27 except where indicated by a number next to the sample mean.

Distance→ Depth↓	**0.5m**		**1m**		**1.5m**		**4m**	
	sample mean	**95% CI**	**sample mean**	**95% CI**	**sample mean**	**95% CI**	**sample mean**	**95% CI**
0-10 cm	0.9	0.4 - 1.8	0.5	0.1 - 0.9	1 (n=25)	0.7 - 1.4	0.3 (n=25)	0.1 - 0.5
10-20 cm	0.3	-0.1 - 1.4	1.4	0.6 - 2.4	0.2 (n=25)	-0.8 - 1.2	0.3 (n=25)	-0.1 - 1.4
20-30 cm	-0.5	-1.3 - 0.2	-0.2	-0.9 - 0.4	-0.3 (n=25)	-1.1 - 0.4	-0.4 (n=25)	-1.2 - 0
30-40 cm	-0.8 (n=26)	-1.3 - 0.2	-0.6	-1.4 - 0	-0.4 (n=25)	-1.0 - 0.1	-0.5 (n=25)	-1.2 - -0.2
40-50 cm	-0.7 (n=26)	-1.4 - -0.2	-0.2	-0.7 - 0.3	-0.4 (n=25)	-1.0 - 0.1	-0.4 (n=25)	-1.0 - 0.1
50-60 cm	0.1 (n=26)	-0.5 - 0.8	-0.3 (n=26)	-0.7 - 0.2	-0.1 (n=25)	-0.4 - 0.2	-0.3 (n=25)	-0.6 - 0.2
60-70 cm	0.3 (n=25)	-0.4 - 1.0	0.2 (n=25)	-0.3 - 1.0	0.1 (n=25)	-0.4 - 1.0	-0.3 (n=25)	-0.8 - 0.1
70-80 cm	0.8 (n=22)	0.2 - 1.7	0.1 (n=24)	-0.4 - 0.4	0.4 (n=23)	-0.1 - 1.8	0 (n=25)	-0.3 - 0.8
80-90 cm	1.3 (n=14)	0.4 - 2.4	0.7 (n=19)	-0.1 - 1.5	0.1 (n=20)	-1.3 - 0.6	-0.5 (n=22)	-1.0 - 0.2
90-100 cm	1.9 (n=8)	0.4 - 3.5	1.5 (n=13)	0.6 - 2.3	3.7 (n=13)	0.7 - 14	-0.4 (n=17)	-1.1 - 0.1

Table 11: Bootstrapped 95% confidence intervals calculated from 5000 resampled data sets for the change in hardness for air blast data matched from the **ground up**. Blocks of dark shading indicate locations where a mean increase in hardness is included in the 95% confidence interval generated from bootstrapping. Blocks of lighter shading depict locations where the 95% confidence interval showed a mean decrease. Sample size is 27 except where indicated next to the sample mean.

Depth↓ Distance→	**0.5m**		**1m**		**1.5m**		**4m**	
	sample mean	**95% CI**	**sample mean**	**95% CI**	**sample mean**	**95% CI**	**sample mean**	**95% CI**
0-10 cm	-0.8	-1.4 - 0.1	-0.2	-0.6 - 0.2	0.3 (n=25)	-0.1 - 0.7	0.3 (n=25)	0.1 - 0.5
10-20 cm	-0.3	-1.1 - 0.4	0.9	0.2 - 1.9	-0.5 (n=25)	-1.4 - 0.3	0 (n=25)	-0.4 - 1.0
20-30 cm	-0.2	-0.6 - 0.4	0.1	-0.7 - 0.6	-0.2 (n=25)	-1.0 - 0.4	-0.4 (n=25)	-1.2 - 0
30-40 cm	0 (n=26)	-0.3 - 0.3	-0.4	-1.0 - 0.1	-0.1 (n=25)	-0.3 - -0.2	-0.7 (n=25)	-1.5 - -0.2
40-50 cm	-0.4 (n=26)	-1.4 - -0.2	0 (n=26)	-0.4 - 0.5	-0.2 (n=25)	-0.6 - -0.3	0 (n=25)	-0.5 - -0.6
50-60 cm	0.4 (n=26)	0 - 1.0	-0.4(n=26)	-0.7 - 0	0 (n=25)	-0.5 - 0.3	-0.2 (n=25)	-0.5 - 0.2
60-70 cm	0.1 (n=25)	-0.4 - 0.8	0.4(n=25)	0.1 - 1.1	0.1 (n=25)	-0.2 - 1.1	-0.3 (n=25)	-0.8 - 0.2
70-80 cm	0.4 (n=21)	-0.5 - 1.4	0 (n=24)	-0.8 - 0.3	0 (n=22)	-0.9 - 1.3	0 (n=25)	-0.3 - 0.7
80-90 cm	0.2 (n=9)	-0.4 - 1.3	0 (n=17)	-0.8 - 0.7	-0.2 (n=18)	-0.7 - 0.3	-0.5 (n=21)	-1.0 - -0.1

After explosive detonation the median number of CT taps at 1 m, 1.5 m and 4 m from the blast center showed a decrease (Figure 24). However, statistically significant decreases only occurred 4 m from the blast center (Table 12).

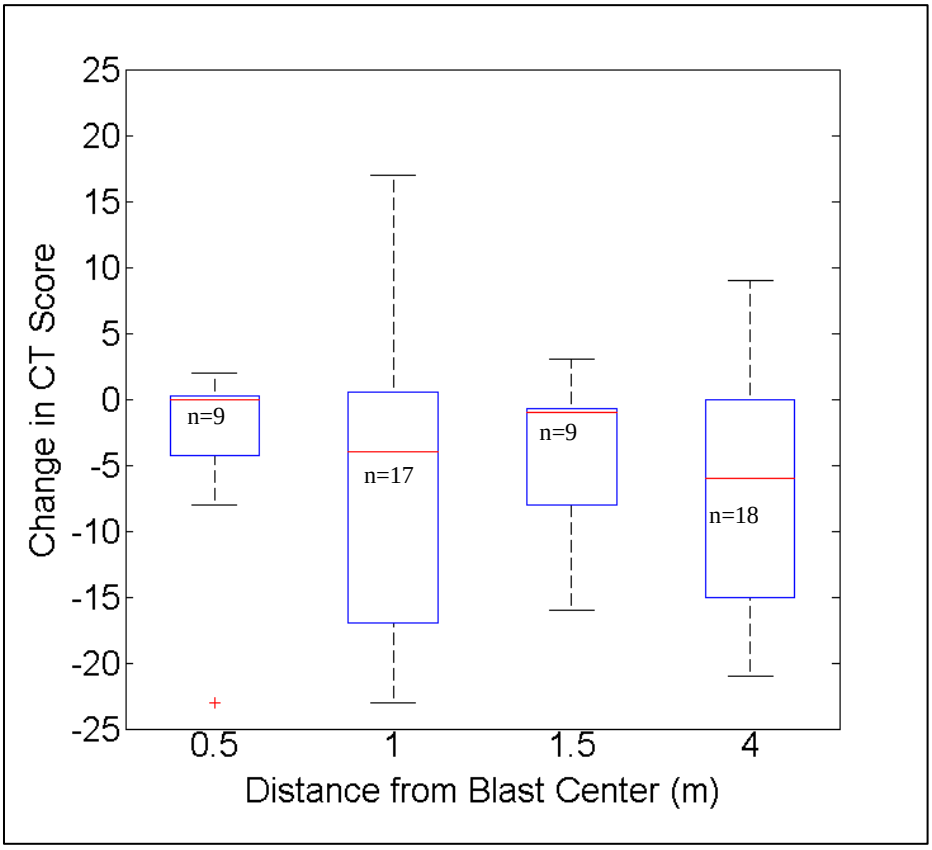

Figure 24: Box and whisker plot showing change in CT results and demonstrating change in number of taps at column failure at all tested distances from the blast center. On each box, the red line is the median, the edges of the box are the interquartile range (IQR) representing the middle 50% of the data and the whiskers extend to 1.5 IQRs. Outliers are represented by red plus signs.

ECT results 1 m from the blast center indicate no median change in ECT score after a blast, and a very small median decrease 4 m from center (Figure 25). Statistical tests of ECT data indicate no median change at either distance (Table 12). The 10 sets of pre- and post-blast ECT results show roughly the same number of tests with no change,

an increase in tap number and a decrease in tap number (Table 13). Results also demonstrate no change in propagation during ECTs at both distances in the majority of the tests (Table 13). When there were changes in propagation, these were different 1 m from the blast center from those occurring 4 m away (Table 13).

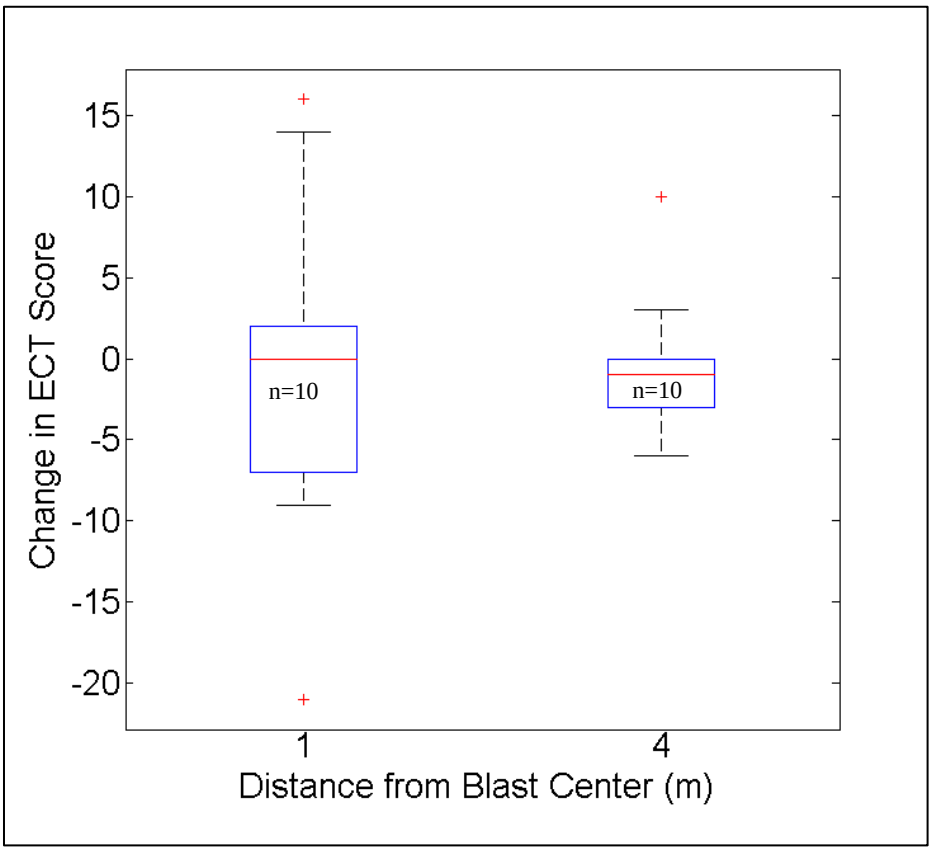

Figure 25: Box and whisker plot showing change in ECT results from air blasts and demonstrating change in number of taps at column failure at all tested distances from the blast center. On each box, the red line is the median, the edges of the box are the interquartile range (IQR) representing the middle 50% of the data and the whiskers extend to 1.5 IQRs. Outliers are represented by red plus signs. Sample sizes are indicated on the plots.

Table 12: P values generated from the Wilcoxon sign-rank test, testing change in CT or ECT score for a median of zero. P values less than 0.05 are shaded and indicate a statistically significant change in CT score. Data set sizes are included for each location.

Test Type	**0.5 m**	**1 m**	**1.5 m**	**4 m**
CT	0.19 (n=9)	0.067 (n=17)	0.062 (n=9)	8.2×10^{-3} (n=18)
ECT	N/A	0.94 (n=10)	N/A	0.83 (n=10)

Table 13: Changes in ECT results showing how the number of taps at column failure changed and how propagation changed after air blasts at both distances sampled. Numerical results show the number of ECTs out of 10 that displayed each result.

Total Number of ECTs: 10	**1 m**	**4 m**
no change in taps	3	3
increase in taps	3	2
decrease in taps	4	5
no change in propagation	6	8
pre-blast propagation/ no post-blast propagation	3	0
no pre-blast propagation/ post-blast propagation	0	2

Shear quality data from CTs at locations 1 m from the blast center show no median change with 13 of 16 observations showing zero change or a decrease in shear quality defined by an increase in Q number and a less sudden, less planar shear (Figure 26). This result is consistent with field observations of cracks, holes and obvious discontinuities in the snowpack 1 m from the blast center after detonations. The data show no median change in shear quality for CTs 4 m from the blast center, and 12 of 16 observations at this distance also indicate zero change (Figure 26). Shear quality data for ECTs were too few to use in statistical testing (n=8 at 1 m, n=7 at 4 m).

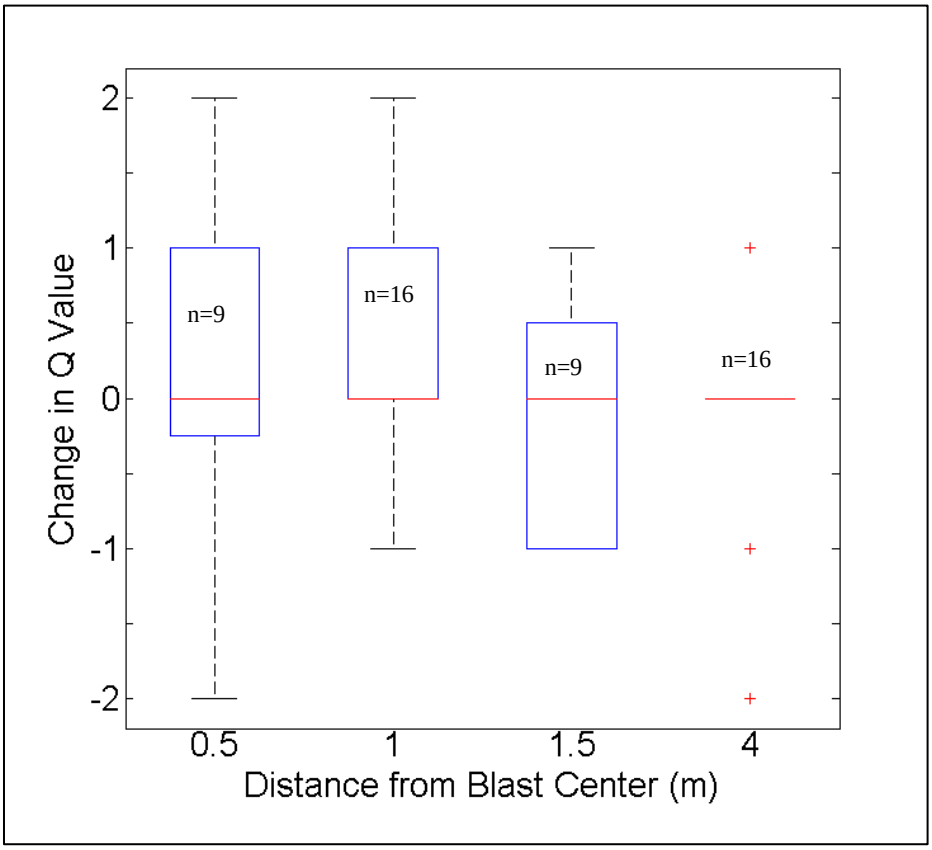

Figure 26: Box and whisker plot showing change in shear quality at all distances from the blast center for CTs at each location for air blasts. An increase in Q number indicates a decrease in shear quality and a less sudden, less planar shear. On each box, the red line is the median, the edges of the box are the interquartile range (IQR) representing the middle 50% of the data and the whiskers extend to 1.5 IQRs. Outliers are represented by red plus signs. Sample sizes are indicated on the plots.

4.3 Laboratory Density Gauge Comparisons

Median density values of the low density snow were 170 kg/m^3 for all three sampling methods (Figure 27). The bulk snow density obtained through using the box weight and inside dimensions, was 162 kg/m^3, 5% less than the sample medians. This indicates an accuracy of $\pm$ 5% for each of the three methods. The median absolute deviation of data sampled with the WE density gauge was 20 kg/m^3, which represents a

precision of ± 12% (Table 14). The Kruskal-wallis test of equal medians returned a p-value of 0.91, indicating no statistically significant difference between the three medians.

Measurements made in the medium density snow resulted in median density values of 300 kg/m^3 for all three sampling methods (Figure 28). The bulk snow density obtained through using the box weight and inside dimensions, was 286 kg/m^3, 5% less than the sample medians. Accuracy for each of the three methods was again determined to be ± 5%. The median absolute deviation of data sampled with the WE density gauge was 10 kg/m^3, which represents a precision of ± 3% (Table 14). The Kruskal-wallis test of equal medians returned a p-value of 0.21, indicating no statistically significant difference between the three medians.

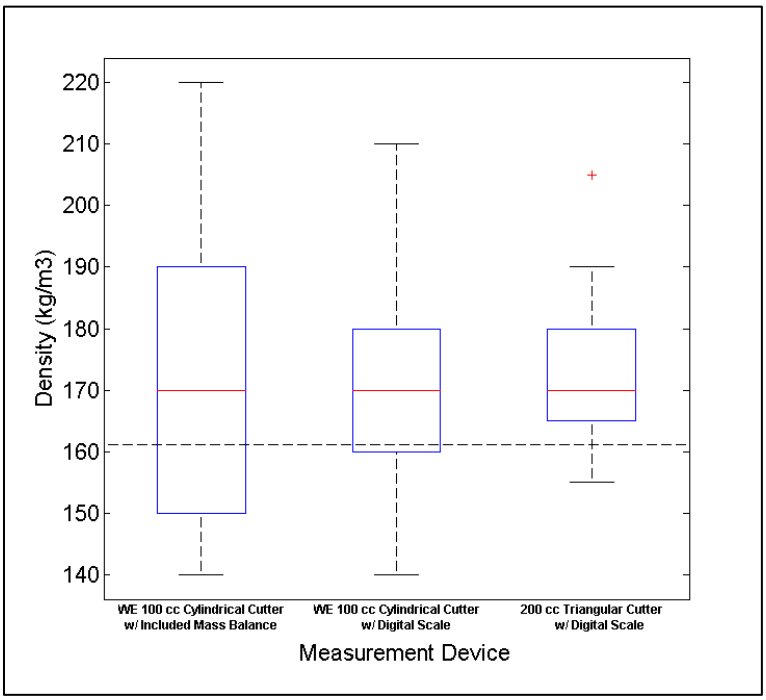

Figure 27: Box and whisker plot showing the results of 30 density measurements from each measurement device in **low density snow**. On each box, the red line is the median, the edges of the box are the interquartile range (IQR) representing the middle 50% of the data and the whiskers extend to 1.5 IQRs. Outliers are represented by red plus signs. The dashed line represents the bulk snow density of 162 kg/m^3.

Table 14: Statistics and measures of variance obtained using each of the three sampling methods in both low density and medium density snow.

	WE 100 cm^3 cylindrical cutter w/ included scale	**WE 100 cm^3 cylindrical cutter w/ digital scale**	**200 cm^3 triangular cutter w/ digital scale**
Test #1: Low Density Snow			
Sample Median (kg/m^3)	170	170	170
Interquartile Range (kg/m^3)	40	20	15
Median Absolute Deviation (kg/m^3)	20	16	8.5
Test #2: Medium Density Snow			
Sample Median (kg/m^3)	300	300	300
Interquartile Range (kg/m^3)	21	15	11
Median Absolute Deviation (kg/m^3)	10	10	5

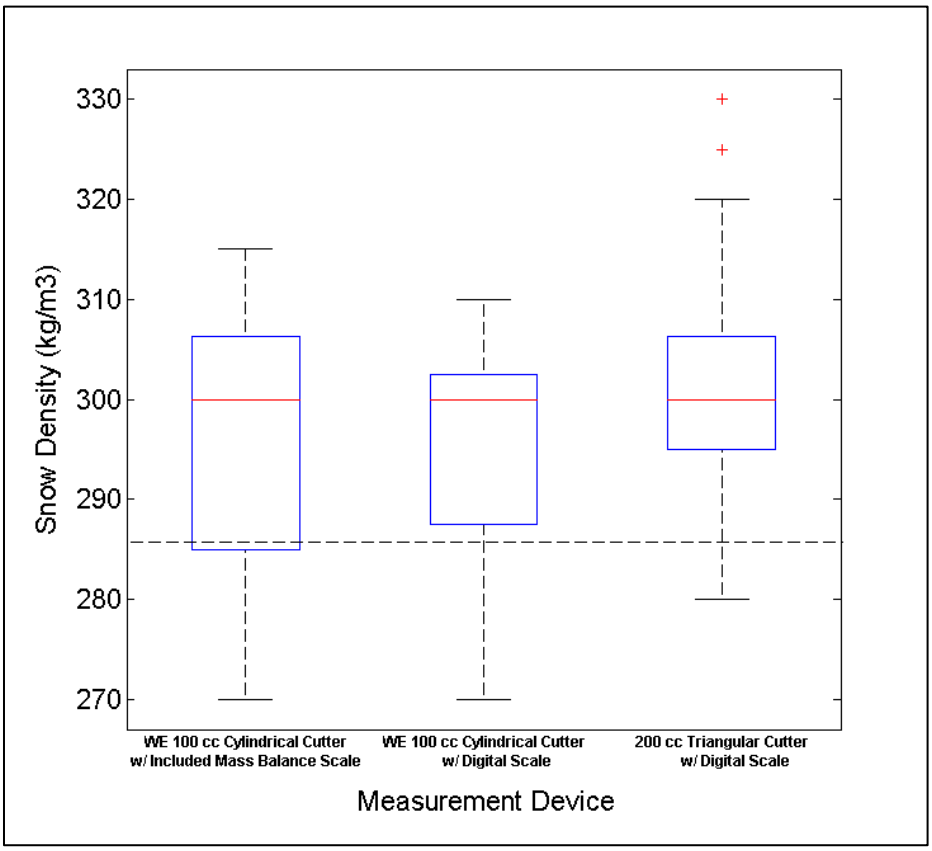

Figure 28: Box and whisker plot showing the results of 29 density measurements from each measurement device in **medium density snow**. On each box, the red line is the median, the edges of the box are the interquartile range (IQR) representing the middle 50% of the data and the whiskers extend to 1.5 IQRs. Outliers are represented by red plus signs. The dashed line represents the bulk snow density of 286 kg/m^3.

The range of data obtained using the WE gauge and scale in low density snow was 100% larger than with the WE sampler and digital scale and 167% larger than with the triangular cutter and digital scale (Table 14). The range associated with using the WE gauge in medium density snow was 40% larger than that associated with the WE cutter and digital scale and 90% larger than with the triangular cutter and digital scale. The median absolute deviation of data sampled with the WE density gauge ranged from 3-12% depending on the type of snow sampled. This value represents the precision associated with the same WE density gauge used for all data measurements presented in this study. In low density snow the Median Absolute Deviation associated with the WE gauge was 25% larger than the MAD resulting from use of the WE cylindrical cutter and digital scale and 135% larger than the MAD associated with the triangular cutter and digital scale. In medium density snow, the MAD resulting from use of the WE gauge and scale was the same as with the WE gauge and digital scale and 100% larger than that associated with the triangular cutter and digital scale.

The Winter Engineering 100 cm^3 cylindrical cutter displayed the largest interquartile range followed by the same cutter used with a digital scale. The smallest interquartile range was obtained using the 200 cm^3 triangular cutter with the digital scale (Table 14). Median absolute deviations (MADs) followed the same patterns with the largest resulting from the WE 100 cm^3 cylindrical cutter and scale and the smallest from the 200 cm^3 triangular cutter used with a digital scale. Regardless of the method used, all but 3 sampled densities in total fell within 1.5 IQRs of the median densities. The

outlying density values were sampled with the triangular cutter and digital scale (Figure 27; Figure 28).

5. DISCUSSION

5.1 Laboratory Density Gauge Comparisons

The three density sampling methods resulted in equal medians in laboratory measurements of both low and medium density snow. These median values were 5% greater than the bulk density of both the low and medium density snow. The accuracy of the WE gauge and scale was determined to be $\pm$ 5% in both types of laboratory snow, indicating that regardless of the initial snow density, the accuracy of the device as determined through lab tests is the same. It should be noted that while all methods provided an equal median, the Winter Engineering density gauge yielded data with the greatest range and MAD and therefore was the least precise. Because the data are not normally distributed, unbiased estimators such as median, range and MAD, that are more resistant to outliers and extreme values, are more reliable for use in interpreting these results.

Conger and McClung's (2009) comparison of density cutters yielded similar results. They documented a combined undersampling and weight measurement error, defined here as an accuracy, of $\pm$ 1 to 4% using the WE cutter and a digital scale. This is less than the $\pm$ 5% accuracy determined from the measurements made in the laboratory with the WE cutter and WE mass balance. Conger and McClung showed that the WE cutter and digital scale had the greatest range of error out of the five cutters used with the digital scale. This is consistent with the results of the laboratory tests conducted in the SSERF where the WE cutter and scale demonstrated the largest MAD. When comparing

these methods of measuring density, greater precision is expected with the triangular cutter and digital scale because the cutter volume is twice that of the cylindrical cutter and the digital scale is presumed to be more precise than the WE mass balance.

Lower precision was accepted in using the WE gauge because of its convenience as a field measurement tool. Furthermore, the majority of statistically significant density increases were greater than the 12% median absolute deviation measured in the laboratory. Although the WE gauge demonstrated less precision, statistically significant increases in density were nonetheless observed, further reinforcing these measured changes due to explosives.

5.2 Surface Blasts

After 8 surface blast explosions at Snowmass Ski Area, the data were examined and field methods were reviewed. Percent change in density data showed some increases, with the greatest seen at the snow surface (a depth of 0-10 cm) out to 3 m from the blast center. Because snow height changed very little after a blast, this is most likely a product of snow being displaced from the crater region to the pit locations and possibly from soot mixing with snow at this depth, thereby increasing snow density (Figure 29).

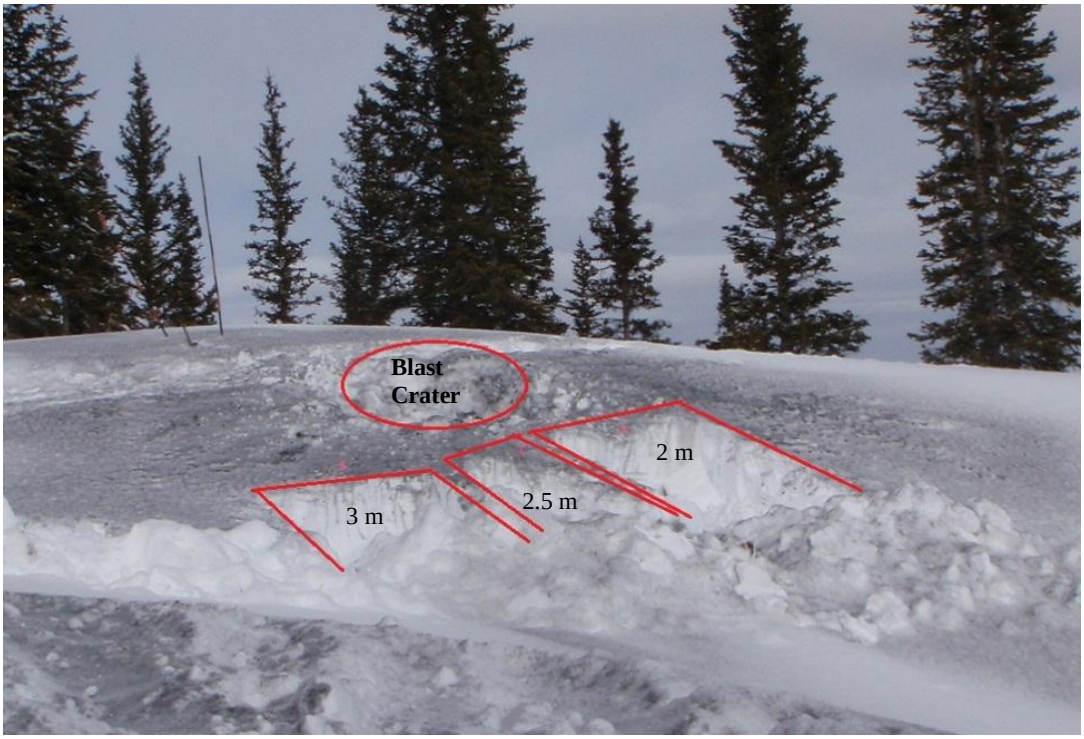

Figure 29: Snowmass study site after a surface blast showing after-blast pits at 2, 2.5 and 3 m from the blast center. The blast has disturbed the snow near the blast center creating a crater and displacing snow. Black soot covers the snow surface in the sampling area.

Below 10 cm in depth, the majority of density increases appear to be approximately 10% or less and occur in no apparent pattern. Deeper in the snowpack (depths of 80-100 cm) there appears to be a slight decrease in density closer to the blast center. These increases are smaller than the 12% maximum error in the density gauge, indicating they could be due to measurement error alone. Because sample sizes were small (n=8) it is difficult to interpret these results with confidence. Furthermore, sampling techniques were not ideal for measuring changes from a surface blast. In designing this study, it was necessary to plan the post-blast pits at a distance from the blast center that would allow for sampling of undisturbed snow after blasts. The 2 m pits were located as closely as possible to the blast center without being inside in the crater

zone. Surface blasts result in more extensive craters than suspended blasts, so pits associated with surface blasts had to be situated farther away than pits associated with suspended blasts. Because surface blasts are expected to affect snow to a deeper extent, but within a smaller area than suspended blasts (Miller et. al, 2011), these pit locations should be closer to the blast center. Because the closest pit was 2 m away from the blast center there is a strong likelihood that these pit locations were too far from the blast center to capture changes other than those occurring at the snow surface. Furthermore, due to operational limitations within the ski area, pre-blast pits were excavated and sampled one day prior to explosive detonations which were conducted in the mornings before opening the controlled terrain where the study area was located. This method of sampling on two different days was only conducted when there was no overnight precipitation or heavy wind, but there are still questions about whether changes could have taken place that were not a result of explosives use. Diurnal and nocturnal temperature changes could lead to snow metamorphism and subsequent snowpack changes which may be difficult to separate from changes occurring due to the explosives. Because no control to compare snow density over two days was established, there is little way of knowing if any of the changes seen in density, hardness or stability test results were caused by the explosives alone. Limitations associated with the surface blast sampling design along with only small density changes occurring in no apparent pattern led to the inference that there was no detectable change at the locations sampled and that measurements were made beyond the immediate area affected by the explosives.

Hardness data show little to no change in median hardness. Any visible changes are decreases in hardness and are no more than a one-step difference, but because a less sensitive hand hardness scale was used in the surface blast tests, any changes that occurred are larger than those that are demonstrated by suspended blast data. In the scale used for surface blast hardness measurements, a one number change in hardness corresponds to a one step change in hand hardness value (Table 1). Most of the data show no median change in hardness at all distances to a depth of 40 cm and below depths of 40 cm, some decreases in hardness occur, but again, the data are too few to use in statistical testing and as discussed previously, field methods raise some questions about the validity of this data. In addition, pre- and post-blast ram hardness profiles show no consistent pattern of hardness change. Comparing pre- and post-blast hardness was more complicated than expected when using the ram profiles for each distance sampled during each test (Figures 12-15; Appendix Figures A1-A21). Even when there was no post-blast snow loss, ram profile layers matched up in a logical way only part of the time and mismatched layers made it difficult to compare pre- and post-blast profiles. This could be an indication of measurement error in the ram or sampling error due to multiple operators of the penetrometer. Alternatively, it could be a product of measuring the spatial hardness variability present in the snowpack.

Ram profiles were also used to validate the matching of density and hand hardness measurements from the snow surface down rather than the ground up. Matching data measurements from the snow surface down involves no adjustment for the decrease in post-blast snow height. Matching measurements from the ground up involves

adjusting the starting point of the measurements. These ram profiles do not provide evidence that matching measurements from the ground up improves layer alignment. Additionally, 10 of the 21 profiles showed either adequate alignment of layers or the need for slight adjustments that did not account for the entire post-blast decrease in snow surface height. This provides further support for matching measurements from the snow surface down rather than from the ground up.

CT data displayed small changes in CT score at locations 2 m from the blast center and no change at locations 3 m from the blast center. At this farther distance, both the median and the interquartile range were zero. Because CT data were few (n=6), statistical tests were not performed. Due to the small size of the data set and issues with field methods, these results are not conclusive to this study.

The surface blasts performed in Snowmass did provide information that helped in designing a better sampling plan for the air blast tests, but they did not provide conclusive data to the analysis, and as a result were discontinued after questions were raised concerning the validity of the study design. In designing methods for air blasts, concerns about snowpit distances from the blast center were addressed, continuous measurements to a depth of 1 m were planned and post-blast sampling was scheduled to occur immediately following pre-blast measurements rather than the following day. These improvements resulted in more reliable data from air blast tests, thereby providing more conclusive results.

5.3 Air Blasts

Results of air blasts show an increase in density in the region extending out to a distance of 1.5 m from the blast center and down to a depth of 50 cm (Figure 17; Table 7). It should be noted that percent increases in density are not always greatest near the blast center. For example, at a depth of 0-10 cm there is a greater median increase in density 1.5 m from the blast center than there is 1 m away. At a depth of 40-50 cm, a greater median change is seen 1 m from the blast center than 0.5 m away. This could be a sign that there is a similar effect over this whole area (extending out to 1.5 m) regardless of proximity to the blast center. Alternatively, this could be the effect of a negative pressure pulse that is greatest at the center, resulting in rebound in the area where density increases are highest. Density increases occurring at a distance of 4 m from the blast center suggest that explosives have limited effect on density except in the upper snowpack (depths of 0-20 cm) at this distance (Table 7). Contrary to Frigo et al.'s inconclusive findings regarding density change, these results show statistically significant changes in snow density and indicate that density is a useful parameter for measuring changes in snow resulting from explosives. These measurements provide field-based observational data that could be incorporated into future predictive models to produce a more robust picture of explosive effects on snow density and the area affected. These observations also provide a permanent measure of explosive effects that has been verified through both statistical tests and bootstrapping, and shows that these effects decrease with range and depth from the blast center.

The area over which statistically significant density change occurred can help to define the effective range of avalanche explosives. Aside from at the snow surface, density increases do not extend past a distance of 4 m from the blast center. This distance is smaller than the distances at which Bones et al. (2012) measured overpressures. Bones et al. (2012) placed sensors at distances of 3 and 5 m from the blast center, but moved their farthest sensor to 7 m away because blast overpressures were still detectable at this distance. While the above results are not exactly the same they are much more similar than Gubler's findings. Gubler (1977) determined the effective range of a 1 kg suspended charge to be 17 to 120 m, but used very sensitive instrumentation that may have been detecting the explosives at a range where they were no longer having a physical effect on the snow.

These field measurements of density increase are also consistent with modeled increases in the area directly below a suspended explosive (Miller et al., 2011). Miller et al. (2011) did not state the exact distance at which they modeled increases, but they did show a 20% density increase in snow with an initial density of 400 kg/m^3, a higher density than any of the pre-blast snow measured in this field study. As suggested by Johnson et al. (1993), greater increases in density are seen in snow with lower initial densities. They illustrate that initial snow densities determine the amount of force needed to compact snow to a critical density where much higher pressures are necessary for further compaction. This implies that lower density snow will undergo more densification than higher density snow at the same pressures. Because 99.4% of sampled pre-blast snow densities in this study were less than the 400 kg/m^3 initial density used in

Miller et al.'s (2011) model, it is logical that higher percent increases were seen in these field data than in their model.

Johnson et al. (1993) used a power law to describe the relationship between pressure and density, therefore it was thought that this could be used to describe the relationship between initial density and the percent change in density after a blast. A power function did fit the data moderately well at the snow surface (down to 20 cm) out to a distance of 1.5 m from the blast center (Table 9). Below a depth of 20 cm, a power relationship was incapable of explaining the majority of variability in the data and other fits were tested. Quadratic, exponential and rational functions all resulted in poor fits. Application of a linear function to the data showed improvement over the power function at the snow surface (down to 20 cm) out to a distance of 1.5 m from the blast center (Table 9). Linear fits also showed improvement over power fits deeper in the snowpack close to the blast center. While the linear fits were not capable of explaining all of the variation in the initial density versus percent change in density data, they did demonstrate that a power law is not the best way to characterize this data. This is most likely because the pressure and density variables described by Johnson et al. (1993) were not the same variables as those explored here. Here, initial density was compared to percent change in density (Figures 19-21) and Johnson et al. compared pressure to density change.

Inspection of hardness data shows no change in median snow hardness regardless of how layers are matched. The nonparametric Wilcoxon sign-rank test was not used because one of its underlying assumptions is a symmetric distribution. The hardness data was highly skewed with the lower end of the distribution lying at the median in many

cases, making it unsuitable for analysis with the Wilcoxon sign-rank test. Therefore, bootstrapping techniques were used to provide a platform on which parametric statistics could be applied. The 95% confidence intervals for mean change in snow hardness show increases in hardness both on the snow surface and at depths of 90-100 cm for data matched from the snow surface down (Table 10). These increases are less than one increase in the modified hardness scale used to classify this data. When compared to the hardness plots it is evident that the increases indicated by the confidence intervals are extremely small and are not reflected in the hardness change plots except at a depth of 90-100 cm where statistically significant changes are most likely a product of small data sets (n=8, 13, and 13) rather than a true reflection of hardness change (Figure 22). Both plots and confidence intervals agree that there is very little to no change in hardness after the application of explosives.

Although hardness changes were expected in this study, no changes were measured. The modified hardness scale used in this study (Table 2) should have allowed for identification of changes because it is more sensitive to small changes than a hardness scale that assigns one value to each category (Table 1). While increases in density are associated with increases in hardness (Kinosita, 1960), only density increases were measured here. This could indicate that the explosives are affecting bonding or microstructure within the snowpack. The breaking of bonds between snow grains was measured acoustically by Gubler (1977), and Johnson et al. (1994) discuss breaking of bonds by the shock wave prior to snow compaction during a blast. Evidence of changes in bonding displayed through poorer post-blast cohesion between grains was also

observed during data collection (Figure 31). Alternatively, it is possible that the hand hardness test is too coarse a tool for detecting hardness change under these conditions and that a more sensitive measurement tool, such as the snow micro penetrometer (Pielmeier and Schneebeli, 2003), may have the ability to show more subtle changes that occur during a blast.

Significant decreases in CT taps at 4 m, but not closer to the blast center; and poorer shear quality at 1 m, but not at 4 m from the blast center imply that the shock wave may be disrupting the failure plane or the consistency of the slab in the immediate area (1 m) of the blast. It should be noted here that if the significance level for the statistical tests of CT data had been set at $p < 0.1$ instead of $p < 0.05$, statistically significant decreases in CT score would have been indicated at a distance of 1 m (Table 12) from the blast center. A clear and continuous region of density increase affecting depths to 50 cm and extending out to 1.5 m from the blast center (Table 7) could hint at a change in slab consistency. As noted above, density is observed to increase beyond this area; however, increases are less consistent beyond this specific region (Table 7). Because densification of snow occurs higher in the snowpack, slabs may be gaining strength while the underlying snow is not. Denser snow can assist the transmission of force (Lang and Nakamura, 1985) which could allow forces to affect deeper snow when densification occurs in the upper snowpack after a blast. Additionally, breaking of bonds as documented by Gubler (1977) or changes in microstructure may be enabling easier CT failures even without added force. Simultaneously, poorer shear quality is observed in the region with the greatest increases in density which may be compensating for this

effect and inhibiting failure at weak layer interfaces. It is possible that weak layers near the blast center collapse during densification, thereby affecting shear quality. Visual observation of the snowpack after field tests exposed cracks, holes and wandering fractures within the snowpack at all distances within 4 m from the blast (Figures 30-32). These are an indication of discontinuities in the snowpack which could arrest fracturing on a horizontal plane.

Figure 30: Example of discontinuities found within the snowpack looking down into the snowpack where a portion of the top layers of snow has been removed. These holes were found while excavating a pit 1 m from the blast center.

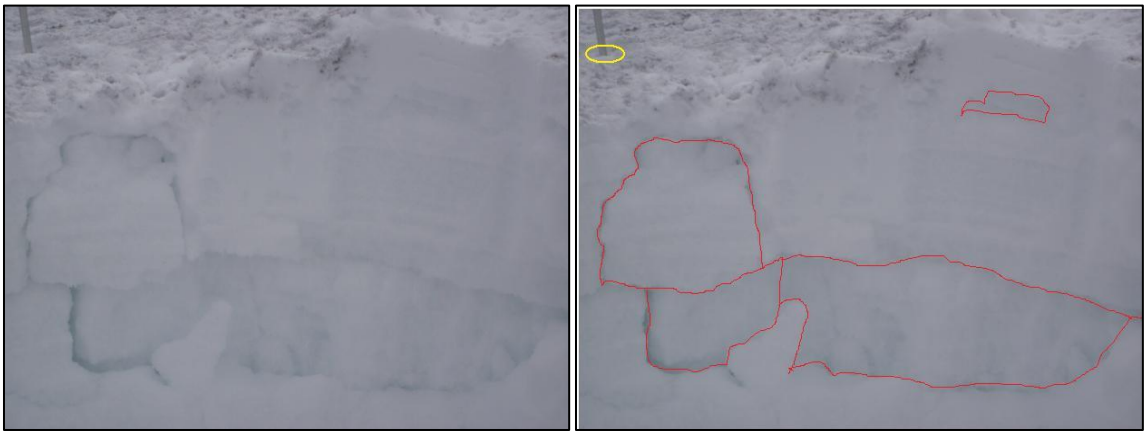

Figure 31: Cracking and separation of layers (outlined in red) at interfaces 0.5 m from the blast center (circled in yellow). Near the bottom of the snowpack a horizontal crack is visible. Snow below the crack was less cohesive than that above it and crumbled as the pit was being excavated, leaving a denser slab hanging above like a shelf.

Figure 32: Post-blast ECT column 1 m from the blast center showing top view on left and facing view on right. The top portion of the column above the failure layer has been removed. Arrows highlight cracks and holes that were both inside the snowpack and visible from the front when the column was excavated.

Destratification, the destruction of layer interfaces and therefore failure planes, is one of the primary goals in avalanche mitigation (Carvelli, 2008) using explosives. This is characterized by these cracks and discontinuities, providing evidence in support of the theory that the use of explosives is likely to be effective in disrupting the failure plane. Carvelli (2008) highlighted this idea of failure plane disruption as part of the rationale for bootpacking and systematic explosives use at Aspen Highlands. Furthermore, Kronholm

and Birkeland (2005) used a cellular automata model to demonstrate how shear plane disruptions might increase overall stability by arresting fracturing through lack of continuous propagation pathways.

Because of the limited number of ECTs performed (n=10 at 1 and 4 m), strong conclusions cannot be drawn from these tests. The majority of pre- and post-blast ECT results show a nearly even distribution between no change, an increase in taps and a decrease in taps, and very little change in pre- and post-blast propagation. The few changes in propagation that occurred at 1 m have results contrary to those at 4 m and hint at what was observed in pre- and post-blast CTs. At 1 m from the blast center the only changes in propagation were from pre-blast propagation to none post-blast. Propagation changed in the opposite way 4 m from the blast center, where two tests that exhibited no pre-blast propagation showed propagation after the blast. Close to the blast center, where the snowpack and shear plane seem to be more affected, only 1 of 4 ECTs that demonstrated pre-blast propagation showed propagation after the blast. At this distance there were zero ECTs that propagated after a blast when they had not before. While these results did not occur often, they could be the product of a disrupted shear plane as discussed previously. At a distance of 4 m from the blast center two of the 10 tests propagated after the blast when there had been no propagation before. Although these results are very few, it is notable that there were zero ECTs 4 m from center in which propagation was observed before a blast and none occurred after the blast. This could be related to the shear plane being more intact at this distance. A larger set of ECT results is needed to further explore these findings.

Snow height decreased in the region near the blast center due to snow compaction, therefore small inconsistencies in layering in before- and after-blast measurements occurred. The layer identifiers measured from the snow surface down rather than the ground up were highlighted in this discussion for two key reasons. It was more important to accurately match layers at the top of the snowpack because presumably there should be a greater effect closer to the blast center. Analysis undertaken comparing pre- and post-blast metrics as measured from the bottom up displayed similar trends to those presented here from the top down. Furthermore, inspection of pre- and post-blast ram profiles showed satisfactory to good alignment of layers in 10 of the 21 profiles with available height data without making any adjustment to compensate for decreases in post-blast snow height that may have occurred. While this is just less than half of the ram profiles that were examined, little evidence was available in support of matching pre- and post-blast measurements from the ground up.

6. CONCLUSION

These findings are the first field-based observations that show changes in the physical properties of snow occurring as a result of explosives use. The results of air blast tests demonstrate a statistically significant increase between pre- and post-blast snow density close to the blast center. However, results of pre-and post-blast hardness measurements show no change. Interestingly, snow stability test scores as measured using a CT (n=16) only showed statistically significant decreases in CT score 4 m away from the blast center and not at closer distances. Changes at farther rather than closer distances are counterintuitive at first. However, observations suggest that the shear plane at closer distances to the blast center was disrupted and this may have resulted in higher test scores than if the shear plane had been unaffected. At farther distances, observations indicate that the shear plane was still relatively intact and the taps to failure decreased. While ECT data are limited in quantity (n=10), changes in pre- and post-blast fracture propagation, like CT shear quality, also suggest an interrupted shear plane closer to the blast center. These results imply that the potential for triggering an avalanche after explosives have been applied to a slope could be declining in the immediate area of the blast (out to 1.5 m). There are still questions about what is occurring in the region 4 m from the blast center and whether there is a greater or lesser likelihood of triggering an avalanche at this distance after a blast. More CTs and ECTs are seen as an important addition to this data set and would offer not only a larger data set of stability test results for use in statistical tests, but would supply additional data, such as on fracture propagation, not available from CTs alone.

As mentioned earlier, the results of this study could provide a measure of the area affected by the specific explosive type and size used for these tests and can also be used to either reinforce or question the findings of prior studies. Density increases of up to 51% reinforce Miller et al.'s (2011) modeled density increase of 20% in the region directly below the blast with the difference in the amount of densification being due in part to different initial densities. The area influenced by the explosive, indicated both by these density increases and by changes in stability test results, extends out to a distance of 4 m from the blast center and some smaller effects could extend farther. This is consistent with Bones et al.'s (2012) research, but contradicts Gubler's (1977) earlier estimates of the area affected by explosives.

These results provide new information to avalanche practitioners and will hopefully enable a better understanding of the size of the area affected by explosives and whether snow stability is changing due to a blast. Future work should include repeated explosives tests with measurements at distances between 1.5 m and 4 m from the blast center and additional stability tests. A more continuous data set may give a better view of changes over the entire 4 m area. Future work should also explore methods of evaluating change from surface blasts with measurements made closer to the blast center.

REFERENCES CITED

Bones, J., Miller, D., and Savage, S. 2012. An experimental dynamic response study of hard slab seasonal snow to explosive avalanche mitigation. In: *Proceedings International Snow Science Workshop*, Anchorage, AK. 142-148.

Brown, R.L., 1981. A method for evaluating shockwave propagation in snow. *Cold Regions Science and Technology* 5, 151-156.

Carvelli, P., 2008. Boot Packing and "Systematic application of explosives": Shear plane disruption techniques in the continental climate. In: *Proceedings International Snow Science Workshop*, Whistler, British Colombia, Canada. 337-344.

Conger, S.M., and McClung, D.M., 2009. Instruments and Methods: Comparison of density cutters for snow profile observations. *Journal of Glaciology* 55(189), 163-169.

Efron, B., and Tibshiriani, R.J., 1994. *An Introduction to the Bootstrap, Volume 57*. Chapman and Hall/CRC. Boca Raton, FL, USA. 437 pp.

Frigo, B., Chiaia, B., Cardu, M., Giraudi, A., Godio, A., Rege, R., 2010. Experimental analysis of snowpack effects induced by blasts. In: Osterhuber, R., Ferrari, M. (Eds.), *Proceedings International Snow Science Workshop*, Squaw Valley, CA, USA. 66-71.

Gray, D.M., and Male D.H., 1981. *Handbook of Snow: Principles, Processes, Management and Use.* The Blackburn Press. Caldwell, NJ, USA. 776 pp.

Greene, E., Atkins, D., Birkeland, K., Landry, C., Lazar, B., McCammon, I., Moore, M., Sharaf, D., Sternenz, C., Tremper, B., Williams, K., 2010. *Snow, Weather and Avalanches: Observation Guidelines for Avalanche Programs in the United States*. Pagosa Springs, CO, Second Printing Fall 2010: American Avalanche Association. 152 pp.

Gubler, H., 1977. Artificial release of avalanches by explosives. *Journal of Glaciology* 19(81), 419-429.

Higgins, J. J. 2004. *An Introduction to Modern Nonparametric Statistics*. Brooks/Cole-Thomson Learning. Pacific Grove, CA, USA. 366 pp.

Jamieson, B., and Johnston, C. 1996. The Compression Test for Snow Stability. In: *Proceedings International Snow Science Workshop*, Banff, Alberta, Canada. 118-125.

Johnson, J.B., Solie, D.J., and Barrett, S., 1994. The response of a seasonal snow cover to explosive loading. *Annals of Glaciology* 19, 49-54.

Johnson, J.B., and Solie, D.J., 1993. Shock response of snow. *Journal of Applied Physics* 73(10), 4852-4860.

Kinosita, S., 1960. The Hardness of Snow. *Low Temperature Science "A"*, Institute of Low Temperature Science, Hokkaido University, 19, 119-134.

Kronholm, K., and Birkeland, K., 2005. Integrating spatial patterns into a snow avalanche cellular automata model. *Geophysical Research Letters* 32, LI9504.

Kruskal, W.H., and Wallis, W.A., 1952. Use of Ranks in One-Criterion Variance Analysis. *Journal of the American Statistical Association* 47(260), 583-621.

Klieger, P., and Lamond, J.L., 2006. *Significance of Tests and Properties of Concrete and Concrete Making Materials*. American Society for Testing And Materials. West Conshohocken, PA, USA. 623 pp.

Lang, T.E., and Nakamura, H. 1985. Settlement Force on a Beam in Snowpack by Computer Modeling. *Annals of Glaciology*, 6. 95-99.

Livingston, C.W., 1968. Explosions in snow. *Technical Report 86*, Hanover, USA CRREL. 59 pp.

Lyakhov, G., Salitskaya, V., Averchenko, A., Zakharov, S., and Bakhushina, L., 1989. Explosive waves in snow. *Combustion, Explosion and Shock Waves*, 25(4), 493-499.

McClung, D.M., Schaerer, P.A., 2006. *The Avalanche Handbook*. The Mountaineers Books, Seattle, WA. 342 pp.

Mellor, M., 1968. Avalanches. *monograph*, Hanover, USA CRREL, 1968. 215 pp.

Mellor, M., 1973. Controlled release of avalanches by explosives. Symposium on Advances in Avalanche Technology, Reno, NV, *US Forest Service Technical Report RM-3*, 37-49.

Miller, D., R. Tichota, and Adams E., 2011. An explicit numerical model for the study of snow's response to explosive air blast. *Cold Regions Science and Technology* 69, 156-164.

Mock, C.J., and Birkeland, K.W., 2000. Snow Avalanche Climatology of the Western United States Mountain Ranges. *Bulletin of the American Meteorological Society* 81(10), 2367-2392.

Orica Ltd., 2010. *avtrolTM Avalanche DUO Cast Boosters Technical Data Sheet*. Orica Mining Services, http://www.oricaminingservices.com/us/en (accessed October 6, 2012).

Pielmeier C., and Schneebeli, M., 2003. Stratigraphy and changes in hardness of snow measured by hand, rammsonde and snow micro penetrometer: a comparison with planar sections. *Cold Regions Science and Technology* 37, 393-405.

Simenhois, R. and Birkeland, K., 2006. The Extended Column Test: A Field Test for Fracture Initiation and Propagation. In: Gleason, J.A. (Ed.), *Proceedings International Snow Science Workshop*, Telluride, CO, USA. 79-85.

Ueland, J., 1992, Effects of explosives on the mountain snowpack. In: *Proceedings International Snow Science Workshop*, Breckenridge, CO, USA. 205-213.

Wilcoxon, F., 1945. Individual Comparisons by Ranking Methods. *Biometrics Bulletin*, 1(6): 80-83.

Wisconsin Geological and Natural History Survey. 2011. *Rock properties: Porosity and density*. http://wisconsingeologicalsurvey.org (accessed July 17, 2012).

Wisotski, J. and Snyer, W.H., 1966. A study of the effects of snow cover on high explosive blast parameters. *Final Report submitted to United States Naval Ordinance Laboratory*, Air-Ground Explosions Division, Denver: Denver Research Institute - University of Denver. 97 pp.

APPENDIX A:

RAM RESISTANCE PROFILES FROM SURFACE BLASTS

Appendix Figures: A total of 21 Ram Resistance profiles from 7 surface blast tests. For each surface blast, there is a pre- and post-blast profile for each pit location. In each profile, the numbers along the x-axis at the top of the profile show force in newtons, the y-axis axis shows snow depth in cm, the solid line is the pre-blast profile and the dotted line is the post-blast profile. Aligning obvious layers in the pre- and post-blast profiles reveals no clear pattern in hardness change.

The following 9 ram profiles are from locations where there was a 0-3 cm decrease in snow height:

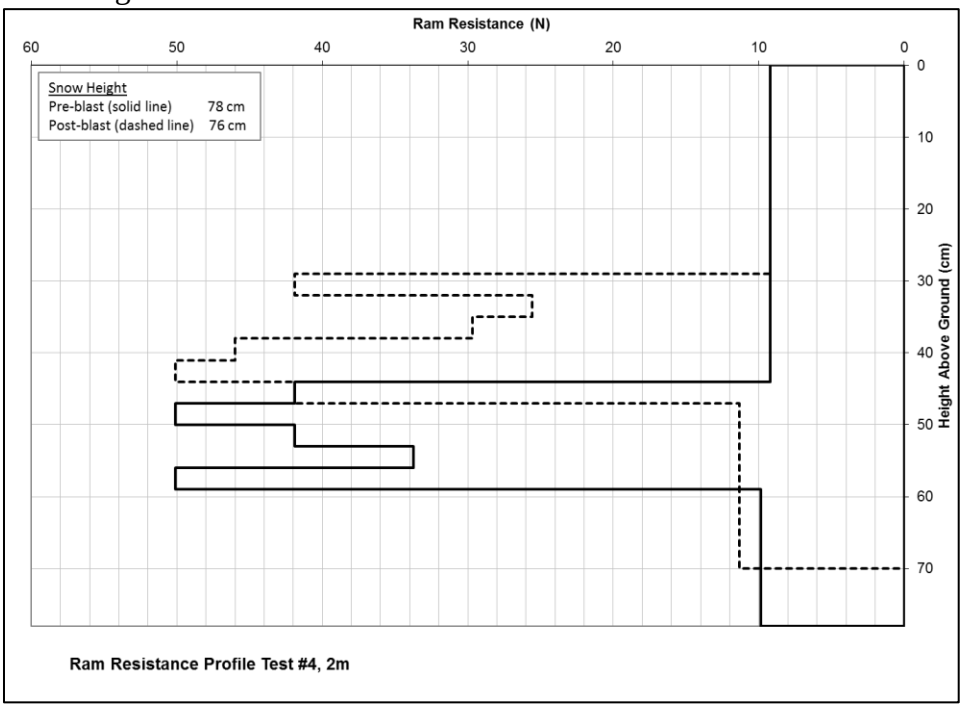

Figure A1: Ram resistance profile with poor alignment of layers and very little decrease in snow height. Layer alignment is not improved by adjusting for the decrease in snow surface height. With layers aligned, there appears to be no change in hardness.

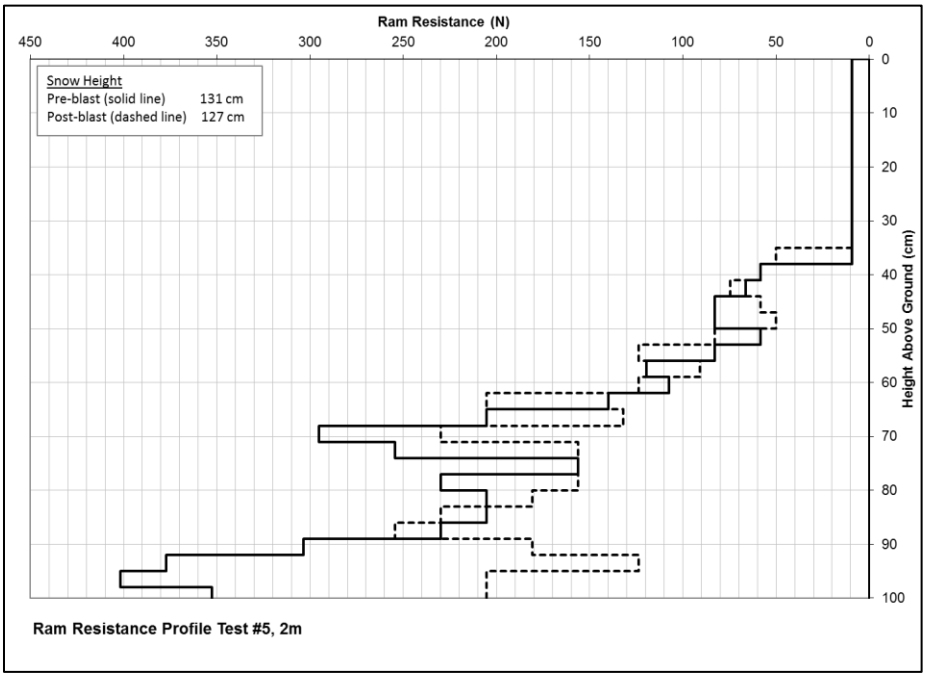

Figure A2: Ram resistance profile with poor alignment of layers and very little decrease in snow height. Layer alignment would be improved by adjusting post-blast snow height to account for the decrease in snow surface height. Alignment of layers shows small hardness decreases in the middle and bottom of the profile.

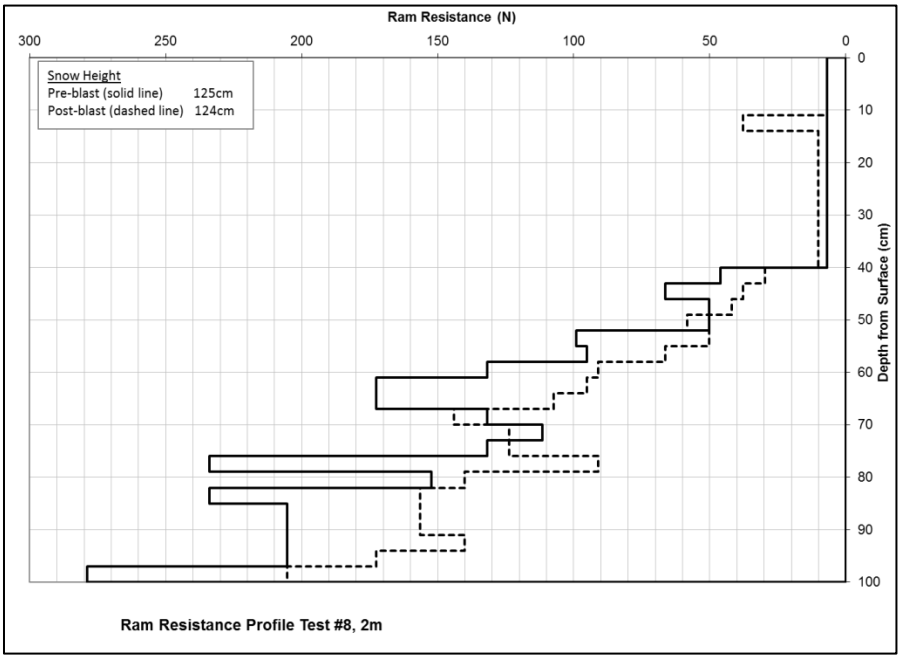

Figure A3: Ram resistance profile with poor alignment of layers and very little decrease in snow height. Layer alignment is not improved by adjusting for the decrease in snow surface height. Aligning layers indicates hardness decreases.

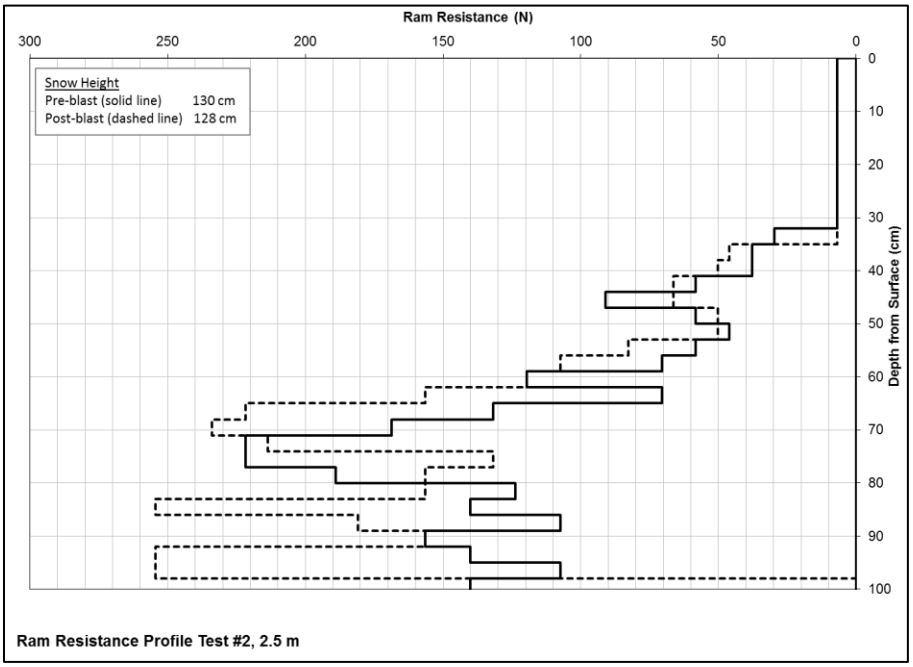

Figure A4: Ram resistance profile with poor alignment of layers and very little decrease in snow height. Layer alignment is not improved by adjusting for the decrease in snow surface height. Increases in hardness are evident at the bottom of the profile.

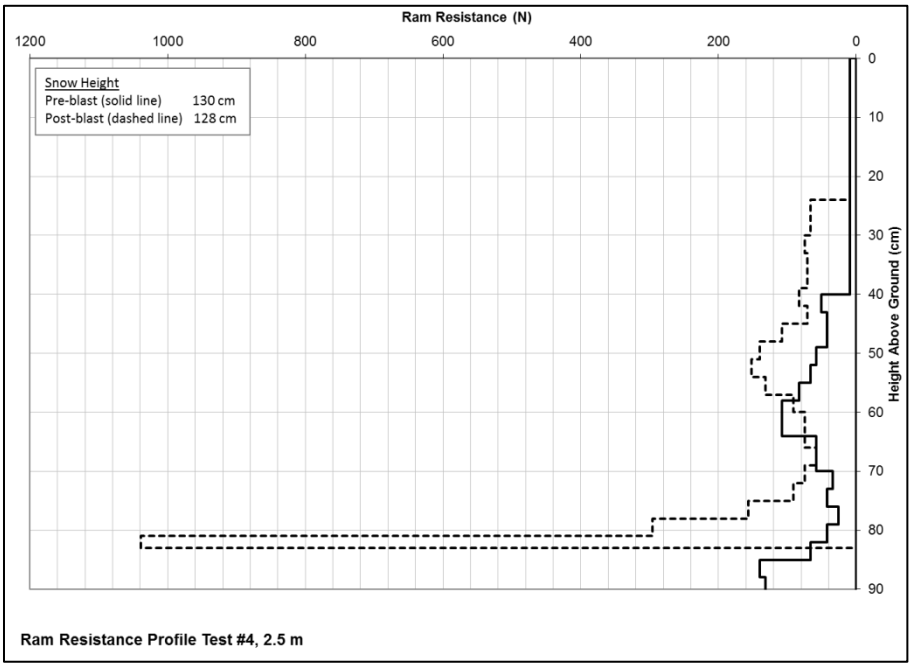

Figure A5: Ram resistance profile with poor alignment of layers and very little decrease in snow height. Layer alignment is not improved by adjusting for the decrease in snow surface height. Change in hardness is only apparent as an increase in hardness at the bottom of the profile.

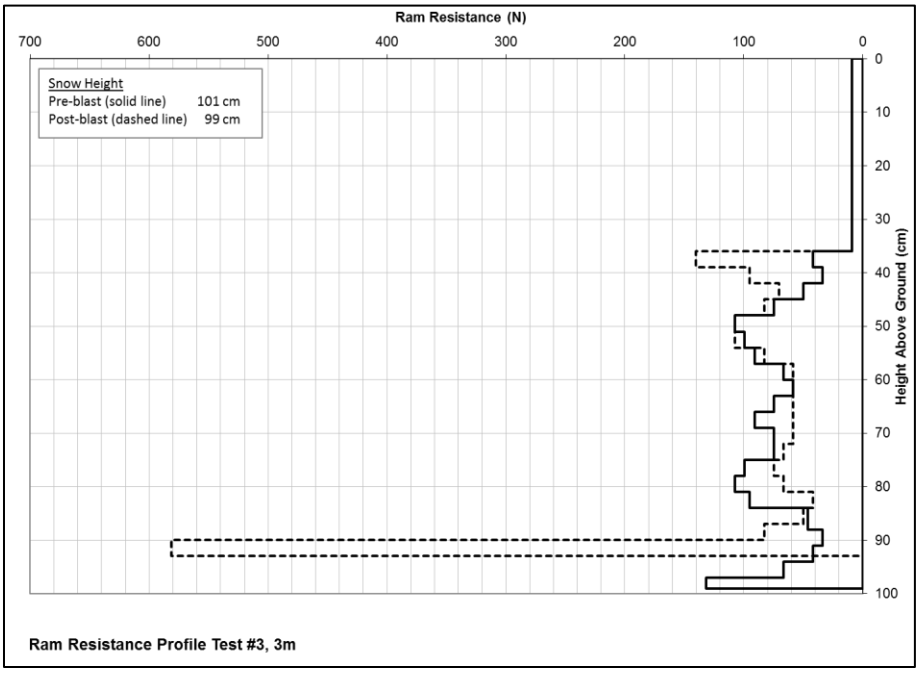

Figure A6: Ram resistance profile with poor alignment of layers and very little decrease in snow height. Layer alignment is not improved by adjusting for the decrease in snow surface height. With layers are aligned, small increases in hardness occur in the upper portion of the profile with a larger increase at the bottom.

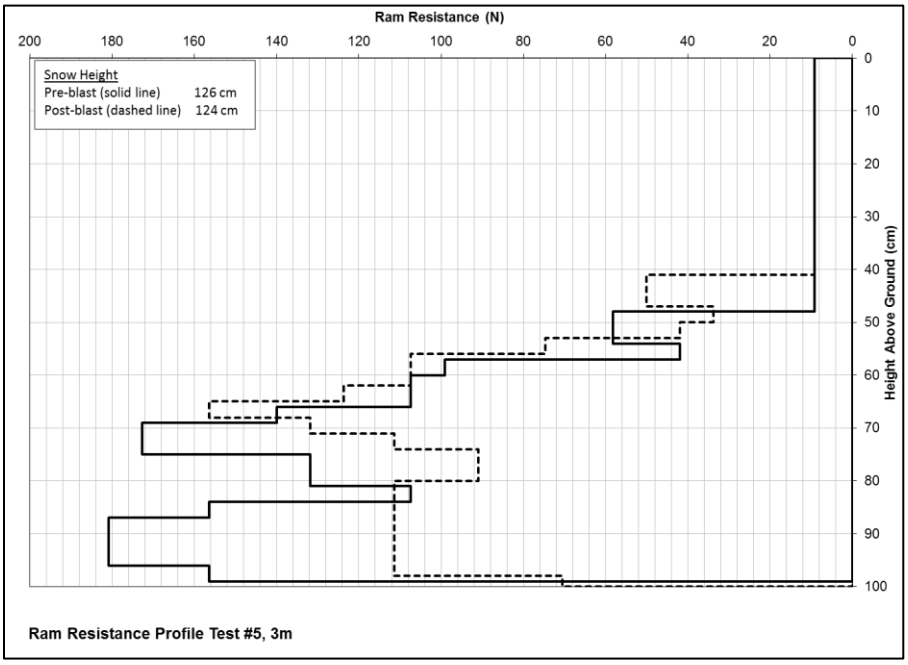

Figure A7: Ram resistance profile with poor alignment of layers and very little decrease in snow height. Layer alignment is not improved by adjusting for the decrease in snow surface height. A decrease in hardness is evident at the bottom of the profile.

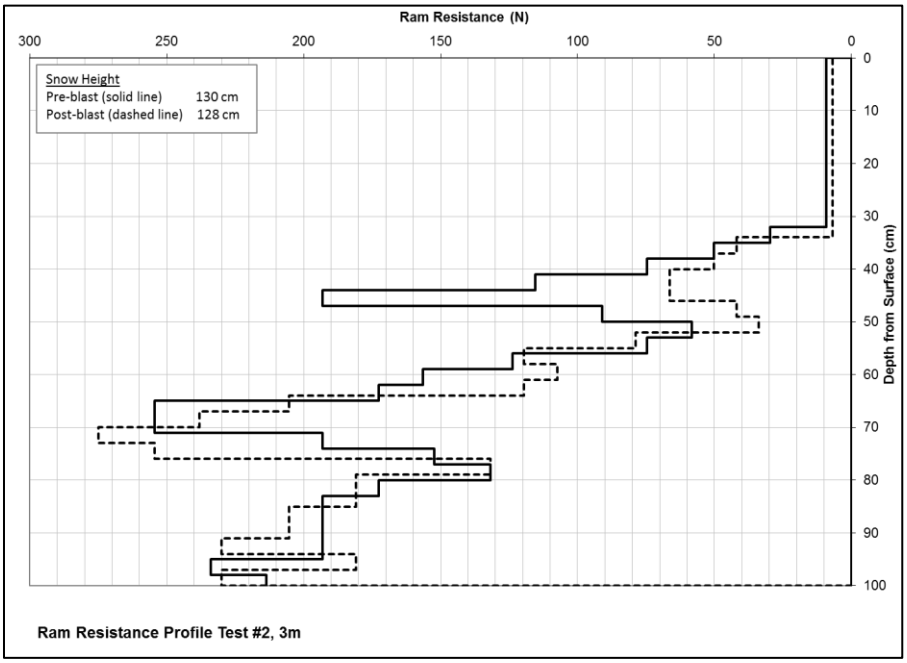

Figure A8: Ram resistance profile with satisfactory alignment of layers and very little decrease in snow height. A slight decrease in hardness is shown in the upper portion of the profile with no other apparent change.

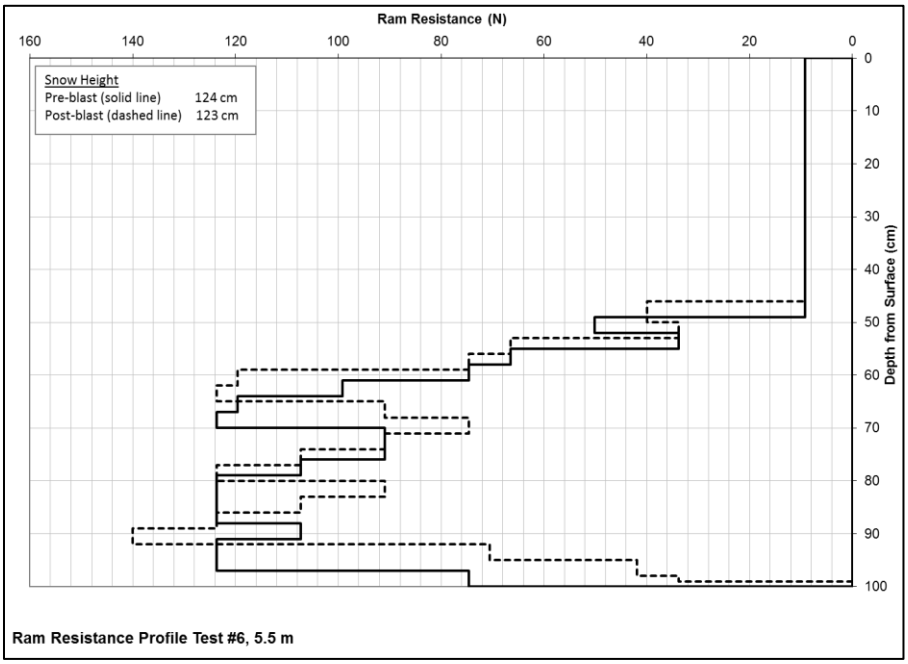

Figure A9: Ram resistance profile with satisfactory alignment of layers and very little decrease in snow height. This profile shows no strong evidence of hardness change.

The following 7 ram profiles are from locations where there was a 4-8 cm decrease in snow height:

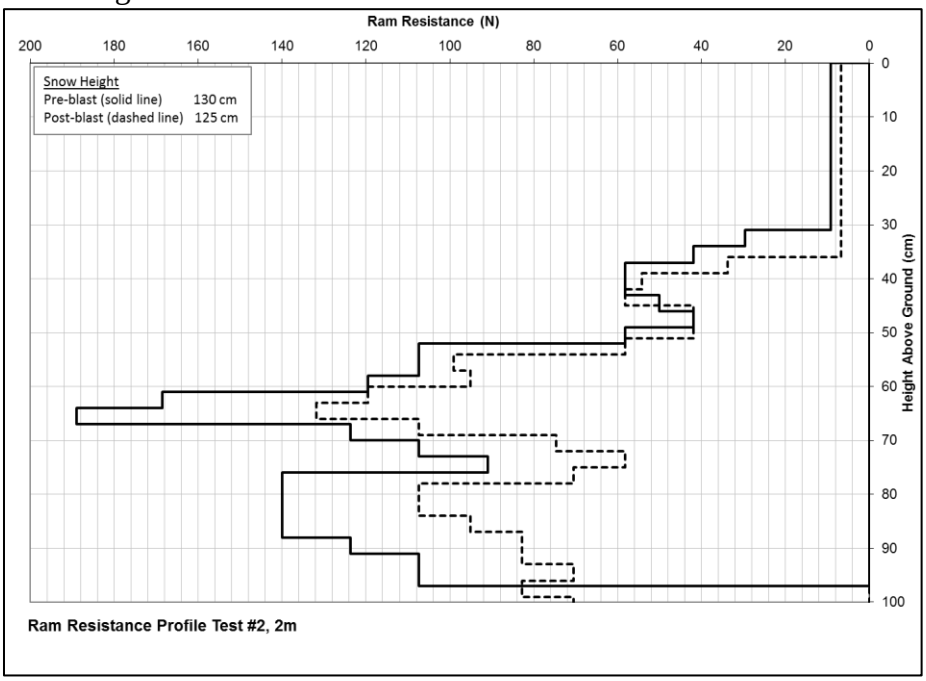

Figure A10: Ram resistance profile with satisfactory alignment of layers and a 5 cm decrease in snow height. Decreases in hardness below a depth of 50 cm are evident.

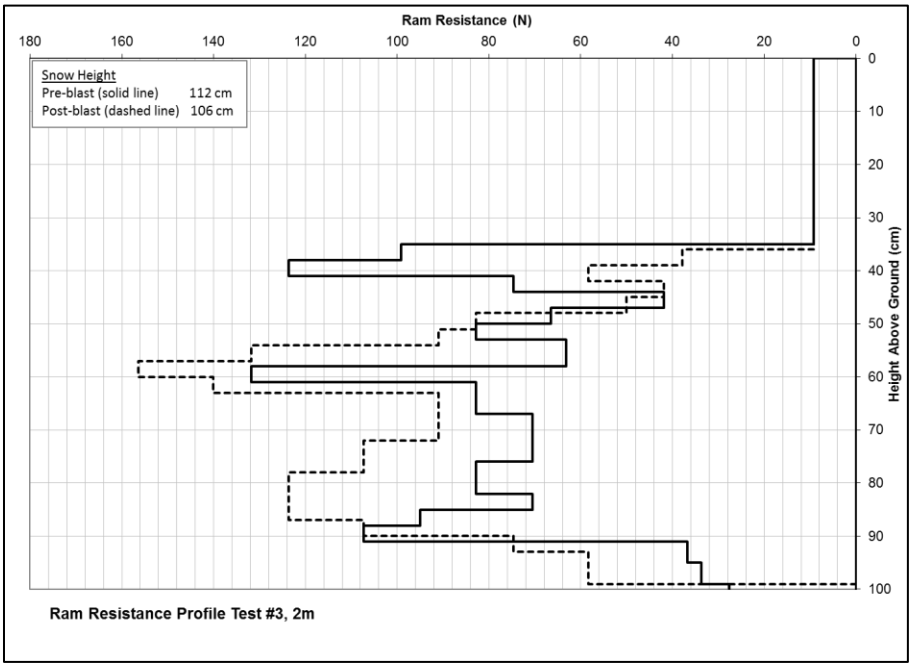

Figure A11: Ram resistance profile with satisfactory alignment of layers and a 6 cm decrease in snow height. Both increases and decreases in hardness are indicated in this profile.

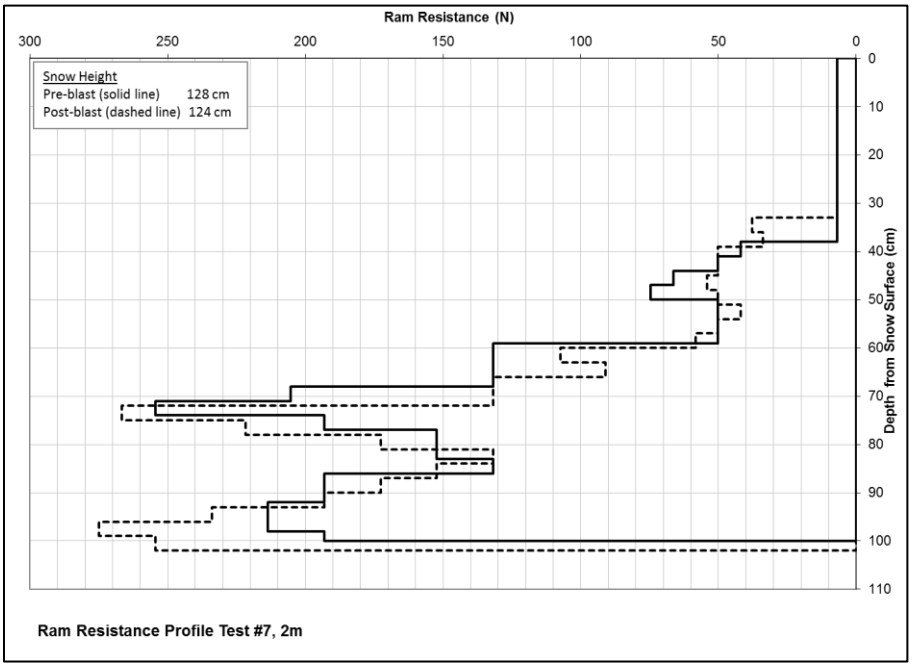

Figure A12: Ram resistance profile with satisfactory alignment of layers and a 4 cm decrease in snow height. An increase in hardness can be seen from a depth of approximately 90-100 cm.

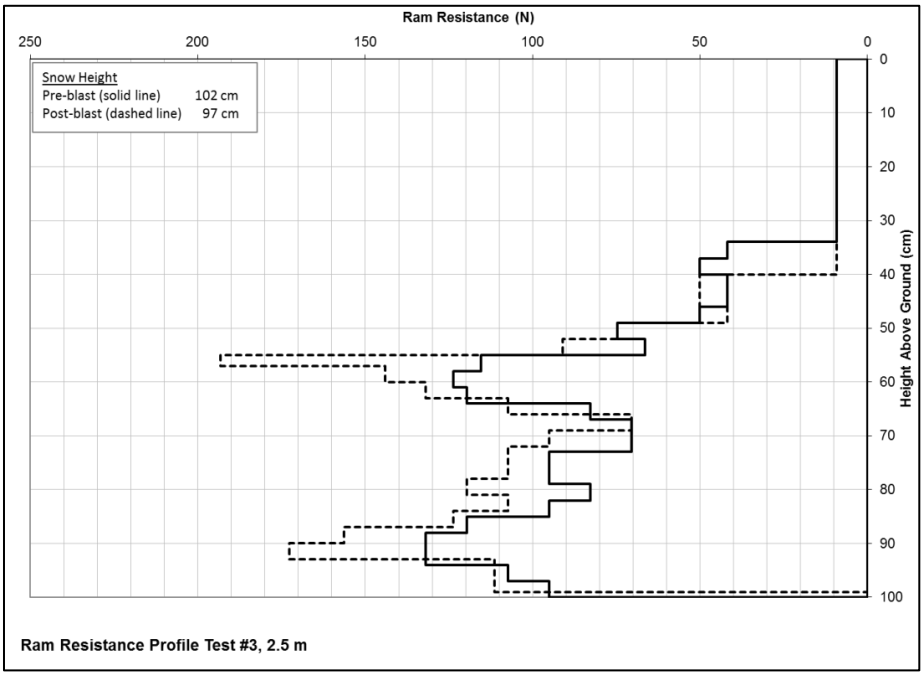

Figure A13: Ram resistance profile with satisfactory alignment of layers and a 5 cm decrease in snow height. Hardness increases occur at various points.

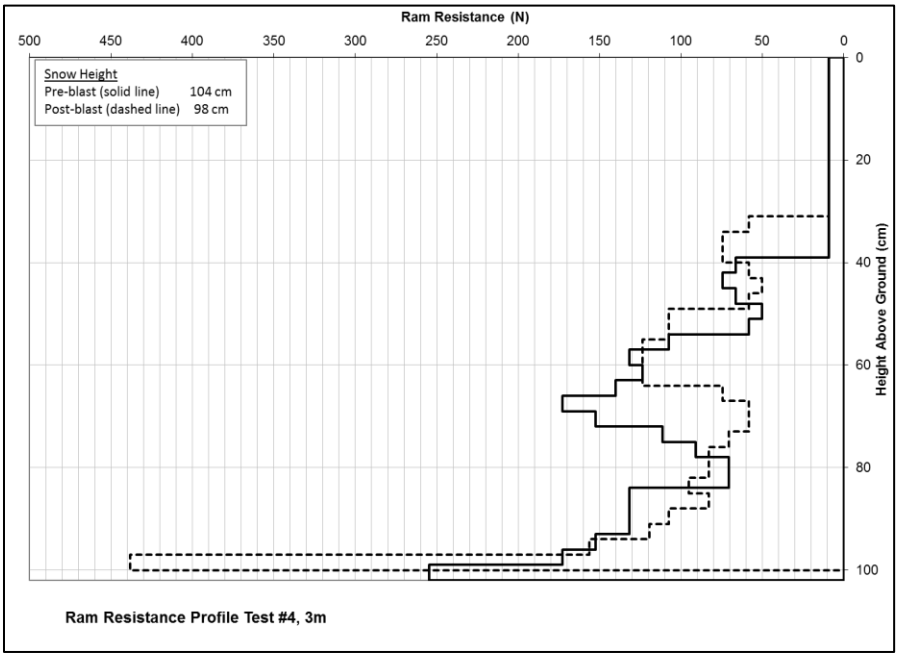

Figure A14: Ram resistance profile with poor alignment of layers and a 6 cm decrease in snow height. Layer alignment would be improved by adjusting post-blast snow height to account for the decrease in snow surface height. A small region of hardness increase is indicated at a depth of approximately 95-100 cm.

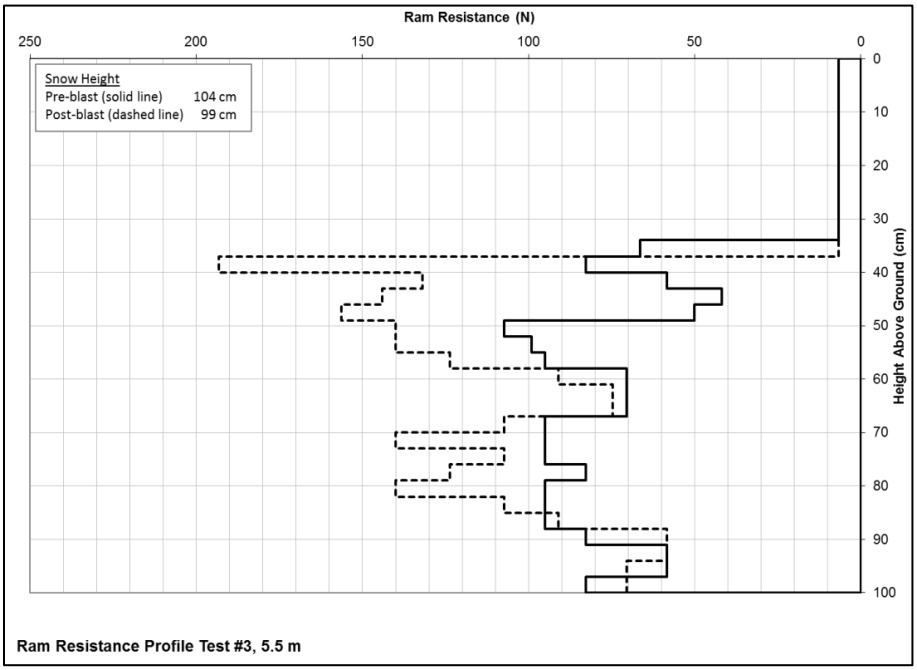

Figure A15: Ram resistance profile with poor alignment of layers and a 5 cm decrease in snow height. It is not likely that adjusting for the decrease in snow surface height would improve layer alignment. Increases in hardness are indicated throughout the profile.

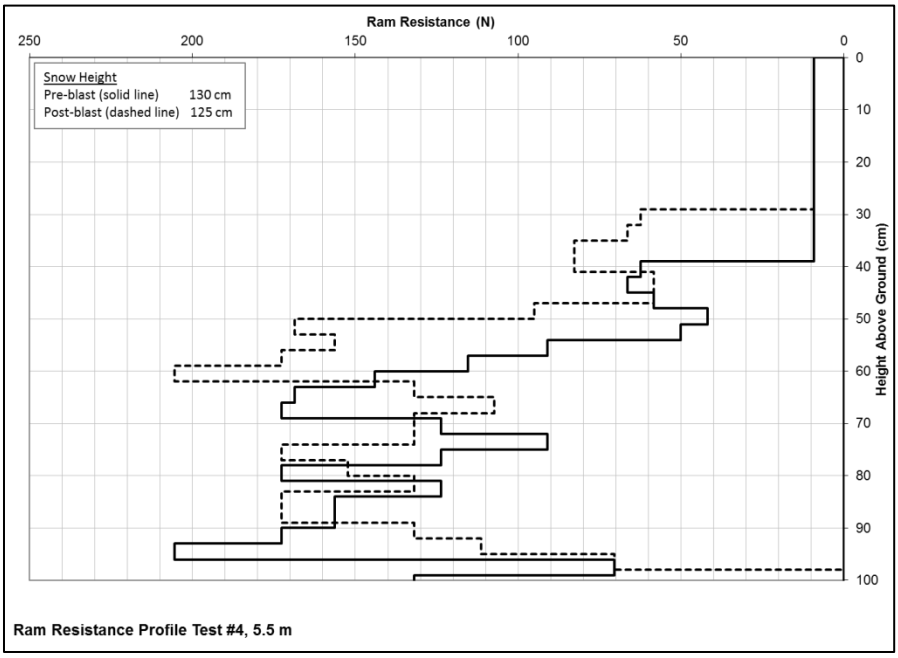

Figure A16: Ram resistance profile with poor alignment of layers and a 5 cm decrease in snow height. Layer alignment would be improved by adjusting post-blast snow height to account for the decrease in snow surface height. There appear to be both small increases and decreases in hardness in this profile.

The following 5 ram profiles are from locations with a 9 cm or greater decrease in snow height:

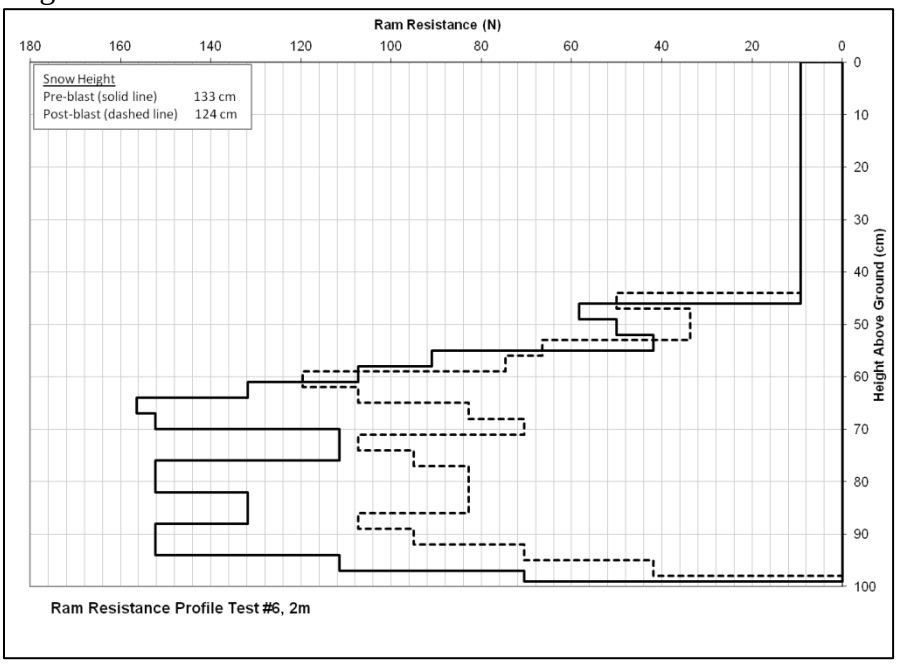

Figure A17: Ram resistance profile with poor alignment of layers and a 9 cm decrease in snow height. Layer alignment would be improved with a partial height adjustment. An overall decrease in hardness is apparent.

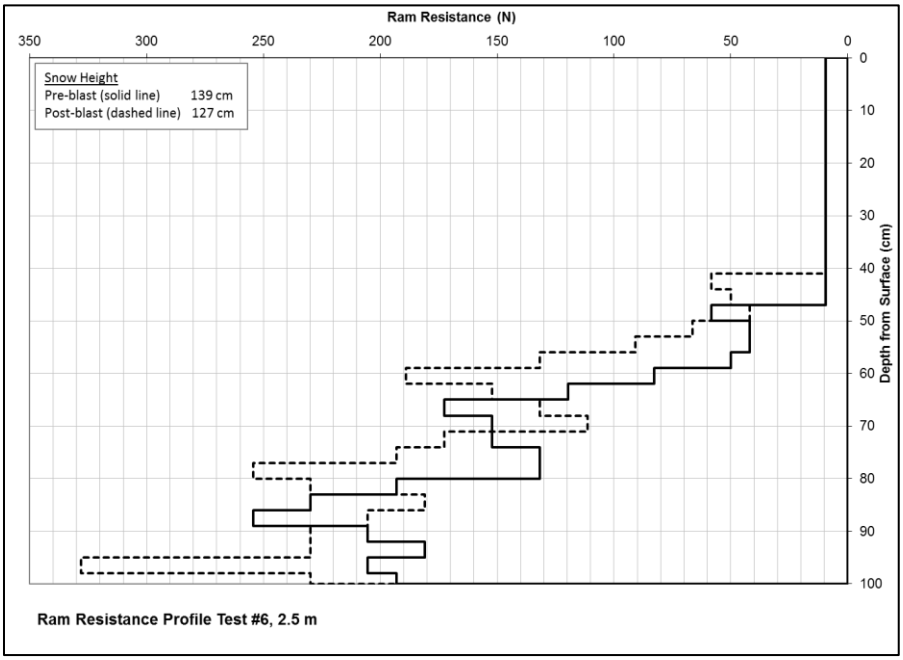

Figure A18: Ram resistance profile that would be improved by shifting the depth of the post-blast profile. Layer alignment would be improved with a partial height adjustment. Aligning layers indicates no change in hardness.

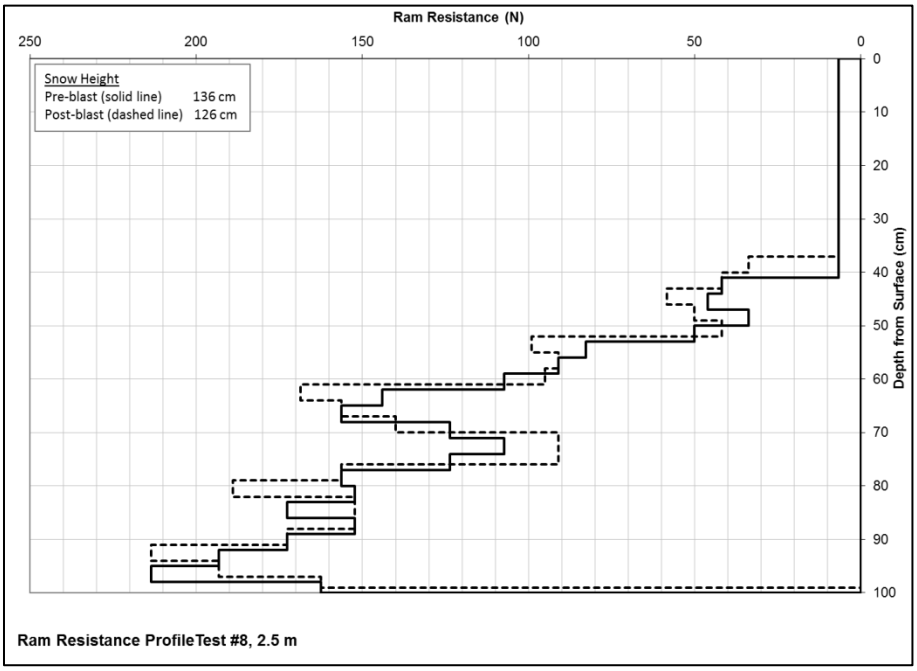

Figure A19: Ram resistance profile with good alignment of layers and a 10 cm decrease in snow height. Very small increases in hardness are indicated at various depths.

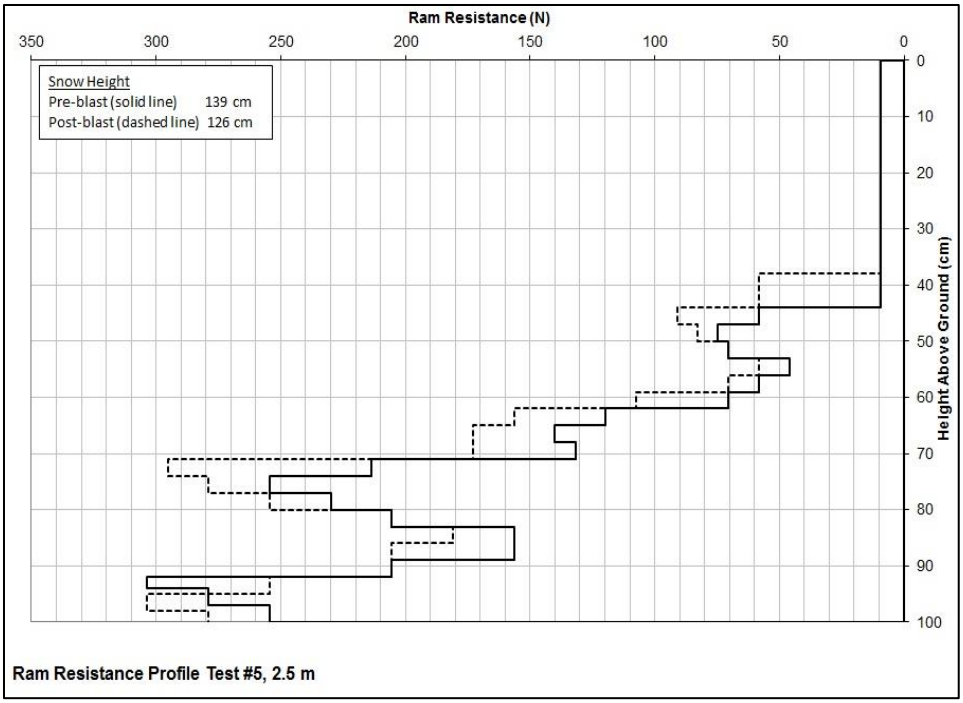

Figure A20: Ram resistance profile with a 13 cm decrease in snow height. Layer alignment would be improved with a partial height adjustment. Increases in hardness are visible to a depth of approximately 80 cm.

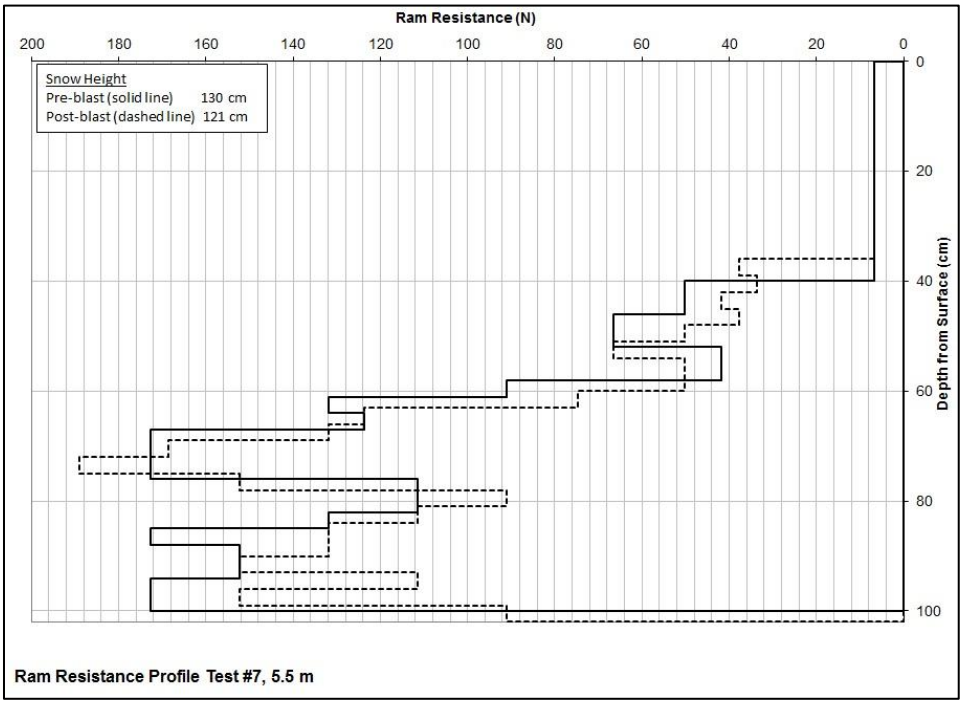

Figure A21: Ram resistance profile with a 9 cm decrease in snow height. Layer alignment is adequate with no height adjustment. Small decreases in hardness are visible to a depth of approximately 80 cm.